The Dissertation Committee for Ellen Kathleen Wagner Certifies that this is the approved version of the following dissertation:

ENGINEERING AND APPLYING NEXT-GENERATION ANTIBODY THERAPEUTICS FOR INFECTIOUS DISEASES

Committee:

Jennifer Maynard, Supervisor

George Georgiou

Lauren Ehrlich

Jason Upton

Lydia Contreras

ENGINEERING AND APPLYING NEXT-GENERATION ANTIBODY THERAPEUTICS FOR INFECTIOUS DISEASES

by

Ellen Kathleen Wagner, B.S.

Dissertation

Presented to the Faculty of the Graduate School of

The University of Texas at Austin

in Partial Fulfillment

of the Requirements

for the Degree of

Doctor of Philosophy

The University of Texas at Austin

May 2017

Acknowledgements

I would first and foremost like to thank my advisor, Jennifer Maynard, for her unwavering support and excellent scientific mentorship. I would not have been successful in lab without Annalee Nguyen, who taught me most of the techniques I use in lab. My labmates are some of my closest friends and scientific sounding boards, and I would not have remained relatively sane without their companionship. Finally, my committee members George Georgiou, Lauren Ehrlich, Lydia Contreras, Jason Upton, and Pengyu Ren have provided helpful feedback on my work, and encouraged my development as a scientist.

Science does not exist in a vacuum, and I am humbled by my many exceptional peers in chemical engineering and other departments at UT. Their friendship and research stories are a continual reminder to always keep things in perspective. I am inspired by my fellow female scientists, and I am honored to have been a part of CHEetahs flag football and the Chemical Engineering Women's group.

To my mom, dad, and brother; thank you for teaching me to be brave, curious, hard-working, independent, and adventurous. Dad, thank you for encouraging me to look at the stars, and Mom, thank you for showing me how to get there. To my brother Paul; thank you for being a patient and positive teacher and always inspiring me to try new things. Thank you to my grandparents and extended family, who have always been kind and supportive. And finally, thank you to my dog Donovan McTwist, who doesn't give a crap about science and makes me laugh every day.

ENGINEERING AND APPLYING NEXT-GENERATION ANTIBODY THERAPEUTICS FOR INFECTIOUS DISEASES

Ellen Kathleen Wagner, Ph. D.

The University of Texas at Austin, 2017

Supervisor: Jennifer Maynard

Antibodies have been engaging with infectious diseases since the evolution of cartilaginous fish, though it is only in very recent history that humans have been able to harness this expertise. The concept of using antibodies as therapeutics was first put into practice in the late 1890's and was called serum therapy. Although this remedy was revolutionary for the treatment of virulent infections, significant side effects as well as the introduction of modern antibiotics caused a rapid decline of the practice in the 1930s. It is now 80 years later and antibodies for infectious indications are experiencing a renaissance. In particular, the evolution of antibiotic-resistant bacteria, the emergence of new pathogens, a growing population of immunocompromised individuals, and the continual search for the next cure has caused many to take a second look at antibodies. The exceptional specificity and biocompatibility of antibodies makes them agreeable therapeutics, and the invention and maturation of protein engineering has given us a toy box of new strategies for their design. In particular, next-generation formats, such as antibody mixtures, bispecific antibodies, and T-cell-receptor driven approaches, are proving useful for the treatment of infectious diseases. These new formats are able to provide broad coverage against mutable pathogens and open new therapeutic avenues by redirecting the immune system. In this dissertation I will lead you through my last 5 years of research and show you what I have learned about engineering and applying next-generation antibody therapeutics for infectious diseases.

Table of Contents

List of Tables

List of Figures

Chapter 1: Engineering principles and pipeline for therapeutic antibodies for infectious disease

ABSTRACT

Parasitic and infectious diseases cause over 9.5 million deaths worldwide annually*(1)*. Antibodies, a fundamental component of the natural immune response to infectious pathogens, are rarely developed for these indications due to cheaper small molecule drugs and effective vaccines. However, a growing niche of specialty applications and the emergence of antibiotic-resistant pathogens has spurred development of antibodies targeting infectious diseases. There are currently 4 such recombinant antibodies approved in the US, with 40 in clinical trials. These high-affinity antibodies are commonly targeted toward secreted toxins, the pathogen's surface, or cellular receptors, and can make for a potent, fast-acting therapeutic. Fc engineering is often employed to provide a longer half-life or enhanced effector function. In particular, next-generation formats such as antibody mixtures and bispecific antibodies have a bright future for infectious applications due to their ability to recognize wider target variability and induce novel mechanisms of clearance. The recent growth of the biologics industry, along with a demonstrated need for novel anti-infective agents, makes it likely that recombinant antibodies will become a more common approach for the treatment and prevention of infectious disease.

INTRODUCTION

Global sales of monoclonal antibody products have grown from ~$39 billion USD in 2008 to nearly $75 billion in 2013, and are projected to reach ~$94 billion in 2017*(2)*. Monoclonal antibodies, already the driver of the biotech industry with 24.6% of US sales in 2012*(3)*, are set to capture an even larger share of the market due to a faster growth in sales and higher approval rate over other pharmaceuticals*(2, 4)*. Although the first recombinant antibody was approved in 1986, 29 of the 56 therapeutic monoclonal antibody products currently marketed in the US (as of April 2017) have been approved in the last 5 years (Fig. 1A), including the first bispecific antibody approval in 2014*(5)*. Of the currently marketed products, ~43% are for cancer indications and ~39% are for inflammatory or autoimmune disorders, while only ~7% are for infectious diseases (Fig. 1B). These include palivizumab (Synagis), approved in 1998 for the prevention of respiratory syncytial virus (RSV) in infants*(6)*; Raxibacumab*(7)* (Abthrax) in 2012 and obiltoxaximab*(8)* (Anthim) in 2016 for the treatment and prevention of inhalational anthrax, respectively; and bezlotoxumab*(9)* (Zinplava) in 2016 for prevention of recurrent *C. difficile* infection (Table 1). We have identified 40 recombinant antibodies in US clinical trials for infectious indications, with 30 currently in phase II or III trials. With a historical success rate of ~26% and an average time to approval of 7 years*(2)*, it is likely that several more anti-infective antibodies will enter the market in the foreseeable future.

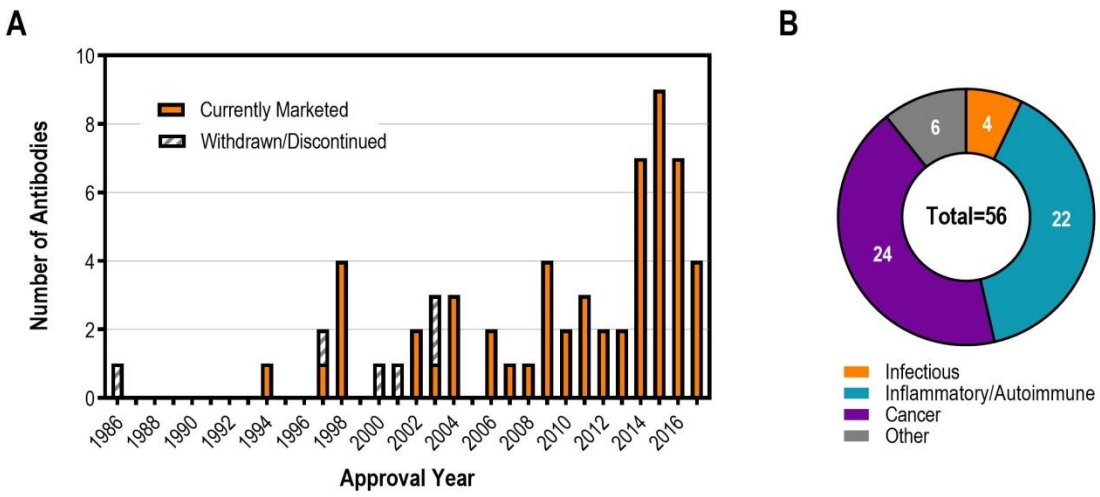

Figure 1. Therapeutic antibodies approved in the United States*(5)*.

A, US therapeutic antibody approval by year. Solid- currently on the market, striped- withdrawn or discontinued. B, Approved indications of currently marketed therapeutic antibodies. Orange- infectious, blue- inflammatory or autoimmune, purple- cancer, grey-other. Inflammatory/autoimmune includes other diseases related to immune system hyperactivity such as transplant rejection and asthma, cancer includes other neoplastic diseases such as Castleman disease. Other includes bone loss, macular degeneration, blood clot prevention and high cholesterol.

Table 1. Anti-infective monoclonal antibodies approved in the United States.

Name	Disease	Target	Affinity **(nM)**	Isotype	Approval **(US)**	Developer
Palivizumab*(6)* **(Synagis)**	RSV	Viral glycoprotein-RSV fusion (F) protein	2.6*(10)*	Humanized IgG1	1998	Medimmune
Raxibacumab*(7)* **(Abthrax)**	Anthrax	Bacterial toxin-protective antigen	2.8*(11)*	Human IgG1	2012	GlaxoSmithKline
Obiltoxaximab*(8)* **(Anthim)**	Anthrax	Bacterial toxin-protective antigen	0.3*(12)*	Chimeric IgG1	2016	Elusys Therapeutics
Bezlotoxumab*(9)* **(Zinplava)**	*C. difficile*	Bacterial toxin-enterotoxin B	0.05-0.8*(13)*	Human IgG1	2017	Merck

Although using antibodies for infectious diseases may seem like somewhat of a niche field, there are many applications for which antibodies are uniquely suited. As compared to small-molecule drugs, antibodies possess two unique traits which can be leveraged to create quality therapeutics. First, antibodies are highly specific, allowing differential targeting of pathogens, receptors, or even specific glycoforms*(14)* in a sea of similar neighbors. In contrast, commonly-used antibiotics can have significant impacts on natural populations of commensal or symbiotic bacteria in addition to the targeted species, for example in the gut microbiome*(15)*, opening the door to overgrowth of opportunistic pathogenic bacteria in the absence of normally present competitors*(16)*. This mechanism is a common cause of recurrent *C. difficile* infections, and was the driving force behind the development of anti-toxin antibodies which can prevent symptomatic reinfection*(17)*. Another potential advantage of high specificity is a reduction in the spread of resistance, especially in non-target organisms*(18)*. While constantly evolving pathogens certainly respond to selective pressure from antibodies*(19)*, such mutations will only impact that particular antibody therapeutic, rather than a whole class of antibiotics. In light of increasing incidence of antibiotic-resistant infections*(20)*, there is now significant interest in developing antibody therapeutics to treat or prevent bacterial infections like methicillin-resistant *S. aureus(21)*.

A second unique characteristic of antibodies is that they are natural molecules of the immune system and can be engineered to interact with or avoid various immune pathways. Therapeutic development often involves discovery of antibody binding regions capable of neutralizing pathogens, followed by engineering efforts directed toward affinity improvement*(12)*. The resulting antibodies can block the interaction of pathogenic antigens with host receptors and/or facilitate clearance of antigen or

pathogens when immune complexes are formed. Importantly, antibodies which function by neutralization can be potent prophylactic agents even in those without a fully-functioning immune system. This passive immunization approach is useful for short-term protection of high-risk individuals, such as infants or transplant patients, from common infections such as RSV*(6)* or Hepatitis C Virus (HCV)*(22)*. In contrast, there is increasing evidence of the importance of Fc-mediated effector functions, which can contribute to complement-mediated lysis and phagocytosis of pathogens*(23)*, and antibodies with improved efficacy can be identified through Fc engineering. Such antibodies include high-value therapeutic agents against elusive targets like HIV*(24)*, which has so far outlasted small molecule drugs and vaccine discovery efforts. In either case, antibodies are typically safe and well-tolerated, have few off-target effects, and do not interfere with other drugs.

A growing list of antibiotic-resistant bacteria, emerging pathogens, and immunocompromised individuals shows that new anti-infective drugs are urgently needed. In the next section we will detail the essential considerations in optimizing antibodies for infectious diseases, which include traditional areas such as specificity, affinity, and Fc engineering, as well as emerging technologies such as antibody mixtures and novel formats. Finally, we will survey indications for which antibodies are in clinical trials or preclinical development, and comment on future directions in the field.

ENGINEERING ANTIBODIES FOR INFECTIOUS DISEASES

The efficacy and mechanism of action of an antibody is defined and refined by several key parameters, including specificity and affinity, clonality, format, and Fc function (Fig. 2). A therapeutic candidate is usually first isolated for its specificity, which can be further enhanced to improve potency. Fc engineering can be used to increase half-life or alter immune system interactions, which in some cases is the major therapeutic mechanism. Antibody mixtures and alternative formats are emerging as strategies with particular relevance to infectious diseases, and may be crucial for broad coverage of a mutable pathogen or for inducing novel clearance mechanisms of elusive targets. In this section we will discuss considerations of each of these areas in the context of targeting pathogenic diseases.

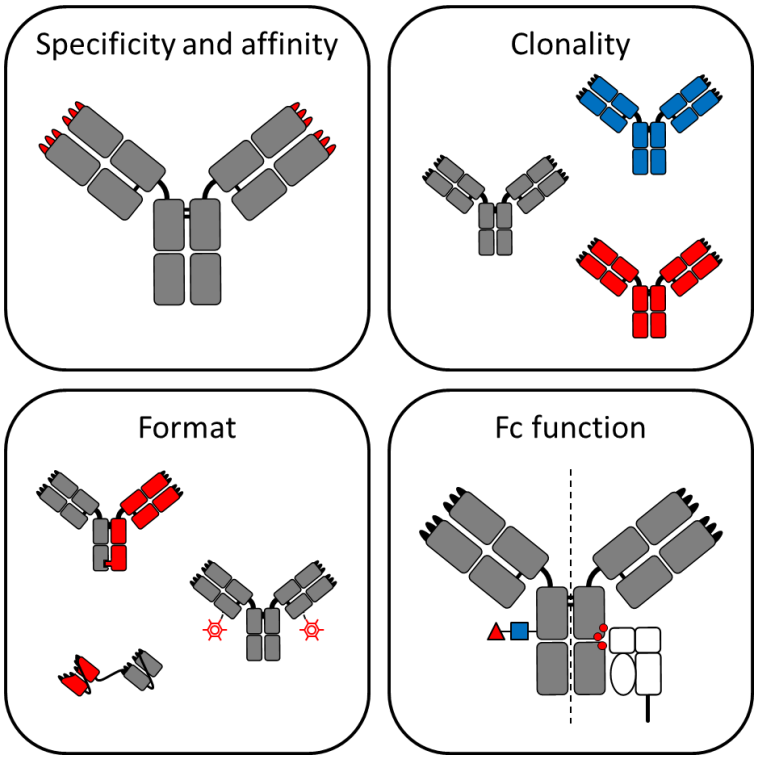

Figure 2. Key tenets of antibody engineering.

Designing an antibody therapeutic requires conscious consideration of several parameters, incuding what the antibody targets and how tightly it binds (specificity and affinity), the number of specificities to include (clonality), interaction with the immune system (Fc function, e.g. glycoslyation or half-life extending mutations), and how the antibody is formatted (format, e.g. bispecifics or ADCs).

Selection of target and affinity maturation

Antibody engineering begins with specificity; antibodies can be raised against nearly any target, but the choice will define the mechanism of action and efficacy. In the case where the desired specificity is known, antibodies are relatively easily isolated by immunization of wild-type or humanized mice, followed by library screening to identify neutralizing antibodies. In a desire to reduce immunogenicity, there is a push toward developing fully-human antibodies, which can be isolated from vaccinated or immunized human volunteers*(25)*. In many cases an effective target may not be known intuitively,

but can be inferred based on what dominates the natural immune response to the pathogen in protected hosts. In other cases, for example HIV, broadly-neutralizing antibodies are an extremely rare natural event, but therapeutic antibodies can be isolated from the few individuals who are naturally resistant to disease progression*(26)*. Most anti-infective antibodies fall into one of three major categories; antibodies that neutralize soluble antigens, antibodies that target intact pathogens, and antibodies that block host receptors.

Bacterial toxins are not infectious themselves, but are the causative agents of morbidity in bacterial infections such as *B. pertussis(27)*, *S. aureus(28)*, and *C. difficile(29)*. Antibodies binding the toxin are therefore not directly anti-infective, but rather can prevent physiological damage, inflammation, and other symptoms while antibiotics and the host immune system clear the infection*(17)*. In some cases the toxin is also immunosuppressive*(30)*, and anti-toxin antibodies may lead to a reduction in the bacterial load*(8)*. Neutralizing antibodies commonly function by blocking receptor-binding sites on the toxin*(27, 31)*, but can also work by preventing conformational changes*(32)* or enhancing immune complex formation and removal*(33)*. Anti-toxin antibodies are also an ideal prophylactic agent for bioweapons such as anthrax*(34)* and botulism*(35)*, as they can provide "instant immunity" against highly-lethal toxins for several months.

Antibodies can also directly target bacteria by binding surface proteins*(36)* or lipopolysaccharides (LPS)*(37)*. In such cases the antibodies can initiate complement- or antibody- mediated cytotoxicity or phagocytosis, and are considered bactericidal*(37)*. This mechanism is therapeutically relevant for treating infections of antibiotic-resistant

bacteria like *P. aeruginosa,* which is cleared in healthy individuals by complement-mediated opsonophagocytosis or killing*(37)*. A recombinant IgM antibody directed against a common *P. aeruginosa* surface LPS serotype is able to recruit host immune cells*(37)* and is in clinical trials for the treatment of nosocomial pneumonia*(38)*. Binding the extracellular surface is also a convenient way to deliver other drugs to the area, as demonstrated with an antibody-antibiotic conjugate that targets intracellular S. aureus*(14)*.

Antiviral antibodies are typically directed against surface glycoproteins on the capsid (naked viruses) or envelope. For example, most influenza A antibodies in development target hemagglutinin (HA), which mediates fusion of the virus to the host cell. These antibodies can therefore neutralize the virus through two mechanisms; direct blocking of membrane fusion in the endosome and lysis of coated particles via antibody-dependent cellular cytotoxicity (ADCC)*(39)*. Even within a particular glycoprotein antigen, antibodies targeting different epitopes may utilize distinct mechanisms for neutralization. The RSV F protein has significantly different pre- and post-fusion structures, and while epitopes within the antigenic site II are mostly conserved between these two structures, epitopes in the more recently described antigenic site Ø are only present in the pre-fusion structure*(40, 41)*. Thus, an antibody targeting site II may be neutralizing even after viral attachment, while a neutralizing antibody targeting site Ø likely functions by preventing the conformational change required for fusion*(40)*. Interestingly, only anti-RSV antibodies targeting antigenic site II were found to have Fcγ-dependent mechanisms*(42)*, which is yet another example of how the fine epitope specificity can drive mechanism.

An alternative approach to treating diseases with antibodies is to target host receptors that are involved in disease progression. For example, there are several therapeutic HIV antibodies in development that bind the host receptors CD4*(43)* or CCR5*(44)*, and prevent required conformational changes to allow viral entry. A benefit of targeting the host receptor is that the therapeutic can work on a broad spectrum of viral isolates, as long as they have the same entry mechanism. Checkpoint inhibitors such as anti-PD1 antibodies, which have recently been approved for several cancers, also have potential for treating infectious diseases by reversing T-cell exhaustion associated with chronic antigen stimulation*(45)*. Other immune modulating antibodies targeting cytokines*(46)* or complement*(47)* are also in clinical trials for infectious indications.

A key consideration in all of these approaches is that the targeted epitope needs to be highly conserved. Pathogens can escape a therapeutic either at the population level, where a diversity of circulating strains with different antigenic properties is available to infect a host; or within a single host, where high mutation rates in the pathogen can quickly generate escape mutants in response to therapeutic pressure. For example, naturally-elicited influenza A antibodies are targeted against the highly-variable hemagglutinin (HA) head, necessitating a constantly evolving vaccine formulation to keep up-to-date with the year's dominant strain*(48)*. In contrast, promising recombinant antibodies against influenza A typically recognize the less-variable HA stalk, and are chosen based on their ability to neutralize both group1 and group 2 strains*(49, 50)*. One influenza A antibody in clinical trials was computationally designed to bind a conserved epitope by rationally targeting highly networked residues that are less likely to be mutated*(51)*. Similarly, the quest for broadly neutralizing antibodies against HIV has

focused on conserved features in the gp120 envelope protein*(52)*, which reduces the chance of functionally-active escape variants.

Affinity maturation is the process by which tighter binding antibodies are generated and selected for, which happens naturally *in vivo* over the course of an infection. Accordingly, substantial protein engineering effort has traditionally been placed on affinity maturation of therapeutic antibody candidates. This is often done by generating targeted libraries to the complementary-determining regions (CDRs) that bind the epitope, transfecting those libraries into a phage or yeast display library, and using a panning or flow cytometry method to select for improved binders. In many cases a clear correlation can be seen between antibody affinity and *in vitro* and *in vivo* efficacy, as nicely demonstrated for antibodies targeting the anthrax PA toxin*(12)* and staphylococcal enterotoxin B*(53)*. The rationale is simple; a higher-affinity antibody will spend more time bound to the antigen, thus is more efficient at providing its protective effect.

While the effects of affinity improvements can be easily spotted *in vitro* or in simple animal models, at a certain point there may be minimal additional protection provided in human disease. This is illustrated by the painful parable of motavizumab, an ultra-high affinity version of pavilizumab. Extensive affinity maturation was performed through saturation mutagenesis of the CDR loops and selection using phage display*(54)*. The final selected variant, motavizumab, exhibited a 70-fold higher affinity, was protective at one-hundredth the dose, and even displayed additional therapeutic mechanisms*(10)*. Unfortunately, clinical trials were unable to show the superiority of motavizumab and also exposed higher rates of hypersensitivity reactions, and ultimately the FDA voted against motavizumab approval*(55)*. Interestingly, during development, it

was noticed that affinity improvement due to faster association rates (k_{on}) rather than a slower off-rate (k_{off}) resulted in improved neutralization of virus *in vitro(54)*, but also increased non-specific tissue binding*(10)*. Although these issues were resolved before clinical trials, the increased hypersentivity reactions may be attributable to this cause, and serve as a reminder that antibody selectivity for the target over non-target antigens is just as important as the overall affinity.

Improving neutralization with oligoclonal antibody mixtures

The natural immune response is polyclonal, and for good reason; infectious pathogens are, by definition, highly variable and highly mutable. A polyclonal mixture therefore is powerful in that it can provide broad protection against a variety of strains in the environment as well as genetic shift inside the host*(56)*. In addition, a natural antibody response includes antibodies specific to many different possible epitopes, and such a mixture could theoretically neutralize a pathogen through several complementary pathways. Although the specific protective agent was not known at the time, this powerful efficacy was appreciated, and "serum therapy" was first deployed in the late 1800s for a variety of diseases*(57)*. Serum therapy for diphtheria consisted of an infusion of purified equine serum from animals immunized with diphtheria toxin, and reduced the mortality rate in children from 50% to 5%*(58)*. Use rapidly declined in the 1930s due to side effects from poor purity and the invention of the first antibiotics*(59)*, but similar approaches are still used today for the treatment and prevention of diseases like tetanus, rabies, and congenital cytomegalovirus (CMV)*(60)*.

Modern serum therapy consists of high titer immunoglobulin (IG) purified from the pooled sera of human (or in certain cases, animal) donors, and is subject to strict

purity and safety standards*(61)*. However, as a human-sourced product, IG suffers from other drawbacks including a limited supply, lot-to-lot variability, and a risk of blood-borne pathogen transmission*(56)*. In addition, even though specialty IG preparations are enriched for pathogen-specific antibodies, extremely high doses (100s of mg/kg) are required for efficacy*(60)*. Recombinant antibody therapeutics can overcome many of the limitations of IG, and there is some precedence for using monoclonals to treat infectious diseases. For example, a single high-affinity recombinant antibody targeting the RSV F protein was able recapitulate or even exceed the efficacy of the IG preparation*(62)*, and is recommended over RSV-IG for high-risk infants*(63)*.

Despite success of several monoclonal anti-infective antibodies, for many applications an antibody mixture may improve efficacy. This may be a critical strategy for the treatment of highly mutable pathogens such as HIV, which is able to escape even from highly potent broadly neutralizing antibodies*(64)*. A mixture of antibodies targeting distinct epitopes would be expected to protect against a broader range of circulating HIV strains, while also reducing the chance of escape variants. In a recent paper, mixtures of two to four antibodies were able to neutralize 100% of viruses from a panel of 125 strains at conditions where the monoclonal only neutralized 25-66%*(65)*. In a macaque treatment model, administration of a mixture of two antibodies controlled viremia for two to five times longer than monotherapy, with loss of efficacy correlated to the decline of antibody in the plasma rather than viral escape*(66)*.

Recombinant antibody mixtures may also benefit from synergy of several components, leading to increased efficacy and lower required doses. In such cases, the individual antibodies often utilize distinct neutralization pathways for efficient clearance

of a pathogen. This is illustrated by a mixture of two antibodies that bind staphylococcal enterotoxin B (SEB), a notable superantigen and potential bioweapon. One antibody blocked the TCR binding site on the toxin and was independently neutralizing, but addition of a second non-neutralizing antibody significantly improved efficacy by inducing formation of immune complexes*(67)*. Notably, in some cases antibodies which are minimally protective individually may be potent components of a mixture, such as a ternary mixture of anti-botulism toxin antibodies which exhibited a 20,000-fold increase in potency compared to each individual antibody*(35)*. Synergy is not limited to antibodies; potent synergy has been observed between antibodies and small-molecule antiviral drugs*(68)*, and such combination therapy is a viable therapeutic strategy.

Oligoclonal antibody mixtures are an exciting maturation of the field of antibody technology; we are now able to better understand and appreciate the enormous capability and finesse of the natural immune response, and finally have the technology to begin to replicate it. High-throughput screening of antibody mixtures remains a challenge, and to date most antibody mixtures have been rationally chosen from a small subset of monoclonals . In addition, validation of superior *in vivo* performance of the mixture should be emphasized early on, as antibody mixtures are moderately to significantly more costly to develop*(69)*. The recent approval of bezlotoxumab (Zinplava) serves as a cautionary tale; while preliminary mouse studies supported the idea that a combination of two antibodies (actoxumab and bezlotoxumab) against *C. difficile* toxins A and B improved efficacy, it was not until phase III trials and follow up studies that actoxumab was dropped from the combination due a lack of added benefit*(70)*. That being said, there are currently 9 antibody mixtures for infectious diseases in clinical trials, and many more in development. New strategies for efficient production of these mixtures at

manufacturing scale are being developed*(69)*, including single-pot strategies that can significantly reduce costs*(71)*. FDA approval requirements are evolving to match this new therapeutic modality, and it is no longer required to perform separate efficacy trials for each component*(72)* .

Fc engineering for improved function and half-life

Recombinant antibodies are almost exclusively of the IgG class, which is the most common antibody class found in the serum and most commonly associated with long-term protective effects. The IgG class is further divided into four isotypes (IgG1, IgG2, IgG3, IgG4), which have ~90% sequence homology but differences in some surface exposed residues and the hinge region*(73)*. Distinct structures lend each isotype to different jobs; for example, IgG2 can form covalent dimers and is important for the targeting of repetitive bacterial surface carbohydrates*(74)*, while IgG4 can swap arms to become functionally monovalent and so mediate anti-inflammatory effects*(75)*. In practice, the vast majority of therapeutic antibodies have been developed as IgG1, partly due to historical precedence and prevalence in the natural immune response and partly due to function. There are several approved IgG2 and IgG4 antibodies, typically with stabilizing mutations in the IgG4 hinge to prevent fab arm exchange*(76)*. IgG3 is not commonly pursued as a therapeutic molecule, in part due to hinge instability, more complex manufacturing, and a shorter serum half-life*(73)*.

The four IgG isotypes have subtle differences in surface exposed residues in the Fc region which causes differential binding of Fcγ receptors (FcRs) expressed on immune cells*(77)*. Antibody-mediated effector functions such as antibody-dependent cellular cytotoxicity (ADCC), antibody-dependent cellular phagocytosis (ADCP), and

complement-dependent cytotoxicity (CDC)*(76)* can be powerful mechanisms against infectious pathogens. The balance of binding to particular activating and inhibitory receptors determines the magnitude and type of effector response; IgG1 is highly activating and induces potent ADCC and CDC, whereas IgG4 is mostly inert*(73)*. Although alternative isotypes are not often characterized, proper isotype selection can be a critical factor in antibody efficacy, as demonstrated with an antibody targeting *C. neoformans(78)*. Another approach is to modify the Fc region for altered FcR binding and therefore altered immune interaction. For example, antibodies targeting the influenza hemagglutinin stalk were found to be potent inducers of ADCC, and Fc variants with enhanced binding affinity to activating FcγRs significantly improved survival in a murine challenge study*(79)*. In some instances it may be desirable to have a very inert Fc region, as present on IgG4. For example, activating antibodies against dengue virus are correlated with increased disease severity, due to antibody-dependent enhancement in which opsonization increases infectivity*(80)*.

Post-translational modifications such as glycosylation can impact FcR binding, and need to be considered during antibody optimization. IgG antibodies contain a conserved N-glycosylation site at N297, which is located near the N-terminus of the C_H2 region and helps stabilize an open conformation*(81)*. Mutations at this site which prevent glycosylation result in a significant loss in FcR binding, C1q binding, ADCC and CDC. A wide diversity of glycoforms are generated during manufacturing, and vary significantly between different proteins and different expression platforms*(82)*. Control of glycosylation may be a way to fine-tune antibody effector functions further; a recent paper generated IgGs with homogenous glycoforms, and found that fucosylation of the core glycans significantly reduced ADCC*(83)*.

The neonatal Fc receptor (FcRN) is expressed throughout the body and functions to transport and recycle circulating antibodies. This transport process is initiated by extracellular binding of the antibody at physiological pH, followed by internalization and acidification of the endosome, subsequent dissociation of the antibody from the receptor at low pH and return of the antibody to the cell surface*(84)*. FcRn binds an epitope at the C_H2-C_H3 domain interface, and engineering of this site can be used to modify the FcRn binding characteristics of the antibody. The well- characterized M252Y/

S254T/T256E (YTE) mutant has improved affinity for FcRn while maintaining the pH selectivity*(85)*, which results in a nearly 4-fold improvement in *in vivo* half-life*(86)*. These and other half-life-extending mutations can have a significant impact on the efficacy and economy of antibody prophylaxis; a YTE variant of an RSV-targeting therapeutic is currently in clinical trials, and is projected to reduce dosing from once per month to once per season*(87)*.

TRIM21 is a recently described cytosolic FcR that binds antibody-bound virus inside the cell. TRIM21 is expressed in most tissues and most antibody classes, and seems to function as a "last line of defense" against virus that has escaped immune evasion*(88)*. The antiviral activity of TRIM21 is sensitive to the kinetics of Fc binding, and engineering of antibodies with improved TRIM21 binding may be a useful strategy for therapeutic anti-viral antibodies*(89)*.

Designing novel antibody formats for novel methods of action

Huge advances in cloning, expression and purification technologies over the past 40 years allow protein engineers today to have a veritable toolbox of antibody bits and pieces to play with. Novel formats, such as antibody-drug conjugates and bispecific

antibodies, have the potential to change the therapeutic paradigm by rewiring the immune system. For evolving, diverse targets such as infectious pathogens, such non-native approaches may be a critical strategy for curing disease.

Antibody-drug conjugates (ADCs) exploit an antibody's natural specificity to deliver a therapeutic to a desired area. While the conjugated drug is the active molecule for therapeutic benefit, the antibody specificity and affinity will define where the payload is delivered. A crucial design element is a linker between the antibody and payload, which is cleaved under specific conditions to release the active drug*(90)*. Although ADCs are mostly being investigated as a way to target toxic chemotherapy agents to cancerous cells, a similar strategy can be used to target antibiotics to sites of bacterial infection. An antibody-antibiotic conjugate is currently being developed for the treatment of *S. aureus*, which is often a stubborn infection in healthcare settings*(14)*. The antibody moiety targets a cell-wall glycopolymer, tethering the antibiotic to the bacterial surface, which is then released when the bacteria are phagocytosed. In this case the antibody-antibiotic conjugate allows the antibiotic to reach a protected infective reservoir which is not accessible to standard antibiotic approaches*(14)*.

Bispecific antibodies bind two distinct targets, the choice of which will define the mechanism of action. There are over 60 formats of bispecific molecules in development, with applications in cancer, inflammatory, and infectious diseases*(91)*. The simplest application is to use a bispecific as a way to target two distinct antigens with the same molecule, which in some cases can be an alternative to an antibody mixture*(92)*. A more nuanced usage is to leverage bispecificity as a way to increase the selectivity and effective affinity for a challenging target. For example, a bispecific antibody for *P.*

aeruginosa can easily find and bind to the ubiquitous exopolysaccharide Psl, and once anchored is then able to more effectively target the rarer but therapeutically relevant PcrV protein*(93)*. Finally, the original and arguably most powerful application of bispecific antibodies is to simultaneously bind and redirect cytotoxic T cells (CTLs) to infected cells*(94)*. This has been demonstrated in the context of HIV infection using a bispecific antibody fragment which targets HIV envelope protein on the surface of infected cells and CD3 of CTLs*(95)*. The bispecific antibody is capable of inducing an effective immune synapse and allows the cytotoxic T-cell to kill the infected target cell.

ImmTAVs function similarly to T-cell redirecting bispecifics, except that the surface-antigen-specific arm is replaced with a soluble T-cell receptor (TCR)*(96)*. Unlike antibodies, which typically recognize conformational epitopes on extracellular pathogens, TCRs recognize linear peptides that are displayed on HLA molecules. The TCR/peptide-HLA interaction is the natural mechanism by which the immune system recognizes intracellular pathogens, and thus is a particularly interesting complex for infectious disease. An ImmTAV targeting an immunodominant HIV epitope has been shown to mediate killing of infected cells *in vitro(96)*, and may be an interesting approach for other elusive viral infections.

A SURVEY OF ANTI-INFECTIVE ANTIBODIES IN DEVELOPMENT

There are currently 40 therapeutic antibodies or combinations in development for infectious indications (Table 2), with many more in preclinical and discovery phases. Herein we briefly survey particular applications for which antibodies are being developed, which can broadly be grouped as common infections, bioterror threats, nosocomial diseases, highly virulent infections, and broad spectrum approaches.

Table 2. Antibodies for infectious diseases in US clinical trials (April 2017)

Name	Disease	Target	Source/Isotype	Clonality/Format/Fc	Status	Developer
Suptavumab*(97)* (REGN2222)	RSV	Viral glycoprotein- RSV F protein	Human IgG1	Monoclonal	Phase III	Regeneron
ALX-0171*(98)*	RSV	Viral glycoprotein- RSV F protein site II	Camel V_HH	Nanobody	Phase II	Ablynx
MEDI8897*(87)*	RSV	Viral glycoprotein- RSV F protein site Ø	Human IgG1	Monoclonal with extended half-life	Phase II	Medimmune
CSJ148*(99)*	CMV	Viral glycoprotein- gB, pentameric compex	Human IgG1	Mixture (2)	Phase II	Novartis
GC1102*(100)*	HBV	Viral glycoprotein- HBV surface antigen	Human IgG1	Monoclonal	Phase II	Green Cross
Bavituximab*(101)* (PGN401)	HCV	Infected cells- Phosphatidylserine	Chimeric IgG1	Monoclonal	Phase II	Peregrine Pharmaceuticals
XOMA3AB*(102)*	Botulism	Bacterial toxin- *C. botulinum* neurotoxin A	Human/Humanized IgG1	Mixture (3)	Phase I	Nanotherapeutics
514G3*(103)*	*S. aureus* bacteremia	Bacterial surface- *Staphylococcus* protein A	Human IgG3	Monoclonal	Phase II	XBiotech
MEDI4893*(21)*	*S. aureus* pneumonia	Bacterial toxin- *S. aureus* alpha toxin	Human IgG1	Monoclonal with extended half-life	Phase II	Medimmune
AR-301*(104)*	*S. aureus* pneumonia	Bacterial toxin- *S. aureus* alpha toxin	Human IgG1	Monoclonal	Phase II	Aridis
ASN100*(105)*	*S. aureus* pneumonia	Bacterial toxin- *S. aureus* alpha toxin/ leukocidins	Human IgG1	Mixture (2)	Phase II	Arsanis
DSTA4637S*(14)*	*S. aureus* pneumonia	Bacterial surface- *Staph* wall techtoic acid	Human IgG1	Monoclonal ADC	Phase I	Genentech
Aerumab*(38)* (panobacumab)	*P. aeruginosa* pneumonia	Bacterial surface- LPS serotype O11	Human IgM	Monoclonal	Phase II	Aridis Pharmaceuticals
Aerucin*(106)*	*P. aeruginosa* pneumonia	Bacterial exopolysaccharide- alginate	Human IgG1	Monoclonal	Phase II	Aridis Pharmaceuticals
MEDI-3902*(93)*	*P. aeruginosa* pneumonia	Bacterial exopolysaccharide-PslI; secretion system- PcrV	Human IgG1-Fab-ScFv	Bispecific	Phase II	Medimmune
Ibalizumab*(107)*	HIV-1	Host viral receptor- CD4	Humanized IgG4	Monoclonal	Phase III	TaiMed Biologics
PRO 140*(44)*	HIV-1	Host viral receptor- CCR5	Human IgG4	Monoclonal	Phase III	CytoDyn

Table 2. Antibodies for infectious diseases in US clinical trials, continued

UB-421*(108)*	HIV-1	Host viral receptor-CD4	Humanized aglycosylated IgG1	Monoclonal	Phase II	United Biomedical Inc.
VRC01*(109)*	HIV-1	Viral glycoprotein-gp120 CD4bs	Human IgG1	Monoclonal	Phase II	NIAID
VRC01-LS*(110)*	HIV-1	Viral glycoprotein-gp120 CD4bs	Human IgG1	Monoclonal with extended half-life	Phase I	NIAID
3BNC117*(111)*	HIV-1	Viral glycoprotein-gp120 CD4bs	Human IgG1	Monoclonal	Phase II	Rockefeller University
10-1074*(112)*	HIV-1	Viral glycoprotein-gp120 V3	Human IgG1	Monoclonal	Phase I	Rockefeller University
3BNC117 + 10-1074*(66)*	HIV-1	Viral glycoprotein-gp120 CD4bs + V3	Human IgG1	Mixture (2)	Phase I	Rockefeller University
PGT121*(113)*	HIV-1	Viral glycoprotein-gp120 V3	Human IgG1	Monoclonal	Phase I	International AIDS Vaccine Initiative
VRC07-523LS*(114)*	HIV-1	Viral glycoprotein-gp120 CD4bs	Human IgG1	Monoclonal with extended half-life	Phase I	NIAID
MB66*(115)*	HIV-1/HSV-2	Viral glycoproteins-HIV-1 gp120, HSV-2 gD	Unknown	Mixture (2) vaginal film	Phase I	Mapp Biopharmaceutical
MEDI8852*(50)*	Influenza A	Viral glycoprotein-G1/G2 Hemagglutinin stalk	Human IgG1	Monoclonal	Phase II	Medimmune/Humabs Biomed
CR8020*(116)*	Influenza A	Viral glycoprotein-G2 Hemagglutinin stalk	Human IgG1	Monoclonal	Phase II	Crucell Holland
CR6261*(117)*	Influenza A	Viral glycoprotein-G1 Hemagglutinin stalk	Human IgG1	Monoclonal	Phase II	Crucell Holland
MHAA4549A*(39)*	Influenza A	Viral glycoprotein-G1/G2 Hemagglutinin stalk	Human IgG1	Monoclonal	Phase II	Genentech
VIS410*(118)*	Influenza A	Viral glycoprotein-G1/G2 Hemagglutinin stalk	Human IgG1	Monoclonal	Phase II	Visterra Inc.
CT-P27*(119)*	Influenza A	Viral glycoprotein-G1/G2 Hemagglutinin stalk	Unknown	Mixture (2)	Phase II	Celltrion
TCN-032*(120)*	Influenza A	Viral surface protein-M2 ectodomain	Human IgG1	Monoclonal	Phase II	Theraclone Sciences
Zmapp*(121)*	Ebola	Viral glycoprotein-Ebolavirus glycoprotein	Human/Chimeric IgG1	Mixture (3)	Phase II	Mapp Biopharmaceutical
REGN3470 + REGN3471 + REGN3479	Ebola	Unknown	Unknown	Mixture (3)	Phase I	Regeneron

Table 2. Antibodies for infectious diseases in US clinical trials, continued

SYN023	Rabies	Viral glycoprotein	Humanized Unknown	Mixture (2)	Phase II	Synermore Biologics
Shigamabs*(122)* (cαSTX1/cαSTX2)	STEC-HUS	Bacterial toxin- Shiga toxin 1/2	Chimeric IgG1	Mixture (2)	Phase II	Taro Pharmaceuticals
Solaris*(47)* (eculizumab)	STEC-HUS	Host complement protein- C5	Humanized IgG2/4	Monoclonal	Phase III	University Hospital Tolouse/Alexion Pharmaceuticals
Pascolizumab*(123)*	Tuberculosis	Host cytokine- IL-4	Humanized IgG1	Monoclonal	Phase II	National University Hospital, Singapore
Nivolumab*(124)*	Sepsis	Host checkpoint inhibitor- PD-1	Human IgG4	Monoclonal	Phase I	Bristol-Myers Squibb

Prophylaxis of common diseases in high-risk patients

Respiratory Syncytial Virus

RSV is a common cause of lower respiratory tract disease in infants and children, and can cause serious morbidity and mortality in infants with heart or lung disease*(62)*. Treatment options in the case of severe options are limited, typically including oxygen and respiratory assistance. Medimmune's pavilizumab (Synagis) was first approved in 1998 for the prevention of RSV*(6)*, and is currently indicated for use in high-risk pre-term infants *(63)*. There are three other similar RSV antibodies in clinical trials. Regeneron has been quietly developing suptavumab, and Medimmune has a follow-up antibody, MEDI8897, which contains the half-life-extending YTE mutations, which should result in once-per-season dosing*(87)*. Finally, Ablynx is developing the nanobody ALX-0171, which can be nebulized and inhaled.

Human Cytomegalovirus

Human cytomegalovirus is one of the most ubiquitous pathogens worldwide, infecting 50-90% of the population by age 50, yet there is still no vaccine available*(125)* . Primary or reactivated CMV during pregnancy can result in congenital infection of the fetus, causing birth defects including hearing loss and neurological defects. Reactivation or infection in transplant patients can cause serious morbidity due to immunosuppression, and current antivirals have significant toxicity profiles. Novartis is in phase II trials with a mixture of two antibodies targeting the gB protein and gH/gL/UL128/UL130/UL131a pentameric complex*(99)*, with the goal of preventing CMV replication after stem cell transplantation. Genentech's phase II study of a mixture of two monoclonal antibodies to prevent CMV in high-risk kidney transplant patients was moderately successful*(126)*, but

the project seems to have been terminated. Recently, a new antigenic "hot spot" was identified on the gH protein, and may be a target for future antibody therapeutics*(127)*.

Hepatitis B and Hepatitis C

Chronic infection with hepatitis B virus (HBV) or hepatitis C virus (HCV) is a major cause of liver fibrosis, liver cirrhosis, and liver cancer*(22)*. In the case of a liver transplant into HBV or HCV seropositive donors, prophylactic measures are necessary to prevent reactivation of the virus. Green Cross has recently completed phase II trials with GC1102, a human monoclonal antibody directed against an unknown epitope of the hepatitis B surface antigen (HBsAg)*(128)*, for prophylaxis of HBV recurrence in liver transplant recipients.

Pertussis

Despite wide-spread vaccination, whooping cough, or pertussis, infects nearly 4 million people worldwide a year. Systemic symptoms are caused by pertussis toxin (PTx), which is secreted by the pathogen *B. pertussis(27)*. Synthetic Biologics and The University of Texas are developing a humanized antibody which neutralizes the toxin*(27)*. A bispecific format of the two antibodies has also been tested as single-molecule alternative to an antibody mixture *(92)*.

Neutralization of bacterial toxin bioterrorism agents

Anthrax

Spores of *B. anthracis* have been developed and used as a bioweapon, with inhalation of these spores leading to ~50% mortality rates even with treatment. Morbidity

and mortality is caused by three anthrax exotoxins lethal factor (LF) and edema factor (EF), which associate with the receptor-binding protective antigen (PA) to target the cardiovascular system and liver*(129)*. Two anti-PA antibodies, raxibacumab (Abthrax)*(7)* and obiltoxaxumab (Anthim)*(8)*, have been approved for the prophylaxis and treatment of inhalational anthrax. Raxibacumab is a human IgG1 with an affinity of ~3nM*(11)*, while obiltoxaxumab is a chimeric IgG1 with an ~10-fold higher affinity*(12)*. Both antibodies are currently maintained at the US strategic national stockpile in case of a bioweapon emergency.

Botulism

Botulinum neurotoxin A is the most toxic substance known to man, and is classified as a high-risk threat agent for bioterrorism*(35)*. The toxin is secreted by the bacterium C. botulinum, and consists of a binding, translocation, and active domain. A study of several antibodies binding distinct epitopes on the translocation domain exhibited enormous synergy in a mouse challenge model, with a mixture of three antibodies showing a 20,000-fold increase in potency compared to any individual antibody*(35)*.

Other bacterial toxins

Other potential bioweapon agents include ricin, which is a potent inhibitor of protein synthesis*(130)*; and staphylococcal enterotoxin B*(53)*, which is a superantigen that can cause massive cytokine release. Neutralizing antibodies have been identified for each of these targets, and may be prophylactic candidates in the future.

Treatment and prevention of healthcare-associated infections

Clostridium difficile infection

C. difficile is a common intestinal bacterium that can cause symptomatic and severe infection when the normal gut microbiome is disrupted. This is frequently associated with individuals who are on long-term antibiotic regimens. Bezlotoxumab (Zinplava) is a recently-approved monoclonal antibody that neutralizes the enterotoxin TcdB, and helps prevent infection recurrence in high-risk individuals*(9)*.

Staphylococcus Aureus Pneumonia

S. aureus is a common infection that is frequently found at hospitals, along with methicillin-resistant strains. *S. aureus* most often presents as a topical skin infection, but can also cause bacteremia or severe pneumonia in weakened individuals, particularly those on a ventilator. There are several antibodies in clinical trials for the treatment of prevention of *S. aureus* in high-risk individuals. Aridis is developing a monoclonal antibody that neutralizes the alpha-toxin which is a critical component of severe disease*(104)*. Medimmune is developing a similar antibody with half-life extending mutations*(21)*, while Arsanis is developing an antibody mixture that not only neutralizes the alpha toxin but several other toxins as well*(105)*. XBiotech is developing an antibody that targets the bacterial surface for bacteremia*(103)*. Of particular interest, Genentech has developed an antibody-antibiotic conjugate that is particularly suited for eliminating niches of infective bacteria hiding inside other cells*(14)*.

Pseudomonas aeruginosa pneumonia

P. aeruginosa is another common nosocomial pathogen, and is particularly implicated for chronic lung infections in cystic fibrosis patients as well as the formation of biofilms. Aridis is developing two antibodies for the treatment of severe *P. aeruginosa* pneumonia; Aerumab is an IgM targeting a common LPS serotype*(37, 38)*, while Aerucin is an IgG1 targeting alginate*(106)*, a common biofilm component. Medimmune is developing an interesting bispecific antibody, which anchors to the bacteria by binding a ubiquitous surface protein and then binds and inhibits the secretion of virulence factors from a type III secretion system*(93)*.

Potent neutralization of deadly viruses

Human immunodeficiency virus - 1

HIV-1 may be the pathogen most people think of when they hear the word "evolution", and rightly so- HIV-1 still remains incurable, and there is a broad pipeline of recombinant HIV antibodies in the pipeline. The first of these antibodies are antagonists that block the host receptors where HIV binds, and include ibalizumab*(43, 107)*, PRO 140*(44)*, and UB-421*(108)*. The second wave of anti-HIV antibodies are those which neutralize conserved epitopes on the viral glycoprotein gp120. These entities include a native and half-life-extended antibody called VRC01*(109, 131)* and VRC01-LS*(110)*, a similar antibody VRC07-523LS*(114)*, and a more recently described, highly potent antibody 3BNC117*(111)*. Several other antibodies that recognize a different region of gp120 include PGT121*(113)* and 10-1074*(112)*. A mixture of two of the most promising candidates, 3BNC117 and 10-1074, is also under investigation*(66)*. Finally, Mapp Biopharmaceuticals is developing a prophylactic vaginal film containing a mixture of two

neutralizing antibodies, which may be an interesting product for the developing world*(115)*.

Influenza A

Influenza A is another highly mutable pathogen that is difficult to vaccinate against. Severe infections in the elderly, not to mention the possibility of pandemic outbreaks, can cause significant healthcare burdens. There are currently 7 antibody products in development for influenza A, which are typically directed against various conserved epitopes in the hemagglutinin (HA) stalk. These include the antibodies CR6261*(117)* and CR8020*(116)* which are specific for group 1 and group 2 HA respectively, as well as Medimmune's MEDI8852*(50)* and Genentech's MHAA4549A*(39)* which are active against a wide variety of strains. The broadly-neutralizing antibody VIS410 is also in development*(51, 118)*, which is notable because it was computationally designed. Celltrion is testing an antibody mixture, CT-P27*(48)*, while Theraclone is developing TCN-032 which targets a different surface glycoprotein*(120)*.

Ebola

The recent Ebola outbreak in west Africa highlighted the potential of prophylactic antibody therapy, and Mapp Biopharmaceutical was able to some testing of its tripartite antibody mixture, ZMapp*(121, 132)*. This mixture is under further development, as is another antibody mixture from Regeneron.

Rabies

Rabies has a nearly 100% fatality rate in humans, and suspected bites are still treated today with prophylactic anti-toxin. A mixture of anti-rabies antibodies from Crucell Holland*(133)* is no longer in development, but Synermore is currently in phase II trials with a different, unpublished cocktail.

Other emerging viruses

Recombinant antibodies may be useful therapeutic agents for emerging infectious diseases. Neutralizing antibodies have been described for Zika*(134)*, MERS*(135)*, and very recently the Marburg and Ravn filoviruses*(136)*.

Broad spectrum and host-mediated approaches

Unusual cell morphology

While the antibodies described above have been exquisitely tailored for a specific pathogen, there are several broad-spectrum approaches for anti-infective antibodies. For example, phosphatidylserine is a common component of the host cell membrane that typically resides on the inside surface. Interestingly, the plasma membrane of virally infected cells is unusual, and phosphatidylserine can be found on the extracellular surface. Thus, an antibody that recognizes the extracellular phosphatidylserine is potentially a broad-spectrum antiviral antibody, and is currently in clinical trials for HCV*(101)*.

Host immune regulation

Another approach is to use antibodies to mediate the host immune response. For example, the damaging outcomes of shiga toxin-producing *E. coli*-associated hemolytic-uremic syndrome (STEC-HUS) is due to severe inflammation of the GI tract mediated by complement, and the already-approved C5 binding antibody, eculizumab (Soliris)*(47)*, is in clinical trials for this indication. Similarly, an anti-IL-4 antibody, pascolizumab*(123)*, may be able to prevent the severe pathology of tuberculosis by neutralizing inflammatory cytokines*(46)*. Finally, checkpoint-inhibitors like nivolumab, which bind PD-1 and reverse T-cell exhaustion, may be useful for stimulating the immune system*(45, 124)*.

CONCLUSION

There are several niches for which antibodies are particularly suited, such as the passive immunization of immunocompromised individuals, neutralization of bioterror agents, potent killing of antibiotic-resistant bacteria, and broad neutralization of emerging and evasive viruses. The key hurdle- and perhaps rightly so- against developing antibodies for infectious disease is the huge costs associated. In the face of much cheaper to manufacture small molecules, and one-shot vaccines, there must be a real unmet clinical or market need for an antibody therapeutic to be an economically viable option. The ultimate success of these therapeutics hinges on efficacy, and careful consideration of antibody specificity and affinity, Fc functionality, clonality and format is crucial for the development of the next generation of antibody drugs.

Chapter 2: A cocktail of humanized anti-pertussis toxin antibodies limits disease in murine and baboon models of whooping cough[1]

ABSTRACT

In spite of wide-spread vaccination, pertussis rates are rising in industrialized countries and remain high world-wide. With no specific therapeutics to treat disease, pertussis continues to cause considerable infant morbidity and mortality. The pertussis toxin is a major contributor to disease, responsible for local and systemic effects including leukocytosis and immunosuppression. Here, we humanized two murine monoclonal antibodies that neutralize pertussis toxin and expressed them as human IgG1 molecules with no loss of affinity or *in vitro* neutralization activity. When administered prophylactically to mice as a binary cocktail, antibody treatment completely mitigated the *B. pertussis*-induced rise in white blood cell count and decreased bacterial colonization. When administered therapeutically to baboons, antibody-treated but not control animals experienced a blunted rise in white blood cell count and accelerated bacterial clearance rates. These preliminary findings support further investigation into the use of these antibodies to treat human neonatal pertussis in conjunction with antibiotics and supportive care.

---

[1] This chapter has been published in final edited form as:
Nguyen AW*, Wagner EK*, Laber JR, Goodfield LL, Smallridge WE, Harvill ET, Papin JF, Wolf RF, Padlan EA, Bristol A, Kaleko M, Maynard JA. A cocktail of humanized anti – pertussis toxin antibodies limits disease in murine and baboon models of whooping cough. Sci. Transl. Med. 7, 1–9 (2015).

E. K. W. planned, performed, and analyzed antibody humanization, antibody characterization, and baboon antibody detection experiments, and designed the humanized antibody sequences.

INTRODUCTION

Despite wide-spread vaccination, pertussis remains a considerable public health concern. In recent decades, infection rates have risen dramatically in industrialized countries reaching a 60-year US high in 2012. This rise appears to be due to a variety of factors including increased surveillance, strain drift, waning immunity after acellular vaccination, and a vaccine-induced Th1/Th2 response instead of the more effective Th1 response induced by whole cell vaccines and infection*(137)*. Worldwide, pertussis remains a major cause of infant death, claiming ~195,000 lives annually*(138)*. Pertussis is of greatest concern for unimmunized infants, as they experience the most severe symptoms, including pneumonia and pulmonary hypertension due to severe leukocytosis*(139)*. In the absence of alternatives, aggressive interventions including leukodepletion and exchange transfusion have been proposed to remove white blood cells*(140)*.

It is generally accepted that, in the long-term, an improved vaccine formulation better able to prevent disease transmission will be required*(137, 141, 142)*. In the meantime, there remains a need for pertussis-specific therapeutics to treat infants with severe disease as antibiotics are only effective in the early stages, typically before diagnosis. Even after bacteria can no longer be cultured, symptoms persist for many weeks, presumably due to residual toxins.

While *B. pertussis* produces a wide array of toxins and adhesins, several lines of evidence point to the pertussis toxin (PTx) as a critical virulence factor. This AB5 toxin is essential for full bacterial pathogenicity*(143)*, exhibiting local and systemic effects through its enzymatically active A subunit and its receptor binding B subunit. The overall

effects of PTx are inhibition of the innate immune response and induction of leukocytosis. Specifically, in mouse models of pertussis infection, the presence of PTx decreases pro-inflammatory chemokine and cytokine production*(144)*, reduces neutrophil recruitment to the lungs, and increases bacterial burden*(145)*. While these effects have not all been demonstrated in human disease, PTx does appear important in primates as well. *In vitro*, PTx has been shown to have an inhibitory effect on human dendritic cell migration that is predicted to slow their recruitment to secondary lymph nodes and subsequent activation of T-cells*(146)*. In human infants, PTx production positively correlates with the extreme lymphocytosis that can lead to pulmonary hypertension*(147)*. Finally, whereas most acellular vaccines are comprised of PTx in combination with other antigens, Denmark relies on a monocomponent PTx vaccine and reports no increase in symptomatic infection*(148)*.

Accordingly, high anti-PTx antibody levels are considered to correlate with protection*(142, 149)*, and passive immunization with anti-PTx serum has been recognized as a potential therapeutic modality for neonatal pertussis. In the past two decades, two human polyclonal anti-PTx immunoglobulin preparations were tested and showed promise for treating pertussis in newborns*(150–152)*. However, treatment with polyclonal antisera can be problematic due to low and variable neutralizing capacities as well as an unreliable supply. For passive immunization, monoclonal antibodies provide a considerable advantage as they can be selected for high affinity and potent neutralizing abilities. For these reasons, the high titer intravenous immunoglobulin product to treat RSV was replaced with a single neutralizing antibody in 1996.

To treat pertussis, we propose a combination of two anti-PTx monoclonal antibodies selected to achieve high potency and to limit the possibility of allelic variants that could escape neutralization. Among the numerous anti-PTx monoclonal antibodies that have been evaluated over the past three decades, the murine antibodies 1B7 and 11E6 stand out as uniquely protective in mouse models of pertussis infection*(153, 154)*. However, murine antibodies are no longer considered suitable for use in humans due to their immunogenicity. Here we cloned and humanized the murine 1B7 and 11E6 antibodies, produced them as human IgG1 antibodies in CHO cells, and extensively characterized them *in vitro*. The humanized antibodies were assessed in a murine challenge model using a recent human *B. pertussis* isolate and compared to the high-titer intravenous immunoglobulin preparation (P-IVIG) used in recent human clinical trials*(151)*. Finally, the antibodies were tested in a newly described baboon model considered highly relevant for the development of pertussis therapeutics*(155)*. Collectively, the data support further animal modeling to assess the potential for passive immunotherapies to mitigate human neonatal pertussis.

MATERIALS AND METHODS

Study design

The objective of this study was to assess the protection conferred by two humanized anti-pertussis toxin antibodies in animal models of pertussis. In both the mouse and baboon model, strain D420, a recent clinical isolate of *B. pertussis*, was used to infect the animals.

An established murine model used to develop the current vaccine was employed to evaluate the prophylactic protection conferred by these antibodies*(153)*. BALB/c and C57BL/6 mice were used for the pharmacokinetic analysis and pertussis challenge, respectively. Based on pilot studies, groups of 6 mice were expected to detect antibodies with 75% of expected activity with 80% confidence in a one-tailed test with p=0.05 (Appendix A Fig. 23). Mouse studies were terminated at day 10, based on pilot studies showing large differences in outcome at this time.

A weanling baboon model was recently developed that may be more representative of human disease progression as evidenced by colonization of the trachea, WBC rise and paroxysmal coughing*(155)*. This model was used to assess protection conferred by these antibodies when administered therapeutically on day 3 after infection, with four control animals and four treated animals. One control baboon became moribund, and data was not available after day 10 for that animal. Baboons were randomly assigned to groups and animal caretakers and laboratory technicians were blinded. The baboon study was terminated after ~21 days, or when WBC and bacterial colonization levels began to approach pre-infection levels.

Antibody variable region cloning and humanization

The murine 1B7 and 11E6 variable region genes*(153)* were amplified from hybridoma cells by RT-PCR using degenerate primers and cloned into pAK100 as described*(156)*. Positive clones were identified by monoclonal phage ELISA using a PTx coated plate (1 μg/ml in PBS; List Labs), followed by sequencing. Humanized variants were designed in silico via five different methods: (a) 'veneering' (ven); (b) 'grafting of abbreviated complementarity determining regions (CDRs)' (abb); (c) 'specificity determining residue-transfer' (sdr); and (d) grafting of intact CDRs onto the hu4D5 framework or (e) a composite framework (fra)*(157, 158)*. The resulting designed variable region genes were synthesized with human IgG1/ kappa constant domains by DNA 2.0 in pJ602 or pJ607 vectors. For chimeric constructs, murine variable regions were similarly cloned with human constant regions*(156)*.

Protein expression & purification

For small-scale expression, plasmid DNA was transiently transfected into CHO-K1 cells (ATCC) and purified using protein A affinity chromatography as described*(156)*. Large scale preps were prepared by Catalent (Somerset, NJ) from polyclonal CHO cell lines, followed by protein A and anion chromatographic steps and buffer exchange into PBS. P-IVIG was obtained from the Massachusetts Public Health Biologic Laboratory (Lot IVPIG-2). P-IVIG was prepared as a 4% IgG solution from the pooled plasma from donors immunized with tetra-nitromethane inactivated pertussis toxoid vaccine*(152)*.

ELISA and binding assays

For indirect PTx ELISAs, a high-binding 96-well ELISA plate (Costar) was coated with 1 μg/ml PTx. The plate was blocked with milk for 1 hr, followed by incubation with duplicate anti-PTx antibody dilutions from 50 μg/ml for 1 hr at 25 °C. After washing and detection with 50 μl of 1 μg/ml goat anti-mouse-Fc-HRP (murine antibodies, Thermo Fisher), goat-anti-human Fc-HRP (chimeric and human antibodies, Thermo Fisher) or goat-anti-monkey IgG (H/L)-HRP (baboon serum; Bio-Rad), signal was developed with TMB Substrate (Thermo Fisher Scientific), quenched with 1M HCl and the absorbance at 450 nM recorded. To monitor antibody concentrations in cell culture supernatant, an Fc capture ELISA was employed, using the protocol above with the following modifications: a 5 μg/ml goat-anti-human Fc (Thermo Scientific) coat and 2 μg/ml goat-anti-human kappa-HRP (SouthernBiotech) secondary antibody. For Fha ELISAs with baboon sera, a 1 μg/ml Fha (List) coat and 1:10,000 dilution of goat-anti-monkey IgG (H/L)-HRP (Bio-Rad) secondary antibody was used. Data were scaled to the maximum response observed for positive control serum collected from an animal 3 weeks post-infection.

PTx binding affinity was determined by both competition ELISA and surface plasmon resonance (SPR). For competition ELISA, an ELISA plate was coated with PTx and blocked as described above. While the plate was blocking, 3.25 nM of each antibody in PBS-T-milk was incubated with different concentrations of PTx (200 nM to 0.1 nM). The ELISA plate was washed and 50 μl of the antibody/PTx mixtures added. The plate was incubated for 15 min at 25 °C. The plate was then washed, secondary antibody added and ELISA developed as above. The resulting curves were fit to equilibrium binding equations*(159)* corrected for bivalent binding.

Surface plasmon resonance analysis was performed using a BIAcore 3000 (GE Healthcare, Uppsala, Sweden; 1B7 variants) or Reichert SR7500DC (AMETEK, Berwyn, PA, USA; 11E6 variants) instrument with dextran chips. Antibodies were immobilized using standard EDC/ NHS chemistry to a level of 500-1000 response units as described*(157)*. PTx was injected in duplicate at 30 µL/min or 100 µL/min (m1B7, ch1B7), with concentrations between 5-200nM diluted in running buffer (PBS or HBS, pH 7.4, 0.05% Tween). The surface was regenerated with a combination of 4M magnesium chloride and 10mM glycine, optimized independently for each antibody. Baseline correction was performed by subtracting simultaneous runs over an in-line control flow cell. The on- and off-rates were calculated using BIAevaluation software (Pharmacia Biosensor) or TraceDrawer (Reichert). Reported values are the average and standard deviation of all on- and off- rates calculated for each protein.

In vitro neutralization

Inhibition of CHO cell clustering was used to determine *in vitro* neutralization of antibody preparations as described*(157)*. Briefly, antibody was serially diluted across a 96-well tissue plate from 50 nM to 1.5 pM in the presence of 5 pM PTx. Antibody and PTx were incubated for 30 minutes at 37 °C after which $2x10^4$ freshly trypsinized CHO cells were added per well. After incubation at 37 °C for 20 hours, the degree of clustering was scored as 0 (no clustering), 1 (equivocal), 2 (positive clustering), or 3 (maximal clustering). Experiments were performed in triplicate and scored independently by two researchers. Neutralizing dose is expressed as the molar ratio of antibody:PTx resulting in a score of 2.

Bacterial strain and growth

B. pertussis strain D420 was isolated from a critically ill infant in Texas in 2002*(160)*. Bacteria were maintained on Regan-Lowe Agar (Becton Dickinson) supplemented with 10% sheep's blood (Hemostat) with 20 µg/mL cephalexin. Liquid cultures were grown overnight in Stainer-Schölte broth with heptakis at 37 °C to mid-log phase.

Ethics Statement

All animal procedures were performed in a facility accredited by the Association for Assessment and Accreditation of Laboratory Animal Care International in accordance with protocols approved by UT Austin (#2012-00084, #13080701), PSU (#40029) and the University of Oklahoma Health Sciences Center (#14-072-I) Animal Care and Use Committee and the principles outlined in the Guide for the Care and Use of Laboratory Animals.

Murine pharmacokinetic assay

An in vivo pharmacokinetic study was completed using groups of six ~12 weeks old female BALB/c mice as described previously*(161)*. Chimeric 11E6, humanized 11E6, humanized 1B7, or a 1:1 mixture of the humanized 1B7 and 11E6 antibodies at the same total antibody concentration were diluted to 250 µg/ml in PBS and 200 µl injected subcutaneously. Blood samples were collected via the tail vein at seven time points between 0 to 336 hours. Antibody concentration in sera was measured by PTx ELISA. After the final time point, mice were euthanized via CO2 inhalation and cervical dislocation. To estimate the beta half-life, the data was fit to a single exponential decay model: $C(t) = bexp(-\beta t)$.

In vivo mouse challenge

Groups of six randomly assigned weanling C57BL/6 mice were each injected intraperitoneally with a single antibody (20 µg), P-IVIG (20 µg), or the antibody combination (10 µg hu1B7+10 µg hu11E6), or PBS two hours before sedation with 5% isofluorane in oxygen and inoculation with $5x10^6$ CFU *B. pertussis* strain D420 in PBS by pipetting 50 µL on the external nares. Investigators were not blinded. The % weight change was calculated by the following formula: ((day 10 weight – day 0 weight/day 0 weight)*100) for each individual mouse. On day 10 mice were euthanized by CO2 inhalation and the respiratory tract was excised for enumeration by serial plating on Regan Lowe agar supplemented with 10% sheep's blood (Hemostat Resources) containing 40 ug/mL cephalexin. Colonies were counted after 5 days at 37oC.

To assess the number of CD45+ white blood cells, blood was collected by orbital bleed (day 10) in a microtainer containing EDTA (Becton, Dickinson, and Company), and 50 µL blood were lysed in 4 mL red blood cell lysis solution (Alfa Aesar) for 6 minutes. Cells were incubated with anti-CD45 APC, washed, and resuspended in 2% paraformaldehyde before acquisition on the LSR Fortessa flow Cytometer (Becton, Dickinson, and Company). List mode data was then analyzed on FlowJo 7.6.1 (Treestar), with data reported as total WBC per 40 ul blood.

Baboon challenge study

Baboon studies were performed at the Oklahoma Baboon Research Resource at the University of Oklahoma Health Sciences Center as described previously*(155)*. Weanling baboons were selected to be 6-9 months old at the time of challenge. Groups consisted of four animals based on published vaccination studies*(155)*. The inoculum for

each direct challenge was between 109–1010 cfu as determined by optical density and confirmed by serial dilution and plating. The bacterial inoculum (1 ml) was delivered on day 0 via intranasal and intratracheal infusion. On day 3 after infection, animals were sedated and humanized anti-pertussis toxin antibodies administered intravenously (20 mg/kg each). Post challenge, baboons were anesthetized and evaluated twice weekly for enumeration of circulating WBC, serum antibody levels, and nasopharyngeal bacterial load. Nasopharyngeal washes were diluted and plated on Regan–Lowe plates to quantify bacterial cell counts. Video recordings of each cage allowed quantification of cough rates. Sera were assessed for antibody titers to Bordetella antigens Fha and PTx by ELISA. At the end of the study, baboons were euthanized with an intravenous injection of euthanasia solution and necropsy was performed. Tissues were embedded and stained with H&E and evaluated by a veterinary pathologist.

Statistical Analysis

Mean ± error values were determined for all appropriate data. For the murine challenge experiment, one-way ANOVA with Tukey's simultaneous test with significance ($p < 0.05$) was used to determine statistical significance between groups. Error bars reported in mouse, baboon, and CHO cell assay experiments represent the standard error. All other error reported is the standard deviation.

RESULTS

Cloning and humanization of murine 1B7 and 11E6 antibodies

As the first step in humanization, the murine 1B7 (m1B7) and 11E6 (m11E6) antibody heavy and light chain variable region genes were cloned via RT-PCR from hybridoma cells using a degenerate primer set and PTx-reactive genes were identified. Next, 3-5 humanized variants of each variable region were generated in silico and the murine and humanized genes cloned into eukaryotic expression vectors encoding human IgG1 heavy or κ light chain constant domains. All pairwise heavy-light chain combinations were expressed by transiently transfected CHO cells and the supernatant used to monitor specific PTx binding activity (Appendix A Fig. 19). Combinations yielding the highest specific activity were further analyzed after medium-scale expression and protein A purification. From these data, a single lead candidate was selected for each antibody which exhibited similar ELISA profiles as the murine parents and high expression (~5-10 pg/ cell/ day). Sequences of these variants are notably more human, as monitored by z-score (Appendix A Table 5)*(162)*.

Hu1B7 and hu11E6 antibodies are biochemically and biophysically similar to their murine predecessors

After transient CHO cell expression and purification, the murine (m), chimeric (ch) and humanized (hu) antibodies were pure (~95%) and migrated at the expected sizes in SDS-PAGE gels (Fig. 3A). Increased thermal stability was observed, indicating that both the human constant and humanized variable regions are stabilized relative to the murine versions (Table 1, Appendix A Fig. 20).

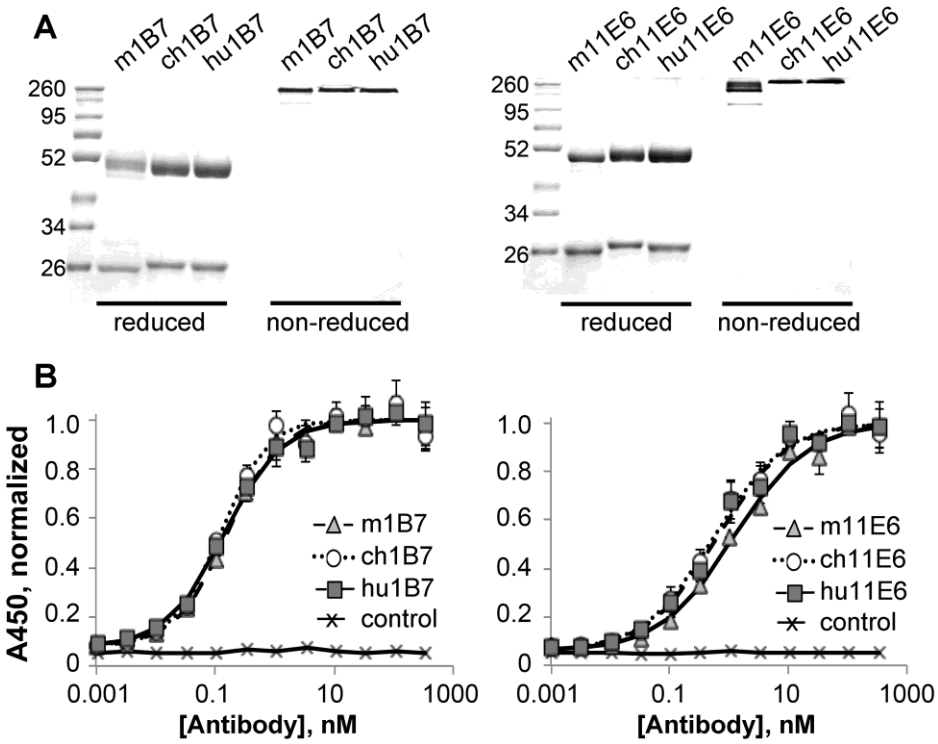

Figure 3. Humanized, chimeric and murine antibodies have similar binding affinities to PTx.

A, SDS-PAGE comparing purified murine, chimeric and humanized variants of 1B7 and 11E6 in reduced and non-reduced forms as indicated. Molecular weights standards (kDa) are shown in lane 1. B, Indirect ELISA comparing the binding of all three versions of each antibody to PTx: murine (▲), chimeric (O) and humanized (□) and isotype control (×) antibodies shown. The absorbance data was normalized such that the maximum signal is 1.0; each sample was run in duplicate and each assay performed at least three times with different protein preparations.

Binding to PTx was initially assessed by ELISA (Fig. 3B) and competition ELISA (Appendix A, Fig. 21). The murine and chimeric versions of each antibody, presenting identical variable region amino acid sequences but appended with murine and human constant domains respectively, exhibited very similar binding affinities as measured by competition ELISA (Table 1). We next collected kinetic binding data using

surface plasmon resonance with immobilized antibody. The SPR-measured association and dissociation rates were similar for the murine, chimeric and humanized variants, yielding affinities within error for all three 1B7 variants (Kd ~0.7±0.5 nM) and all three 11E6 variants (Kd ~2.3 ± 0.7 nM; Table 1, Appendix A Fig. 22).

Table 3. Biochemical characterization of 1B7 and 11E6 antibodies

	Melting temp (°C), second transition	Kd, competition ELISA (nM); (# exp)	Kd, SPR; nM (χ2)	on-rate × 105, SPR (sec-1 M-1)	off-rate × 10-4, SPR (sec-1)
m1B7	74.8 ± 0.7	0.4 ± 0.2 (5)	0.7 ± 0.2 (0.32)	1.7 ± 0.3	1.2 ± 0.3
ch1B7	78.1 ± 0.5	0.5 ± 0.3 (3)	0.5 ± 0.4 (0.74)	1.5 ± 0.1	0.8 ± 0.5
hu1B7	79.0 ± 0.3	1.2 ± 0.7 (6)	0.7 ± 0.5 (0.75)	0.9 ± 0.2	0.7 ± 0.5
m11E6	67.3 ± 0.4	5 ± 1 (3)	2.4 ± 0.9 (2.20)	1.3 ± 0.7	3 ± 3
ch11E6	69.4 ± 0.4	5 ± 2 (4)	nd*	nd*	nd*
hu11E6	74.4 ± 0.4	7 ± 3 (5)	2.3 ± 0.7 (1.25)	0.8 ± 0.4	1.7 ± 0.7

* nd, not determined

The binary combination of hu1B7 and hu11E6 is synergistic

Not only do hu1B7 and hu11E6 bind PTx tightly, but as monoclonal antibodies, they exhibit ~100-fold and 10-fold higher PTx-specific binding titers, respectively, than the P-IVIG used previously to treat human infants*(151)* (Fig. 4A). Furthermore, PTx is able to simultaneously bind hu1B7 and m11E6, suggesting their effects may be synergistic (Fig. 4B). Indeed, while either antibody alone protects CHO cells against PTx-mediated morphological changes at ~70:1 (hu1B7) and ~40:1 (hu11E6) molar ratios, an equimolar binary combination exhibits enhanced protection (~20:1; Fig. 5A) which is

more neutralizing than an equivalent P-IVIG dose (~120:1; Fig. 5B)*(153)*. Accordingly, a 1:1 molar ratio of hu1B7 and hu11E6 was selected for subsequent animal protection studies.

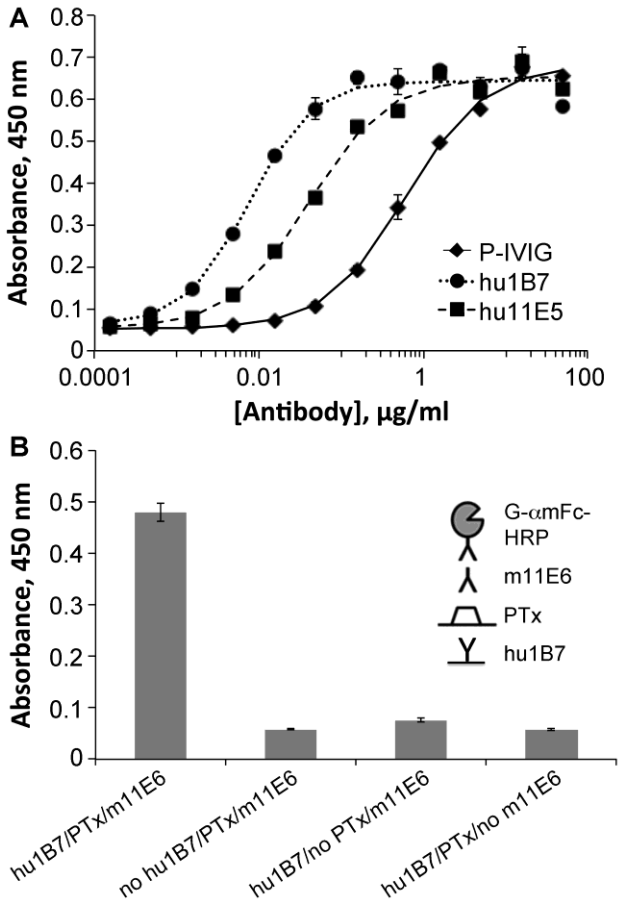

Figure 4. The hu1B7 and hu11E6 antibodies have higher anti-PTx titers than P-IVIG and can simultaneously bind PTx.

A, Humanized 1B7 and 11E6 antibodies and high-titer P-IVIG were assessed for PTx binding by ELISA. An ELISA plate was coated with PTx, blocked, incubated with the indicated concentrations of P-IVIG (◆), hu1B7 (●), or hu11E6 (■). B, Sandwich ELISA to assess simultaneous binding of 1B7 and 11E6. Each sample was run in duplicate and each assay repeated at least three times.

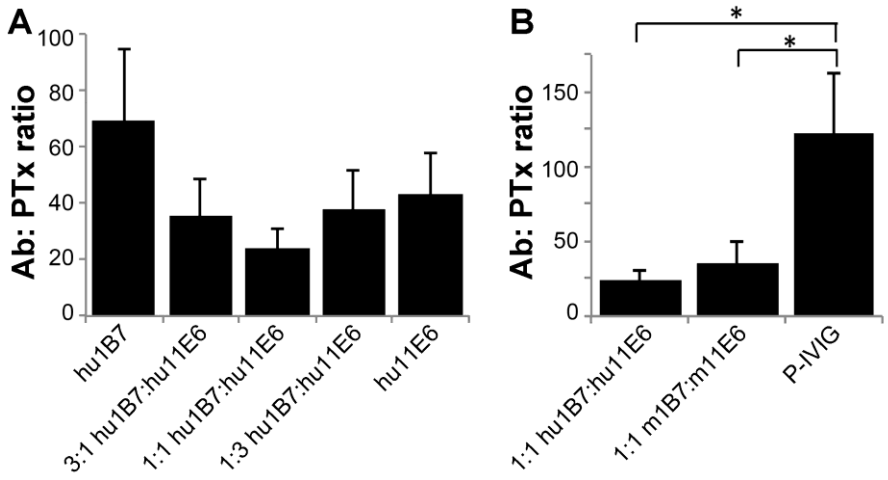

Figure 5. The binary combination of hu1B7 and hu11E6 is synergistic and more potent than P-IVIG *in vitro*.

The CHO cell clustering assay was used to determine the molar ratio of antibodies to PTx required for complete neutralization of CHO morphology changes. A, Different ratios of hu1B7 and hu11E6 were compared to determine the most potent ratio. B, An equimolar ratio of humanized 1B7 and 11E6 was compared to the same ratio of murine antibodies and P-IVIG. Results depict average of three replicate experiments; statistical significance determined by single-factor ANOVA and Tukey's test with α=0.05.

Hu1B7 and hu11E6 protect mice prophylactically from *B. pertussis* infection

While not a natural host for *B. pertussis*, mouse models share some characteristics of human disease and were used to develop all vaccines to date. In particular, the rate of bacterial clearance in immunized mice after aerosol challenge correlates with vaccine efficacy in children*(163)*. Previously, the Sato group performed murine protection studies with m1B7 and m11E6 using intracerebral and inhalation models with *B. pertussis* strain 18-323*(153, 154)*. Since this study was preparatory for non-human primate studies, we replaced strain 18-323, which infects mice efficiently but is a hyper-virulent strain of atypical *B. pertussis* lineage, with strain D420, a recent human clinical isolate used to develop the baboon model and which expresses the dominant alleles of major virulence

factors*(160)*. Pilot studies determined that prophylaxis with 5 μg m1B7 antibody followed by infection with $5x10^6$ cfu D420 resulted in statistically significant differences in WBC, bacterial colonization and weight gain over a 10-day period with groups of six animals (Appendix A Fig. 23).

Recognizing that antibodies with human constant domains will be cleared from the blood more rapidly than murine antibodies, we assessed the murine in vivo clearance rates of the humanized antibodies for comparison to previously measured m1B7 rates. Mice were administered chimeric or humanized antibodies or a binary cocktail of humanized antibodies (2 mg/kg subcutaneously), and sera were collected over 14 days with anti-PTx concentrations measured by ELISA. The beta elimination half-lives of ~100 hrs for humanized and chimeric antibodies with human constant domains were similar, and, as expected, shorter than that for m1B7 (~210 hrs)*(161)*. We used these data to estimate that a 20 μg dose of humanized antibodies would result in similar serum concentrations on day 10 as the 5 μg m1B7 dose used in pilot studies.

Accordingly, weanling mice were administered 20 μg each of a single humanized or chimeric antibody, P-IVIG, the binary humanized antibody mixture or a PBS control (n=6 per group) before inoculation with $5x10^6$ cfu *B. pertussis* strain D420. At ten days post-inoculation, untreated mice exhibited ~five-fold increase in WBC relative to naïve mice (Fig. 6A; Appendix A Table S3), lost weight (Fig. 6B) and were heavily colonized by *B. pertussis* (Fig. 6C). In contrast, all mice receiving monoclonal antibodies exhibited significantly decreased WBC levels as compared to PBS-treated mice ($p<0.001$; Fig. 6A). Animals receiving the 1B7 antibody resembled uninfected mice more closely than those receiving only 11E6 or P-IVIG for all outcomes. This was most pronounced in terms of

weight gain, as mice receiving ch1B7, hu1B7 or the antibody mixture gained significantly more weight than PBS-treated animals ($p<0.05$; Fig. 6B). Mice treated with the antibody cocktail were indistinguishable from naïve animals in terms of WBC and weight gain and had significantly lower WBC than P-IVIG-treated mice ($p<0.05$, Fig. 6A). Finally, mice treated with the binary antibody cocktail had a ~10-fold reduced bacterial colonization levels as compared to untreated mice ($p<0.01$, Fig. 6C), similar to the reduced colonization observed for PTx-deletion strains*(164)*. P-IVIG was previously tested in human clinical trials*(151, 152)* with promising initial outcomes; if the correlation between performance in the mouse model holds for human outcomes, this humanized antibody combination could be more protective than P-IVIG.

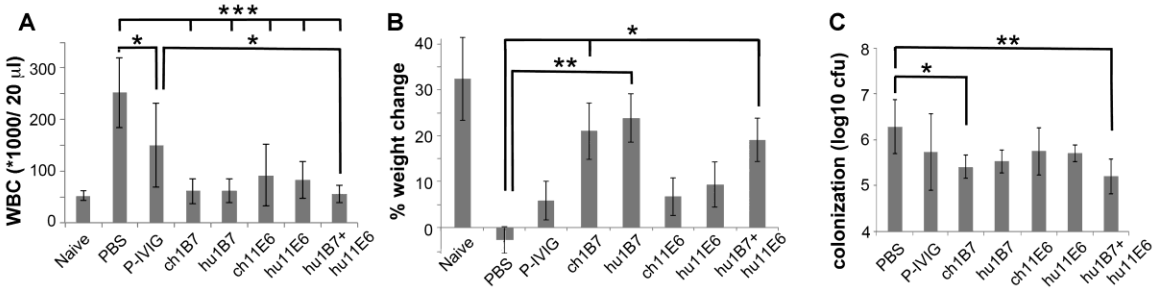

Figure 6. Prophylactic treatment with humanized antibodies protects mice against pertussis.

Mice (n=6) were each administered 20 µg antibody intraperitoneally two hours before infection with $5x10^6$ cfu *B. pertussis* D420 bacteria. The infection severity was assessed on day 10 by A, CD45+ leukocyte count (WBC), B, weight gain and C, bacterial colonization of the lungs. No bacteria were recovered from uninfected animals. Means ± standard error are shown; significance * $p<0.05$, ** $p<0.01$ and *** $p< 0.001$ versus PBS-treatment is indicated, using Tukey's simultaneous test. Additionally, only P-IVIG-treated mice had WBC distinguishable from uninfected naïve mice ($p<0.01$) and mice treated with hu1B7, ch1B7 or the antibody cocktail had lower WBC than P-IVIG-treatment for equivalent doses ($p<0.05$). Only mice treated with P-IVIG and ch11E6 exhibited reduced weight gain relative to uninfected mice ($p<0.05$).

Hu1B7 and hu11E6 protect baboons therapeutically from infection by *B. pertussis*

Finally, we used a recently developed nonhuman primate model to assess the feasibility of our antibody cocktail to treat established disease. In this model, bacteria are administered intranasally and intratracheally to weanling baboons, who then exhibit symptoms of classical pertussis including colonization of the trachea, increased WBC counts, and a characteristic cough. No other clinical changes have been associated with disease*(155)*. *B. pertussis* strain D420 was administered to eight weanling animals on Day 0. Three days later, when the WBC had begun to rise (>14,000/μl; Appendix A Table 6), the humanized antibody cocktail (20 mg/kg each antibody) was administered intravenously to four of the animals. All eight animals were then monitored for WBC, cough and bacterial colonization (Appendix A Table S4).

Disease in the untreated animals (n=4) was typical of the model*(155)*: the WBC rose into the 40,000/μl range by day 5 before beginning to decline, approaching baseline after 23 days (Fig. 7A). These animals were heavily colonized by *B. pertussis* (107-108 cfu recovered by nasopharyngeal wash on days 3-17) and remained elevated for the duration of the study (Fig. 7B). One control animal (C1) became moribund after exhibiting an extremely high WBC. In contrast to the controls, all four animals receiving antibody treatment exhibited a blunted rise in WBC and accelerated removal of bacteria from the nasopharynx (Fig. 7C). At the time of treatment, two of the treated animals had achieved high levels of nasopharyngeal colonization (10^7-$5x10^8$ cfu; denoted H1 and H2), while the other two treated animals experienced moderate levels of nasal carriage (~104 cfu; denoted M1 and M2). These animals exhibited a sharp decrease in WBC coincident with antibody treatment. The measured antibody beta-phase elimination half-life in the treated baboons was 10±4 days, thus the hu1B7 and hu11E6 levels remained high for the

duration of the study (Appendix A Fig. 24). ELISA detection of PTx-reactive antibodies in nasopharyngeal washes indicated that the administered antibodies were present in the mucosa of treated but not control animals (Appendix A Fig. 25).

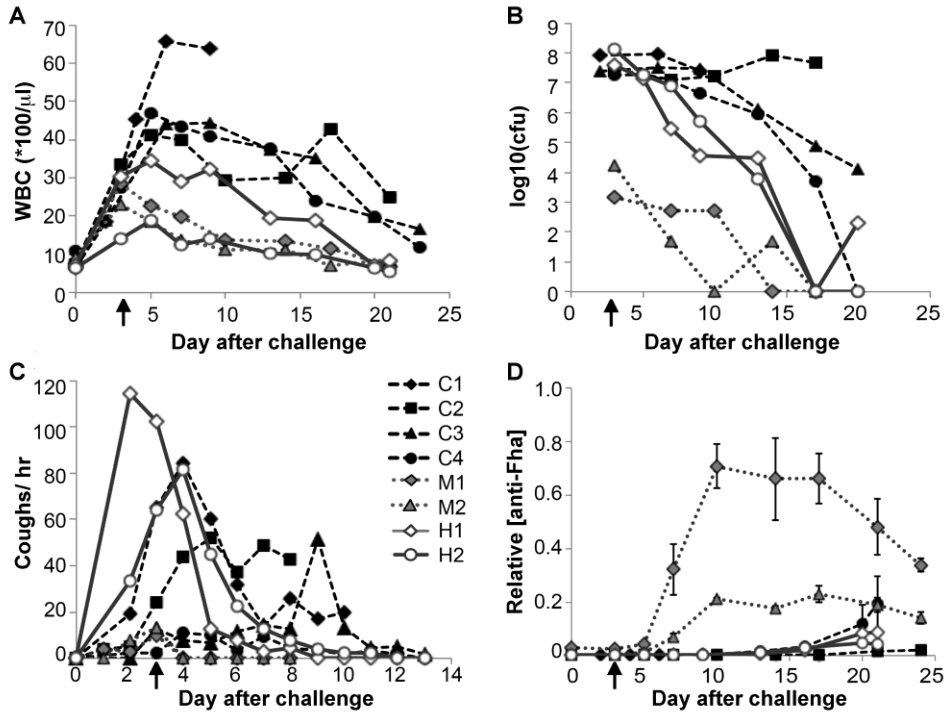

Figure 7. Therapeutic treatment with antibody cocktail reduces leukocytosis and accelerates bacterial clearance in baboons.

Weanling baboons were inoculated with 109-1010 *B. pertussis* D420 bacteria on Day 0. On day 3 after infection (indicated by arrow), animals in the treatment group (n=4) were administered hu1B7 and hu11E6 antibodies intravenously, while control animals (n=4) were given nothing. All animals were subsequently monitored for A, WBC count, B, bacteria recovered by nasopharyngeal wash and C, coughing on the days indicated. Groups shown include controls (solid black icons, dashed line, C1-C4), treated animals who were mildly colonized (grey icons, dotted black line, M1 and M2), and treated animals which were heavily colonized (hollow icons, solid grey line, H1 and H2). D, Serum anti-Fha titers for individual animals are shown to assess endogenous immune responses. Titers were normalized to the maximum response observed for serum from a historical control baboon, collected three weeks after experimental infection. Serum was not available for animal C3.

In this study, the baboon model exhibited variability in cough severity and clinical progression, as is seen in human pertussis*(165)*. All the animals coughed, but this did not strongly correlate with WBC or bacterial colonization levels. Three of the four controls exhibited substantial coughing (>10 per hour) through day 9, while the two heavily colonized, treated animals experienced heavy bouts of coughing (60+ per hour on day 3) which diminished rapidly after antibody treatment (Fig. 7C; Appendix A Table 6). All treated animals exhibited reduced cough rates by day 5, which were reduced to <5 per hour by day 9. No other clinical observations (body temperature, weight, activity level; Appendix A Table S4) were found to correlate with disease and potential variables such as insulin, histamine sensitization and blood chemistry have not been evaluated in this model. Notably, PTx does not appear to be responsible for coughing as B. parapertussis does not express PTx, yet causes a similar cough in humans*(165)*. Thus, we would not expect PTx neutralization to affect the cough except indirectly by protecting the innate immune system and the resulting enhanced bacterial clearance.

Histological examination of moribund control animal C1 noted a normal trachea with dense bronchopneumonia and large abcesses, similar to that seen in post-mortem analyses of infants that died of pertussis*(139)*. *B. pertussis* was recovered from the trachea and right lung of this animal. Histopathology from recovering control and treated animals showed evidence of abcesses and small consolidations. Thus, the damage that occurred to the lung tissue during the first 72 hours of infection may not have had time to repair, consistent with the long-term sequelae following severe pertussis. Histopathological analyses of treated, mildly colonized animals had some abnormalities (fibroses and consolidations) but were overall much healthier (Appendix A Fig. 26).

We were interested in why two treated animals were less efficiently colonized. To explore this, we evaluated baseline serum antibody levels recognizing another major Bordetella antigen, filamentous hemagglutinin (Fha) by ELISA (Fig. 7D). Animals with clear pertussis symptoms had no baseline serum Fha titer but exhibited detectable levels by day 20, consistent with a primary immune response*(155)*. Interestingly, the two co-housed animals with low levels of nasal carriage also had relatively high initial anti-Fha titers, which exhibited rapid increases starting on day 6, as expected for a secondary immune response*(155)*. From one of these animals, B. bronchiseptica was recovered in the nasal wash (<100 cfu) in addition to *B. pertussis*. Therefore, we hypothesize that baboons are subject to B. bronchiseptica infection and that concurrent exposure partially protected these two animals, as does prior *B. pertussis* infection*(141)*.

DISCUSSION

Before widespread vaccination, a number of blood products and polyclonal immunoglobulins were used to treat human pertussis, some with positive, albeit poorly controlled, results*(166)*. More recent preparations were developed on the presumption that PTx is responsible for the severe symptoms of disease and therefore preparations enriched in anti-PTx antibodies would mitigate the symptoms. However, this clinical strategy is limited by the expectation that only a fraction of PTx-specific antibodies in a polyclonal preparation would be neutralizing. In contrast, the monoclonal antibodies utilized in this study were selected specifically for their capacity to neutralize PTx, individually and synergistically. The initial feasibility data using murine and baboon models reported here support the concept of passive immunotherapy to neutralize PTx's pathological effects.

Previously, two polyclonal anti-PTx preparations elicited by immunization with inactivated PTx were assessed in controlled trials. One showed a significant, ~3-fold decrease in the number and duration of whoops versus placebo-treated children, an effect which was most pronounced when treatment was initiated within the first seven days*(150)*. A subsequent P-IVIG preparation used for Phase 1/2 trials in infants showed declines in lymphocytosis and paroxysmal coughing by the third day after treatment*(151)*. Unfortunately, Phase 3 trials did not support this initial promise, as the product expired before study enrollment was completed*(152)*. Given the dosage and blood volume of infants enrolled in these studies, both achieved the goal of high and sustained anti-PTx titers but observed variable effects on clinical outcomes.

The murine antibodies 1B7 and 11E6 are each highly protective alone, and the combination was previously shown to function synergistically in aerosol and intracerebral murine models*(154)*. Notably, they were more efficacious than a polyclonal anti-PTx preparation and provided significant protection when administered up to seven days after infection as measured by survival, leukocytosis and bacterial colonization*(153)*. Since 11E6 is thought to competitively inhibit PTx binding to cellular receptors*(154)*, this antibody appears to prevent the initial PTx-cell interaction, but may require a 2:1 stoichiometry for complete neutralization of the two binding sites on each PTx molecule. Unlike 11E6, 1B7 appears to alter PTx intracellular trafficking such that the toxin never reaches its G-coupled protein target*(157)*. Hu1B7 and m11E6 can simultaneously bind PTx (Fig. 4), indicating that the epitopes do not overlap and supporting the hypothesis that hu1B7 and hu11E6 are synergistic by virtue of complementary mechanisms. This notion is further supported by the *in vitro* CHO cell neutralization data shown here, in which the humanized antibodies displayed synergy when combined in an equimolar ratio (Fig. 5). Based on these data, we think synergy is highly likely, although the murine studies presented here were designed to demonstrate protection conferred by humanized antibodies against a clinically relevant strain as opposed to synergy.

The promising clinical results with P-IVIG and the availability of murine antibodies conferring in vivo protection with complementary mechanisms led us to hypothesize that humanized versions of these antibodies would efficiently block PTx activities and treat pertussis symptoms in humans. The humanized 1B7 and 11E6 antibodies are biochemically similar to the original murine versions, leading to the expectation that they will exhibit similar efficacy. This was initially evaluated in a prophylactic murine aerosol model using a recent human clinical isolate. Not only did the

humanized antibodies protect as well as the chimeric antibodies, but the individual antibodies and the binary combination significantly mitigated disease in terms of weight gain, lung colonization and WBC (Fig. 6).

The murine aerosol mouse model was used to develop current acellular vaccines and support their progression to human clinical trials. However, in 2012 a non-human primate model, which may have better predictive value for human disease, was first reported. Using this model, we observed leukocytosis and bacterial colonization in control animals which resolved after three weeks, typical of the model*(155)*. Antibody-treated animals exhibited a blunted WBC rise and accelerated bacterial clearance (Fig. 7), supporting a role for these antibodies to treat pertussis in critically ill infants.

Notably, the baboon model introduces a large number of bacteria (109-1010 CFU) into the respiratory tract, resulting in rapid onset of disease, with WBC elevation apparent in 2-3 days and heavy coughing in 3-4 days. In contrast, humans are likely infected with a smaller inoculum via contact or aerosols, exhibiting comparable clinical symptoms 2-3 weeks after infection*(167)*. This is similar to baboons experimentally infected by contact or aerosol transmission, who showed peak WBC several weeks after infection*(168)*. Together, these data suggest that the baboon clinical symptoms observed on day three correspond to human symptoms several weeks after infection. As there is no prior data evaluating pertussis therapeutics in baboons, treatment on day three post-infection was selected due to the rapid onset of disease in baboons, the expected antibody serum half-life, and the appearance of endogenous baboon antibody responses as early as 12-days post-infection. Additional animal modeling and human clinical trials would determine the windows during which antibody treatment could affect disease outcomes.

Interestingly, the two baboons that were only mildly colonized with *B. pertussis* were likely partially protected through concurrent exposure to B. bronchiseptica. This organism is endemic in many animal populations but has not been described in baboons*(165)*. Here, two co-housed animals were mildly colonized by *B. pertussis* (103 - 104 cfus recovered), with similar day 3 WBC and coughing as all other animals; symptoms which resolved rapidly upon antibody administration (Appendix A Table 6). Protection against *B. pertussis* infection has been observed for mice previously infected with B. bronchiseptica*(169)*; concurrent exposure in baboons may also provide some cross-protection. An important implication is that baboons must be protected from and monitored for B. bronchiseptica exposure prior to use in *B. pertussis* studies.

By immediately arresting PTx activities, the hu1B7/hu11E6 antibody cocktail appears to have two effects on disease progression, as observed in both the murine and baboon models. First, since PTx is directly responsible for the elevated WBC, blocking this activity prevents further leukocytosis, protecting against pulmonary hypertension and organ failure, the specific causes of infant death from pertussis. Second, by modifying Gi/o proteins, PTx interferes with innate immune responses; in particular, chemotaxis to the lungs and subsequent oxidative burst*(144, 145)*. Antibody-mediated blockade of these activities is expected to allow neutrophils and macrophages to more efficiently phagocytose *B. pertussis*, thereby resolving the pertussis infection and preventing secondary infections. As there is no evidence to support direct antibacterial effects mediated by these antibodies, protection of the innate immune system would explain the ~10-fold reduction in bacterial colonization levels observed in mice (Fig. 6) and baboons (Fig. 7) after antibody treatment. These results are consistent with studies showing similar reductions in murine colonization by PTx-deficient *B. pertussis* and B.

parapertussis strains*(143, 164, 170)* and the inability of acellular vaccination to prevent subsequent bacterial colonization of mice or baboons*(141, 171)*. While the bacteria localize in the lungs, the various murine responses to PTx, including hyper-insulinemia and histamine sensitization, suggest the toxin is widely distributed and thus antibodies are likely required systemically to neutralize PTx activities.

Two potential challenges for an antibody therapeutic to treat pertussis are maternal vaccination and early identification of exposed or high-risk infants. Currently, maternal vaccination is the leading strategy in development to protect newborns from pertussis prior to initiation of standard vaccination schedules at two months of age. The goal is to induce high levels of maternal anti-pertussis antibodies for transfer to the fetus in utero that then confer protection after birth. While maternal vaccination is attractive for many reasons, recent uptake data in the US indicate that with optimal healthcare access, 40% of newborns remain unprotected*(172)*, while 86% of pregnancies covered by Medicare did not receive the vaccine*(173)*. Moreover, the resulting infant anti-pertussis titers can be modest at birth and decay rapidly*(174)*. This will leave many infants unprotected and the need for a therapeutic in urgent situations will remain. The neutralizing antibodies described here could provide a complementary therapeutic strategy when maternal immunization fails. Similarly, therapeutic use of anti-pertussis antibodies will require accurate and timely identification of high-risk cases such that the therapy can be administered when it is most effective. We expect minimal interference with subsequent vaccination since only two of the many epitopes included in the vaccine would be masked by hu1B7 and hu11E6.

We believe these data in aggregate support continued development of the humanized 1B7 and 11E6 antibodies toward clinical application. To this end, we are currently planning experiments in neonatal baboons as these appear to better mimic severe pertussis observed in human neonates*(175)*. While these antibodies have affinities typical of those generated by in vivo somatic hypermutation and similar to approved antibody therapeutics, enhanced efficacy may be attained through additional protein engineering efforts to increase the binding affinity*(12)* or the circulating half-life*(176)*. The evidence presented here and in prior literature suggest that neutralizing PTx will improve recovery when added to the current standard of care, however this notion would need to be clearly demonstrated in controlled human trials with quantitative endpoints prior to broad antibody use. In addition, given the decreasing cost of goods for antibodies and support from non-governmental organizations, the antibodies may be able to prevent disease in the developing world where infants are most likely to die from pertussis. Finally, these results support the notion that PTx is a major protective antigen and should continue to be a focus of future pertussis vaccines.

ACKNOWLEDGEMENTS

We thank J. Keith (NIH) for the 1B7 and 11E6 hybridomas; D. Ambrosino (Mass Biologics) for P-IVIG; T. Merkel (U.S. Food and Drug Administration) for helpful discus- sions; H. Sato and Y. Sato for their publications on the m1B7 and m11E6 antibodies. We acknowledge the following funding sources: NIH grant #AI066239, Norman Hackerman Advanced Research Project #003658-0019-2011, Welch F-1767, and Synthetic Biologics (J.A.M.); NIH grant #P40OD010431 and #P40OD010988 (R.F.W.).

Chapter 3: Synergistic neutralization of pertussis toxin by a bispecific antibody *in vitro* and *in vivo*[2]

ABSTRACT

Bispecific antibodies are a rapidly growing class of therapeutic molecules, originally developed for the treatment of cancer but recently explored for the treatment of autoimmune and infectious diseases. *B. pertussis* is a re-emerging pathogen, with several key symptoms caused by the pertussis toxin (PTx). Two humanized antibodies, hu1B7 and hu11E6, bind distinct epitopes on PTx and mitigate disease severity in murine and baboon models of infection when co-administered. Herein, we describe generation of a bispecific human IgG1 molecule combining the hu1B7 and hu11E6 binding sites via a knobs-in-holes design. The bispecific antibody showed binding activity equivalent to the antibody mixture in a competition ELISA. A CHO neutralization assay provided preliminary evidence for synergy between the two antibodies, while a murine model of PTx-induced leukocytosis definitively showed synergistic neutralization. Notably, the bispecific antibody retained the synergy observed in the antibody mixture, supporting the conclusion that synergy is due to simultaneous blockade of both the catalytic and receptor binding activities of pertussis toxin. These data suggest that a hu1B7/hu11E6 bispecific antibody is a viable alternative to an antibody mixture for pertussis treatment.

---

[2] This chapter has been published in final edited form as:
E. K. Wagner, X. Wang, A. Bui, J. A. Maynard. Synergystic neutralization of pertussis toxin by a bispecific antibody *in vitro* and *in vivo*. Clin Vaccine Immunol 23, 851-862 (2016)

E. K. W. planned, performed, and analyzed all experiments.

INTRODUCTION

Despite vaccination, pertussis infection continues to cause ~195,000 deaths worldwide, primarily of infants *(1)*. Of the estimated 16 million cases of pertussis each year, ~95% occur in the developing world. Even in developed countries, disease incidence has increased dramatically over the last decade, reaching pre-vaccination levels in some countries *(177, 178)*. This rise has been attributed to shortcomings of the current acellular vaccine *(179)* as well as pathogen adaptation *(180)*. In both cases, high levels of circulating disease place young infants at risk, as this population is the most susceptible to severe disease. An antibody therapeutic could be used to treat seriously ill infants in the developing world and prevent disease in high-risk areas.

Pertussis toxin (PTx) is one of several virulence factors secreted by the gram-negative bacterium *B. pertussis*. PTx is directly responsible for suppression of the innate immune system *(144)* and systemic leukocytosis, which is the key clinical indicator of severe disease and appears directly responsible for pulmonary hypertension and organ failure *(181)*. In addition, low titers of PTx-neutralizing antibodies correlate with susceptibility towards clinical infection *(149)*. We previously developed a binary mixture of two humanized anti-pertussis toxin antibodies which was able to mitigate whooping cough in mouse and baboon models of infection *(27)*. The antibody hu11E6 blocks binding of the toxin to host cells, while the antibody hu1B7 interferes with the catalytic pathway. At a dose selected to demonstrate efficacy but not synergy, the individual antibodies and mixture were able to completely suppress leukocytosis in a murine infection model. The mixture also reduced bacterial colonization ~20-fold.

A concern when developing therapeutics for a mutable pathogen is the risk of escape variants that are no longer affected by the therapeutic. One approach is to target multiple epitopes to reduce this risk and enhance therapeutic efficacy *(70)*. Antibody mixtures are able to provide better protection against pathogen adaptation, and can also provide broader coverage against a target, such as HIV-1, which exhibits high antigenic diversity *(65)*. In addition, combinations of antibodies exhibiting complementary mechanisms can be highly synergistic, as was demonstrated with antibodies targeting botulinum neurotoxin that were only able to significantly neutralize the toxin when formulated as a tertiary antibody mixture *(35)*. Recently, a combination of three investigational antibodies was used to treat patients in the 2014 Ebola outbreak after it demonstrated efficacy in non-human primates *(132)*. A number of other antibody mixtures to treat infectious diseases are in pre-clinical development *(70)*. While antibody mixtures have shown promise as therapeutic agents, additional manufacturing steps for formulation and quality control of the mixture can add significant complexity and cost. Antibody mixtures are typically classified as combination drugs, and documentation of the safety of each individual component as well as the mixture is required *(72)*.

In contrast, bispecific antibodies are a new class of therapeutic in which two binding specificities are combined in the same molecule. The original application of bispecific antibodies was to direct non-specific CD8+ T cells to cancerous cells by simultaneously binding the T cell surface protein CD3 and a tumor cell antigen. This approach is demonstrated by the first approved bispecific antibody in the US, Blinatumomab *(94)*, and modifications of this strategy are currently being pursued for a number of other cancer applications. Bispecific architecture has more recently been explored as a way to crosslink two surface antigens, and shows promise as a mechanism

to enhance neutralization potency against infectious targets such as antibiotic-resistant P. aeruginosa *(182)* as well as HIV-1 *(183)*. The applications of bispecific antibodies are rapidly expanding, and the development of better methods to make bispecific antibodies is an active area of research.

We previously observed that an equimolar mixture of the hu1B7 and hu11E6 anti-PTx antibodies was more effective *in vitro* than either antibody alone *(27)*. This led us to hypothesize that a bispecific antibody containing these two binding sites would capture the therapeutic potential of the mixture in a single molecule. Importantly, this construct would also provide insight into the structural basis of synergy exhibited by these two antibodies. Herein, we describe the development of a bispecific anti-PTx antibody with human IgG1 architecture. The bispecific antibody was able to bind the two cognate PTx epitopes simultaneously and exhibited an effective affinity similar to that of the antibody mixture. A murine neutralization assay demonstrated clear synergy between the hu1B7 and hu11E6 antibody combination as well as within the bispecific antibody. This evidence supports the conclusion that synergy between hu1B7 and hu11E6 is due to more complete neutralization of toxin activity from simultaneous blockade of the receptor binding and catalytic pathways, and also suggests that a bispecific antibody may be a viable alternative to an antibody mixture for the treatment of pertussis.

MATERIALS AND METHODS

Protein preparation and purification

Large-scale preparations of hu1B7 and hu1E6 were prepared by Catalent (Somerset, NJ) using polyclonal CHO cell lines followed by protein A chromatography, anion chromatography and buffer exchange into PBS pH 7.0 *(27)*. Fab fragments were prepared by digestion of the parent monoclonal antibodies using immobilized papain (Thermo Scientific Pierce), followed by protein A chromatography and buffer exchange into PBS pH 7.4.

Bispecific antibody expression plasmids were generated by introducing the previously described T366Y (knob, hu1B7H+) or Y407T (hole, hu11E6H-) point mutations *(184)* into an antibody expression vector containing human IgG1 constant heavy domains *(185)*. The modified heavy chain and native light chain plasmids were transfected in a 1:1 ratio into confluent T-150 flasks containing adherent CHO-K1 cells using Lipofectamine 2000 (Life Technologies). Supernatant was collected over one week, purified using protein A chromatography and stored in PBS pH 7.4. Bispecific antibody was prepared by incubating a 1:1 molar ratio of the hu1B7H+ and hu11E6- parental antibodies at ~2 mg/mL in PBS pH 7.4 with 10mM EDTA and 50mM 2-MEA (Thermo Scientific Pierce) for 90 minutes at 37 °C. The partially reduced sample was then buffer exchanged into PBS pH 7.4 and stored overnight at 4 °C to allow re-oxidation and heterodimerization *(186)*.

The PTx holotoxin (PTx) and its B subunit (PTx-B) were obtained from List Biological Laboratories. The A subunit (PTx-220K), a version of the pertussis toxin A subunit truncated at residue 220 and appended with a terminal lysine residue and hexa-

histidine tag, was expressed from plasmid pAK400 as described *(157)*. Briefly, BL21(DE3) cells containing the expression vector were grown in TB at 25°C to an OD600 of 1.5, then induced with 1mM IPTG for 5 hours. Cell pellets were collected and the periplasmic contents recovered by osmotic shock. PTx-220K was purified by immobilized metal affinity chromatography followed by size exclusion chromatography (Superdex S75 column on an ÅKTA FPLC). Purified PT-220K was biotinylated via its sole lysine by incubation with a 50-fold molar excess of EZ-Link Sulfo-NHS-Biotin (Thermo Scientific) at 4°C overnight, followed by buffer exchange into PBS pH 7.4. Biotinylation was confirmed with ELISA, in which a hu1B7 coat was used to capture PTx-220K which was then detected with streptavidin-HRP (BD Pharmingen).

Modeling hu1B7 and 11E6 epitopes on PTx

The hu11E6 antibody sequence was submitted to a public Rosetta antibody server *(187, 188)* for modeling. Four models with diverse structures were selected and submitted to PatchDock *(189, 190)* for an initial docking estimate, using the residues within 10 angstroms of the sugar residues on PTx structure 1PTO *(191)* as a constraint for binding area. The best docking run for each antibody structure was submitted to Rosetta Docking2 for refinement. The epitope for the top docking runs was defined as all residues on the PTx structure within 4 Å of the CDRs. The final consensus epitope was defined as residues consistently contacted in both the S2 and S3 subunits. An average plane was calculated from the coordinates of all surface exposed residues in each epitope, and a line normal to this plane was added using a custom PyMol script.

PTx binding assays

All ELISAs followed the same general procedure, with specific modifications detailed below. First, a high-binding 96-well ELISA plate (Costar) was incubated overnight at 4 °C with the coat protein in PBS, pH 7.4. Second, the plate was blocked. Third, protein dilutions were prepared in the plate in duplicate. After any additional protein incubation steps, the secondary antibody was added to the plate. After the final incubation and washes, the plate was developed with TMB substrate (Thermo Fisher Scientific), quenched with 1N HCl and the absorbance measured at 450 nm using a SpectraMax M5. All incubation steps proceeded for one hour at room temperature. Wash steps in between incubation steps used PBS with 0.05% tween-20 (PBST), while the blocking buffer and assay diluent used was PBS with 5% powdered milk (PBSTM).

For the PTx sandwich ELISA, the plate was coated with 1 μg/mL of murine 1B7 or 11E6, blocked, then incubated with dilutions starting from 70-100 nM of PTx-220K, PTx-B, or full PTx. The sandwich was completed with 1 μg/mL human 1B7 or 11E6, labeled with a 1:2500 dilution of goat-anti-human Fc-HRP (Thermo Scientific Pierce), and developed as above.

For the bispecific sandwich ELISA, the plate was coated with 1 μg/mL PTx-B, blocked, then incubated with antibody dilutions starting from 20 μg/mL. Following incubation with 1 μg/mL PTx-220K-biotin, binding was detected with streptavidin-HRP (BD Pharmingen) at a 1:5000 dilution.

For the PTx binding ELISA, the plate was coated with 0.2 μg/mL PTx, blocked, then incubated with antibody dilutions starting from 5 μg/mL (hu1B7 variants) or 10

μg/mL (hu11E6 variants). Binding was detected using goat-anti-human constant kappa-HRP antibody (Thermo Scientific Pierce) at a 1:1250 dilution. Data shown is representative of three independent experiments.

PTx binding affinity was determined by competition ELISA. A high-binding plate was coated with 0.2 μg/mL PTx and blocked as described above. While the plate was blocking, a 3 nM (mAbs and bispecific) or 6 nM (Fabs) solution of each protein was incubated with dilutions of PTx starting from 200 nM. After equilibration for an hour at room temperature, the PTx/antibody mixtures were transferred to the washed ELISA plate in duplicate and allowed to incubate for 15 minutes at room temperature to capture unbound antibody. Binding was detected with goat-anti-human Fc-HRP (monoclonal and bispecific antibodies) or goat-anti-human constant kappa-HRP (Fab fragments) and signal developed as above. The resulting curves were fit to equilibrium binding equations *(192)* corrected for bivalent binding *(193)* where appropriate. Three independent experiments were performed. Statistical significance was determined by 1-way ANOVA and Tukey's Test.

Protein biophysical characterization

For mass spectrometry analysis, 100 μg each of the hu1B7H+, hu11E6H- and hu1B7/hu11E6 bsAb antibodies were digested with the IdeS enzyme (Promega) for 1 hour at 37 °C. The digested products were run on a Superdex S200 size exclusion column using an FPLC instrument (Äkta, GE Healthcare) with PBS pH 7.4 as a running buffer, and the peak corresponding to ~100kD was collected based on MW standards and buffer exchanged into 50mM ammonium acetate using a centrifugal filter (Amicon). The antibodies were analyzed by LC-MS on an Orbitrap Fusion mass spectrometer

(ThermoFisher). A linear gradient of 0.1% formic acid and water and 0.1% formic acid and acetonitrile over 15 minutes was used to elute the antibodies from a ProSwiftTM RP-4H (1 x 50 mm) monolithic column (ThermoFisher). The Orbitrap Fusion was operated in Standard Pressure Mode at 15000 resolution from 1800-4500 m/z, with 20 microscans and a source fragmentation energy of 35V. Following acquisition, data was deconvoluted using MagTran and Protein Deconvolution 4.0.

To assess protein size and purity, 3 μg of each purified protein was analyzed by SDS-PAGE. Proteins were incubated with reducing or non-reducing loading buffer and incubated for 5 minutes at 80°C or 30s at 42°C respectively. The protein was loaded onto a 10% acrylamide gel or 4-20% gradient gel (Bio-Rad) and run at 120V prior to staining with GelCode Blue (ThermoFisher).

To assess protein stability, the antibody thermal melting temperature was measured by differential scanning fluorimetry. Purified antibodies were prepared at 400, 200, and 100 μg/mL in PBS pH7.4 and mixed with protein thermal shift dye (Life Technologies) as described in the product literature. Quantification of fluorescence was measured using a ViiA-7 instrument at a ramp rate of 1°C/minute, with derivative melting temperature (Tm) values calculated from Protein Thermal Shift software (Applied Biosystems, V1.2). Samples were run in triplicate.

In vitro PTx neutralization assay

Inhibition of CHO cell clustering was used to determine *in vitro* neutralization ability of antibody preparations as described *(194)*. Briefly, antibody was serially diluted across a 96-well tissue plate from 800 to ~0.4 nM in the presence of 4 pM PTx. Antibody

and PTx were incubated for 30 minutes at 37 °C, after which $1x10^4$ freshly trypsinized CHO-K1 cells were added per well. After incubation at 37 °C for an additional 48 hours, the degree of clustering was scored as 0 (no clustering), 1 (equivocal), 2 (positive clustering), or 3 (maximal clustering). Neutralizing dose is expressed as the lowest antibody-to-PTx molar ratio resulting in a score of 1. Samples were run in duplicate and three independent experiments were performed. Statistical analysis was performed with the Kruskal-Wallace test (for data not coming from a Gaussian distribution) and Dunn's post-hoc test.

Murine PTx leukocytosis study

An *in vivo* leukocytosis assay was performed as previously described *(195, 196)* with the following modifications: First, 2 μg PTx or 2 μg PTx plus 20 μg of total antibody were pre-incubated for two hours at room temperature to allow for binding equilibration. These preparations were then injected into a lateral tail vein of 5-6 week old female BALB/c mice. Four days later, blood was collected by terminal cardiac puncture and combined with Na2EDTA to a final concentration of 10 mM to prevent clotting. Blood (10 μl) was lysed in 150 μl mouse red blood cell lysis buffer (Alfa Aesar) for 15 minutes, washed with PBS+2%FBS, and stained for one hour on ice with 2.5 μg/mL anti-mouse CD45 antibody or isotype control antibody, each labeled with Alexa Fluor 488 (BioLegend). Samples were run on a flow cytometer (BD LSR-Fortessa) with CountBright absolute counting beads (Life Technologies) to calculate the total number of white blood cells (WBC) per μl blood. Group sizes were based on power calculations from pilot experiment data, with groups of 6 (PBS) or 10-11 (PTx and antibody treated) mice per group. In a pilot experiment, mice were administered PBS or 200 μg of hu1B7 by intra-peritoneal injection (n=3 per group), with blood taken on day 4 from a lateral tail

and processed as above. In addition, blood was also taken on day 0 from the lateral tail vein of these and other mice to assess the variability in baseline WBC counts. Statistical analysis was performed using a 1-way ANOVA and Tukey's test.

Ethics statement

All animal procedures were performed in a facility accredited by the Association for Assessment and Accreditation of Laboratory Animal Care International in accordance with protocols approved by The University of Texas at Austin (AUP-2014-00414) Animal Care and Use Committee and the principles outlined in the Guide for the Care and Use of Laboratory Animals.

RESULTS

Antibodies hu1B7 and hu11E6 can simultaneously bind the same toxin molecule

PTx is an AB5 toxin, with the S1 subunit comprising the "active" A subunit and subunits S2 through S5 comprising the receptor "binding" B subunit. The antibody hu11E6 binds two homologous sites on the B subunit and thus prevents the initial interaction between the toxin and glycosylated receptors on host cells *(154)*, while the antibody hu1B7 binds the A subunit, preventing ADP-glycosylation of cytoplasmic Gi/o receptors *(157)*. We thus hypothesized that the synergy previously observed between hu1B7 and hu11E6 was due to a more complete neutralization of the toxin function when both the binding and catalytic activities of the toxin are blocked *(27)*. This effect would be maximal if the hu1B7 and hu11E6 epitopes on a single PTx molecule could be simultaneously bound by their corresponding antibodies, creating a hu1B7-PTx-hu11E6 complex. To evaluate this as a possible mechanism, we wanted to confirm that binding of one hu1B7 or hu11E6 antibody did not preclude binding of a second antibody to the same toxin molecule.

We addressed this question via a series of ELISA assays in which one antibody (murine 1B7 or 11E6) was used to capture PTx, which was then detected by a second antibody (hu1B7 or hu11E6; Fig. 8A). As suggested by the known binding stoichiometry, the full-length toxin can be sandwiched between two 11E6 antibodies or any combination of 1B7 and 11E6 antibodies: both the m1B7/ hu11E6 and m11E6/ hu11E6 combinations gave strong signals while the m1B7/ hu1B7 combination did not. Similarly, the B subunit alone only had a positive signal by the m11E6/ hu11E6 combination, albeit with lower signals reflecting the lower affinity of 11E6. Similarly, the S1 subunit could not be sandwiched by any combination of 1B7 and 11E6. These data confirm that hu1B7 and

hu11E6 can bind the same PTx molecule simultaneously, and suggest that multiple bispecific antibodies could simultaneously bind a single toxin molecule.

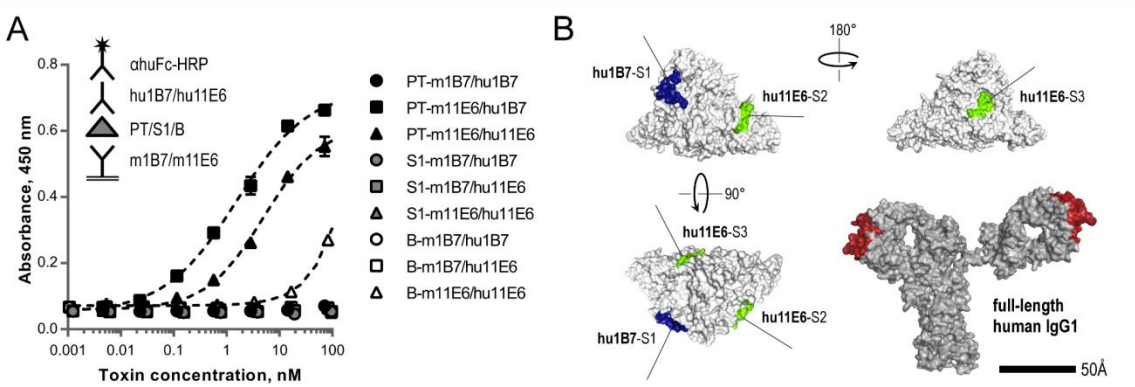

Figure 8. Orientation and stoichiometry of the hu1B7 and putative hu11E6 epitopes.

Antibody hu1B7 binds a single well-defined epitope on the S1 subunit while hu11E6 binds two highly homologous epitopes present on both the S2 and S3 subunits. (A) PTx can simultaneously engage antibodies binding the hu1B7 and hu11E6 epitopes. Shown is a sandwich ELISA in which one antibody is used to capture PTx (solid icons), the A subunit (S1-220K, grey icons) or B subunit (hollow icons), which is then detected by a second antibody. Tested antibody pairs include an m1B7 capture antibody with hu1B7 detection (m1B7/hu1B7; circles), m1B7 capture with hu11E6 detection (m1B7/ hu11E6; squares), or m11E6 capture with hu11E6 detection (m11E6/hu11E6; triangles). Error shown is the range of two duplicate samples in a single experiment. (B) PTx showing the relative locations of the hu1B7 and hu11E6 epitopes. The experimentally defined hu1B7 epitope is shown in dark blue and the two predicted hu11E6 epitopes in light green. The lines extending from the epitopes are normal to the average plane, approximating the angle at which a bound Fab would project. A full length huIgG1 structure (PDB 1HZH, *(197)*) with the antigen binding sites highlighted in red is shown at the same scale. Graphics generated with PyMol.

Crosslinking of two epitopes on a single PTx molecule is likely not required for synergistic neutralization

To further understand the constraints on antibody-PTx binding, we highlighted the amino acid residues recognized by hu1B7 and hu11E6 on the crystal structure of PTx

(191) (Fig. 8B). The hu1B7 epitope has been experimentally defined: it localizes primarily to the S1 subunit *(157)*, and was finely resolved using a combined yeast display/ high-throughput sequencing approach *(198)*. Although experimental epitope mapping of hu11E6 has not been performed, the murine antibody has been reported to bind epitopes present in the homologous S2 and S3 subunits, thereby inhibiting PTx from binding glycosylated and sialylated cellular receptors *(154)*. We further refined the putative hu11E6 epitopes by docking Rosetta models *(187, 188)* of the antibody onto the toxin, guided by the location of oligosaccharides in a relevant crystal structure (PDB ID 1PTO) *(191)*. The resulting structure shows that the two predicted hu11E6 epitopes and single known hu1B7 epitope are located on different faces of PTx and are oriented in opposing directions. The midpoints of any two epitopes are approximately 50Å apart, which is much narrower than the typical ~130Å wingspan of a crosslinking antibody *(199)*. A line normal to the best-fit plane calculated from the solvent-exposed residues was used to approximate the orientation of an antibody bound to the PTx surface. Even considering a large elbow angle of 125° between the variable and constant regions *(200)*, the geometry suggests that a single antibody molecule, whether monoclonal or bispecific, would only be able to interact with a single epitope at a time. Thus, complete blockade of all three epitopes would require a stoichiometry of three antibodies for every PTx molecule.

Expression and purification of a stable hu1B7/hu11E6 bispecific antibody

Since hu1B7 and hu11E6 previously exhibited synergy *in vitro* as native IgG1 antibodies, we chose to develop a bispecific antibody with natural architecture using the knobs and holes platform *(184)* followed by *in vitro* assembly to form the desired heterodimer *(186)* (Fig. 9A). The resulting human IgG1 bispecific is structurally similar

to the hu1B7 and hu11E6 monoclonal antibodies, facilitating comparisons among the variants, with the added benefits of low immunogenicity and enhanced circulating half-life due to FcRn binding *(91)*.

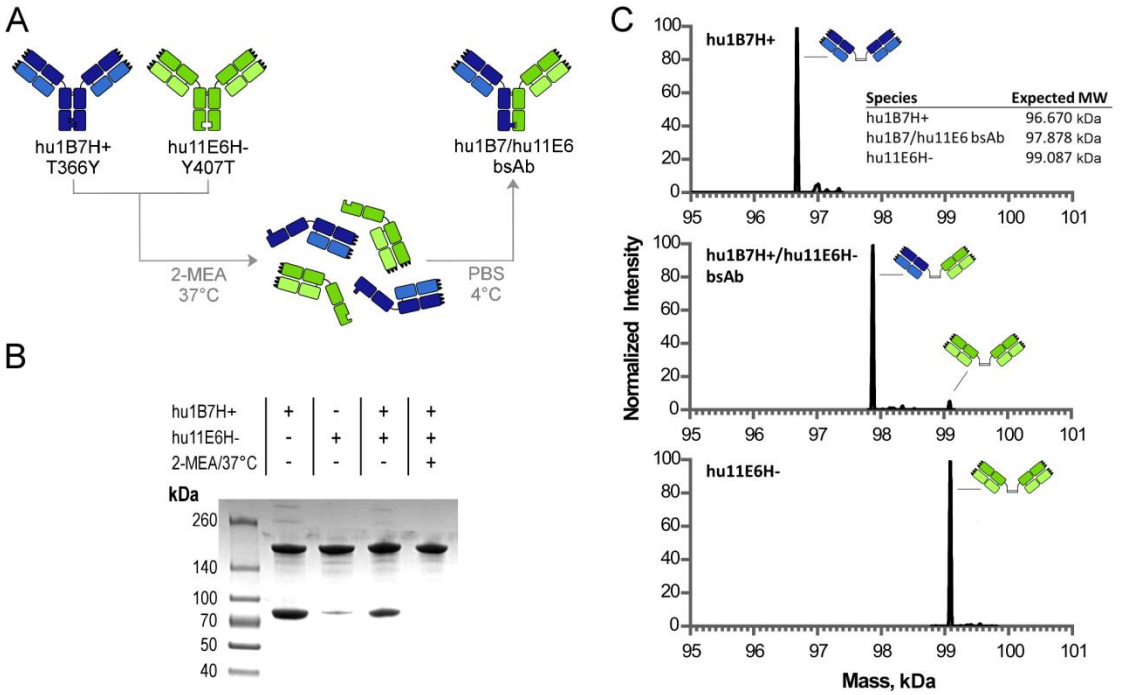

Figure 9. Production of bispecific hu1B7/hu11E6 antibody.

(A) Schematic overview of the process used to create the bispecific antibody. Single amino acid residue changes were introduced into the parent antibody Fc domains to create "knob" (T366Y; hu1B7H+) and "hole" (Y407T; hu11E6H-) variants, which were expressed and purified separately. An equimolar mixture of the two proteins was then subjected to a controlled reduction and re-oxidation reaction, resulting in efficient formation of the heterodimeric, bi-specific antibody. (B) Purity of the knob and hole variants and 2-MEA-catalyzed recombination was monitored by non-reducing SDS-PAGE. Samples shown are with (+) or without (-) the three reaction components: hu1B7H+, hu11E6H-, or the 2-MEA red/ox step. (C) Purified hu1B7H+, hu11E6H-, and the bispecific antibody were digested with IdeS enzyme to yield F(ab')2 fragments. LC/MS was used to determine the purity of the bispecific preparation.

To make the bispecific, the T366Y "knob" mutation was introduced into the CH3 domain of hu1B7 to generate hu1B7H+, while the Y407T "hole" mutation was introduced into the CH3 domain of hu11E6 to generate hu11E6H-. These two parent antibodies were transiently expressed in separate CHO cell cultures and purified via protein A chromatography. Non-reducing SDS-PAGE of the purified proteins revealed mixtures of homodimer and half-antibodies at ~75 kDa after storage in PBS pH7.4 (Fig. 9B). Notably, the hu11E6H- ran primarily as a covalent homodimer at this pH *(201)*, while the hu1B7+ showed bands for homodimer and half-antibody, consistent with previous reports of an Fc anti-parallel knob-knob dimer *(202)*. The hu1B7H+ and hu11E6H- proteins were combined in an equimolar ratio and subjected to a controlled reducing step using 2-mercaptoethanolamine (2-MEA) to generate the heterodimeric bispecific antibody *(186)*. Non-reducing SDS-PAGE analysis of the protein product after this step shows a significantly reduced presence of the half antibody and high molecular weight species, suggesting successful formation of the bispecific antibody (Fig. 9B).

The hu1B7/hu11E6 bispecific antibody was digested with IdeS to generate F(ab')2 fragments, which were purified and analyzed by LC/MS to assess the purity of the bispecific (Fig. 9C). The precursor antibodies hu1B7H+ and hu11E6H- were prepared in the same way as controls. The bispecific fragment had a major peak at 97.878 kDa, which is a unique molecular weight intermediate to the hu1B7H+ and hu11E6H- homodimer weights of 96.669 and 99.087 kDa respectively. The measured masses were nearly identical to the expected values calculated from the primary amino acid sequence. The bispecific also showed a small peak corresponding to hu11E6H- homodimer, representing ~5% of the maximum intensity. As the original reaction was performed at a 1:1 hu1B7H+:hu11E6H- ratio, we expect a similar proportion of unreacted hu1B7H+.

The unreacted fraction hu1B7H+ likely contained a significant amount of half-antibody based on SDS-PAGE of the hu1B7H+ precursor, which would not show up in our IdeS analysis. Thus, assuming there is a similar amount of unreacted hu1B7H+ also present, the final purity of the assembled bispecific antibody is ~90%, consistent with other bispecific antibodies generated using the T366Y/Y407T mutations *(184)*.

Biophysical characterization of monoclonal, Fab, and bispecific antibodies

To provide a point of reference in our functional assays and to assess valency effects, we also produced monoclonal hu1B7 and hu11E6 and their Fab fragments. The monoclonal antibodies were expressed in transient CHO cell cultures and purified by protein A and anion exchange as previously described *(27)*. The Fab fragments were generated by subsequent digestion of purified antibody with immobilized papain, followed by protein A chromatography to remove undigested antibody and free Fc domains. Reducing and non-reducing SDS-PAGE analysis determined that the proteins were highly pure (~90% or higher) and of the expected size (Fig. 10A). Reducing lanes show characteristic bands at ~50 kDa (intact immunoglobulin heavy chain) and ~25 kDa (light chain and Fab heavy chain), while non-reducing lanes show single bands at ~150 kDa (intact immunoglobulin and bispecific antibody) and ~50 kDa (Fabs).

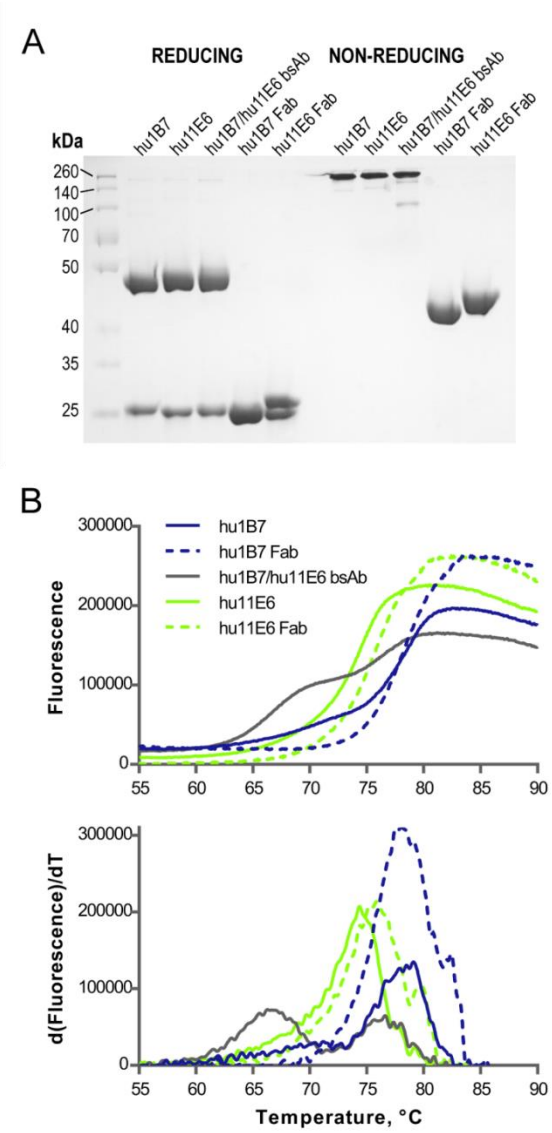

Figure 10. Biophysical characterization of bispecific and parent antibodies.

(A) Reducing and non-reducing SDS-PAGE was used to assess the size and purity of the hu1B7 and hu11E6 full-length and Fab antibody fragments as well as the hu1B7/ hu11E6 bispecific antibody. 3 µg of protein were loaded per lane. (B) Differential scanning fluorimetry was performed to determine the melting profile of full-length hu1B7 and hu11E6 (solid lines, blue or green respectively), the hu1B7 and hu11E6 Fabs (dashed lines, blue or green respectively) and the hu1B7/hu11E6 bispecific antibody (grey line). Samples were prepared in PBS, pH7.4. Derivative data (d(Fluorescence)/ dTemperature) is aligned below the raw melting curves to facilitate identification of transition temperatures. Curves are averages of three replicates at 400 µg/ml.

Antibody thermal stability was assessed using a differential scanning fluorimetry assay to monitor protein unfolding in PBS, pH 7.4 (Fig. 10B). The full-length hu1B7 profile shows two melting regimes, with the first peak (~71°C) likely representing CH2 unfolding and the second peak (~79°C) representing CH3 and Fab unfolding *(203)*. In this buffer, the hu11E6 domains unfold in a more continuous manner, with the most rapid unfolding occurring around 74°C. The Fab formats show similar or slightly higher melting temperatures than their full-length counterparts, with derivative melting points of ~78°C for hu1B7 Fab and ~76°C for hu1E6 Fab. The bispecific antibody exhibited a more complex profile, making it difficult to identify specific melting regimes, but major transitions were observed at ~67°C and ~77°C. The introduction of the knob and hole mutations is expected to have a slight destabilizing effect on the CH3 domain of the bispecific. Derivative traces are also shown to aid in identification of melting transitions (Fig. 10B).

A hu1B7/ hu11E6 bispecific antibody has similar *in vitro* PTx binding activity to the binary mixture

To assess the PTx binding activity of the bispecific antibody and to compare this with the activity of the binary antibody, we performed a series of ELISA assays. To verify that the protein was functionally bispecific, we compared the hu1B7/hu11E6 bispecific and hu1B7H+ and hu11E6H- parent antibodies using a sandwich ELISA (Fig. 11A). The PTx-B subunit was coated on the plate and used to capture any antibodies with the hu11E6 paratope. This was followed by incubation with S1-220K-biotin and streptavidin-HRP to detect molecules also containing the hu1B7 binding site. As hu1B7H+ only binds S1-220K-biotin, this did not bind to coated PTx-B, while hu11E6H- binds PTx-B but cannot be detected with S1-220K-biotin. In contrast, the bispecific

antibody was able to simultaneously bind both PTx-B and S1-220K-biotin, exhibiting a characteristic logarithmic binding curve with an EC50 of ~4nM.

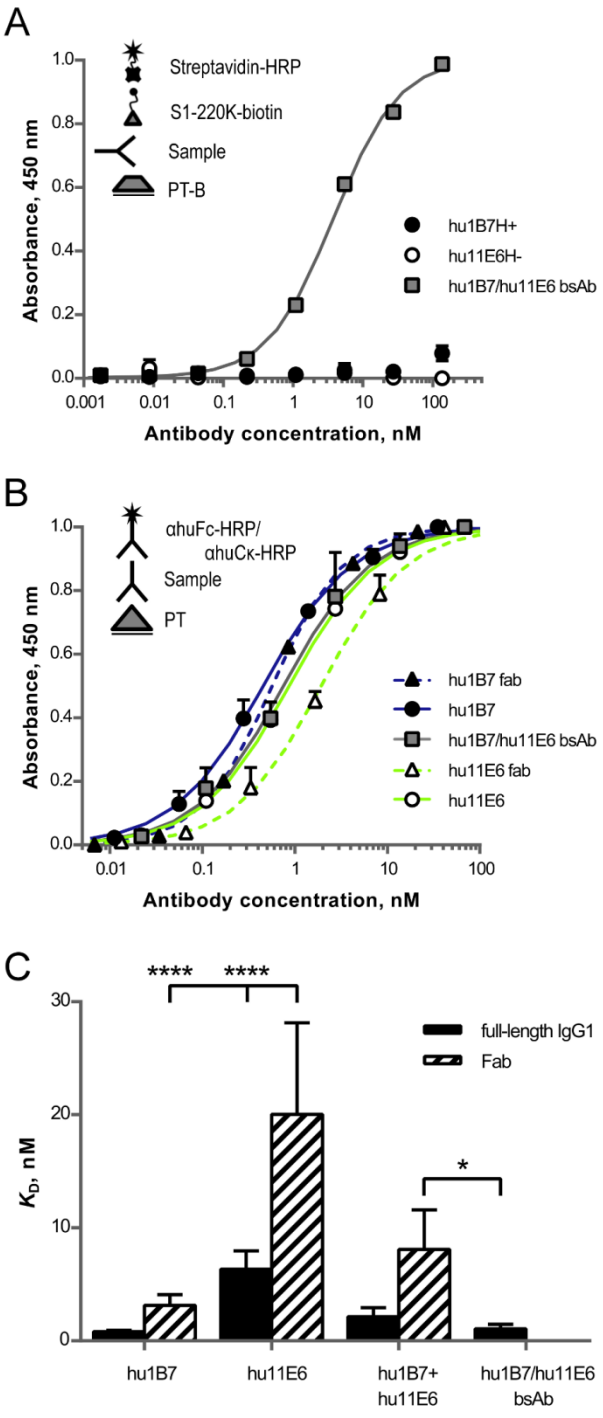

Figure 11. Biochemical characterization of bispecific and parent antibodies.

Figure 11. Biochemical characterization of bispecific and parent antibodies.

(A) The hu1B7/hu11E6 bispecific antibody (grey squares) was assessed for presence of each unique binding site and the ability to simultaneously engage two different epitopes using a sandwich ELISA. Purified PTx-B subunit was used to capture the hu11E6 paratope, followed by biotinylated S1-220K and streptavidin-HRP to detect the hu1B7 paratope. The monospecific parent antibodies hu1B7H+ (solid circles) and hu11E6H- (hollow circles) were used as controls. (B) An ELISA was used to confirm the PTx binding activity of all antibody variants and controls. A PTx-coated plate was incubated with dilutions of full-length hu1B7 or hu11E6 (circles, solid with blue line or hollow with green line respectively), the hu1B7 or hu11E6 Fabs (triangles, solid with dashed blue line or hollow with dashed green line respectively) or hu1B7/hu11E6 bispecific (squares, solid grey line), followed by anti-human-kappa-HRP to detect bound chains. (C) A competition ELISA was used to determine the solution-based equilibrium dissociation constant (KD) of all variants. Data is shown for full length (solid bars) and Fab antibody formats (striped bars). For all panels, the error shown is the standard deviation. The competition ELISA data is averaged from six replicates over three experiments. Statistical significance was determined using 1-way ANOVA and Tukey's test. Statistical significance indicated as: *$p<0.05$, **$p<0.01$, ***$p<0.001$ and ****$p<0.0001$. In addition to the comparisons shown, hu11E6 Fab was significantly different than all other groups (****), and the hu1B7 Fab + hu11E6 Fab mix was significantly different than hu1B7 mAb (*).

We next assessed the binding characteristics of all individual antibodies and fragments using a direct PTx-binding ELISA (Fig. 11B). All variants displayed strong binding to PTx, with the bispecific antibody showing a binding profile nearly identical to those of full-length hu1B7 and hu11E6. While the hu1B7 Fab had a curve similar to full-length hu1B7, the hu11E6 Fab showed a ~2-fold increase in EC50 compared to the full-length version, suggesting there are significant avidity effects for hu11E6.

For a more thorough investigation into the effective binding affinities of different antibody formats, we performed a quantitative competition ELISA wherein antibody dilutions were incubated with a constant amount of PTx, after which unbound antibody was detected by a direct PTx-binding ELISA (Fig. 11C). We fit curves to this data to calculate the equilibrium dissociation constants (KD), with bivalency corrections used for the full-length proteins *(193)*. Due to a simple 1:1 interaction with toxin and a binary "bound" or "not bound" structure, Fabs provide more accurate affinity measurements. The hu1B7 Fab KD was calculated to be 3.1±0.9 nM while the hu11E6 Fab had a significantly weaker affinity with a KD of 20±8 nM. The full-length formats showed an approximately 3-fold improvement in effective affinity compared to the Fabs, likely due to avidity effects. The KD values calculated here for the full-length hu1B7 and hu11E6 were 0.8±0.1 nM and 6±2 nM respectively, and are comparable to our previous competition ELISA and SPR measurements *(27)*.

Both Fab and full-length mixtures as well as the bispecific antibody were tested in this assay, although in these cases KD represents an effective affinity. The mixture of full-length antibodies and bispecific antibody exhibited effective affinities intermediate to those of the two parents at 2.1±0.8 nM and 1.1±0.4 nM respectively, while the Fab

mixture had an effective affinity of 8±4 nM. These affinities are skewed more toward the higher affinity of hu1B7, which in this solution-based assay may capture a larger fraction of available PTx molecules than the hu11E6 binding site. Notably, the bispecific antibody also showed a significant improvement in effective affinity as compared to the Fab mixture, supporting the importance of avidity effects. The data from these three ELISA assays in aggregate demonstrate that the hu1B7/hu11E6 bispecific is functionally bispecific and binds PTx similarly to the antibody mixture in a solution-based assay.

The bispecific antibody neutralizes PTx activities *in vitro*

We next wanted to assess the neutralization capacity of the hu1B7/hu11E6 bispecific antibody in a simple *in vitro* model. The CHO cell assay is a commonly used method to quantify PTx activity and neutralization by observing morphological changes in CHO-K1 cells after incubation with toxin or toxin and antibody *(194)*. This method was previously used to observe synergy between hu1B7 and hu11E6, which was maximal in an equimolar mixture *(27)*.

A constant amount of PTx (4 pM) was equilibrated with a series of antibody concentrations (up to 800 nM) in a 96-well plate. CHO-K1 cells were seeded into the wells and incubated for 48 hours, prior to scoring for the degree of cell clustering. Here we report the neutralizing ratio as the lowest antibody-to-toxin ratio which was able to completely prevent the clustered morphology, corresponding to a score of 1 (equivocal) on the established 0 to 3 scale *(154)*, which is a more rigorous analysis than previously applied *(27)* (Fig. 12). Under these conditions, full-length hu11E6 and hu1B7 completely neutralized toxin at a ~1,100:1 and ~34,000:1 ratios, respectively. This large discrepancy is consistent with previous studies, despite superior performance of hu1B7 in a mouse

aerosol challenge *(27)*. In addition, a similar study using a panel of murine anti-PTx antibodies, including 1B7 and 11E6, also observed enhanced neutralization in the CHO cell clustering assay by anti-B subunit antibodies which did not necessarily correlate with protection *in vivo (195)*. The hu1B7+hu11E6 mixture and hu1B7/hu11E6 bispecific were also able to fully neutralize the toxin, with antibody-to-PTx ratios of ~700:1 and ~900:1 respectively. These values are more similar to those observed for hu11E6 than for hu1B7 alone, despite the presence of fewer hu11E6 binding arms in the mixture or bispecific formulation. This is preliminary evidence of synergy and also demonstrates that the bispecific format does not compromise B subunit neutralization.

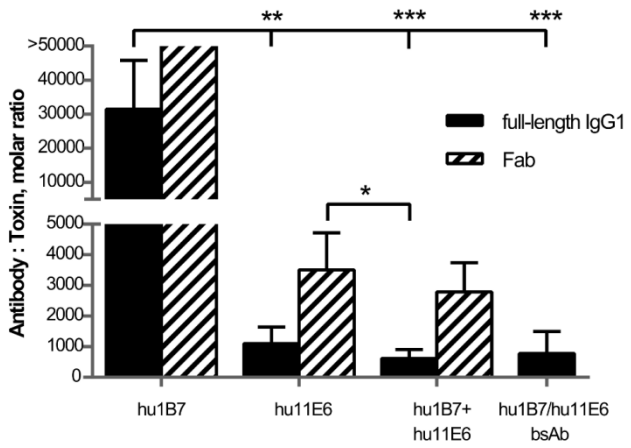

Figure 12. *In vitro* PTx neutralization measured by inhibition of CHO cell clustering.

Adherent CHO-K1 cells were grown in the presence of 4 pM PTx pre-equilibrated with antibody dilutions. The lowest molar antibody-to-toxin ratio able to fully prevent clustering was recorded as the neutralizing ratio. Data is shown for neutralization with the full-length and bispecific antibodies (solid bars) and their Fab fragments (striped bars). The hu1B7 Fab was not able to fully neutralize the toxin at any concentration tested. Data is presented as the geometric mean of six replicates over three experiments, with error bars indicating the 95% confidence interval. Statistical analysis was performed using Kruskal-Wallace and Dunn's post-hoc tests. Statistical significance indicated as: *p<0.05, **p<0.01, ***p<0.001 and ****p<0.0001.

We included the hu1B7 and hu11E6 Fabs as well as a mixture of the two to assess the role of valency in PTx neutralization. In particular, we did not know *a priori* whether the bispecific antibody would better mimic a mixture of monoclonal antibodies or a mixture of Fabs. In this assay the antibody was present at a significant molar excess over PTx, favoring binding of multiple antibodies to a single PTx. For this reason, we did not correct for valency in our ratio calculations. In general, the Fabs required approximately three-fold more protein to achieve the same neutralization level as the full-length antibodies (3,600:1 for hu11E6 Fab, 2,900:1 for Fab mix; Fig. 12), and we were unable to detect neutralization by the hu1B7 Fab under these stringent assay conditions. These results correlate well with the increase in effective affinity seen with the full-length immunoglobulins in the competition ELISA.

In this plate-based cellular assay there is no mechanism for clearance of antibody-toxin complexes; thus, in order to prevent cellular intoxication, antibody molecules must sequester every PTx molecule for the 48 hour duration of the experiment. As transiently unbound PTx molecules are able to bind cellular receptors and enter the cell via receptor-mediated endocytosis, even high-affinity antibodies such as hu1B7 and hu11E6 require very high ratios to fully neutralize PTx. Thus, the neutralizing ratios reported here are much higher than would be expected for an *in vivo* experiment.

The antibody mixture and bispecific antibody synergistically inhibit PTx-induced leukocytosis *in vivo*

Systemic leukocytosis is a primary outcome of *B. pertussis* infection and is predictive of severe disease in infants *(181)*. As a proof-of-concept study to assess the therapeutic potential of the hu1B7/hu11E6 bispecific antibody, we turned to an *in vivo*

leukocytosis assay which measures the ability of an antibody to neutralize the increase in white blood cell (WBC) count induced by the injection of purified pertussis toxin *(195, 196)*. This assay has previously been shown to be more predictive of protection during bacterial infection than the CHO cell assay *(195)*.

In a pilot experiment, juvenile BALB/c mice were injected with 200 μg hu1B7 antibody or PBS. Whole blood was collected from a lateral tail vein and assayed for white blood cells by staining for CD45 and measuring fluorescent cells via flow cytometry. In addition, WBC counts were taken from these and other mice on day 0 to assess the baseline variability. Treatment with a high dose of hu1B7 did not elevate the WBC count as compared to the baseline level or PBS treatment (Fig. 13A).

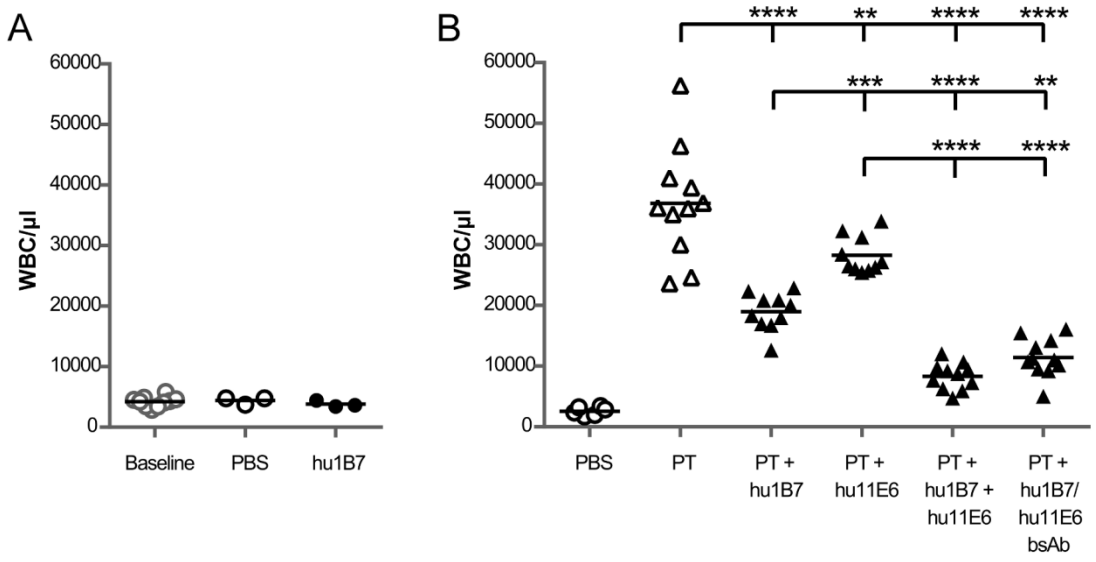

Figure 13. Antibody-mediated suppression of PTx-induced leukocytosis *in vivo*.

(A) Antibody treatment alone did not raise WBC. Five-week old female BALB/c mice were administered 200 µg hu1B7 or an equal volume of PBS via intraperitoneal injection, with the CD45+ WBC measured four days after treatment by flow cytometry. WBC counts of these and other mice were taken on day 0 to assess the baseline variability. (B) Antibody treatment suppresses PTx-induced leukocytosis. Mice were administered equal volumes of PBS, 2 µg PTx in PBS, or 2 µg PTx plus 20 µg total antibody (hu1B7, hu11E6, hu1B7+hu11E6 or the bispecific antibody) in PBS via a lateral tail vein injection, with CD45+ WBC counts measured four days later by flow cytometry. Hollow symbols indicate the WBC recorded for baseline, PBS and PTx-only treated control groups, solid symbols indicate antibody treated groups and triangles represent groups that received PTx. Groups were compared using one-way ANOVA and Tukey's test with statistically significant comparisons indicated. Statistical significance indicated as: *$p<0.05$, **$p<0.01$, ***$p<0.001$ and ****$p<0.0001$. Comparison of the hu1B7+hu11E6 binary mixture with the hu1B7/hu11E6 bispecific antibody was not significant.

In the neutralization experiment, mice were injected with PBS, pre-equilibrated mixtures of 2 µg PTx plus 20 µg antibody, or 2 µg of the toxin alone. Four days later, whole blood was collected via cardiac puncture and assayed for white blood cells as described for the pilot experiment. The toxin alone induced a ~14-fold increase in WBC

as compared to PBS-treated mice, while the full-length hu1B7 and hu11E6 antibodies were each able to significantly suppress this WBC rise ($p<0.0001$ and $p<0.01$, respectively; Fig. 13B). Of these, hu1B7 was significantly more effective than hu11E6 ($p<0.001$), consistent with previous data showing enhanced *in vivo* protection against bacterial challenge by hu1B7 over hu11E6 *(27)*.

A relatively low antibody dose (7:1 molar ratio of antibody to PTx) was selected to provide only partial suppression of leukocytosis by hu1B7 or hu11E6 to allow for the detection of synergy based on pilot experiments (data not shown). Under these conditions, an equimolar antibody mixture (10 μg of each antibody) significantly reduced WBC versus treatment with the same dose of either hu1B7 or hu11E6 alone (20 μg antibody; $p<0.0001$). The resulting WBC count was not significantly different than that for PBS-treated naïve mice. Since the antibody mixture contains equimolar amounts of both the hu1B7 and hu11E6 specificity, simple additivity predicts that the mixture would provide a result intermediate to that of either antibody used alone. Instead, the efficacy of the mixture was significantly enhanced over either monoclonal preparation, indicating synergy between the antibodies.

Synergy of the bispecific antibody can be assessed in a similar way, although avidity effects complicate the analysis. As there is only a single hu1B7 epitope on a PTx molecule, the bispecific antibody can be expected to retain all of the hu1B7 functionality. In contrast, while hu11E6 can also only bind a single epitope at a time, bivalency was beneficial in ELISA and CHO assays, thus the bispecific construct may not be able to capture the full neutralization potential of hu11E6 with only a single paratope. However, treatment with 20 μg of the bispecific antibody still significantly reduced the WBC count as compared to either of the monoclonal preparations ($p<0.01$ vs hu1B7, $p<0.0001$ vs

hu11E6). Notably, there was no difference between WBC count for mice treated with the antibody mixture as compared to those treated with the bispecific antibody at this power level. These data show that the bispecific antibody was able to capture the synergy observed in the mixture.

DISCUSSION

Three of the 52 currently approved antibodies are indicated for the treatment or prevention of infectious diseases *(204)*, with dozens more in clinical and pre-clinical development *(70, 205, 206)*. Palivizumab was approved in 1998 to prevent respiratory syncytial virus (RSV) infection in high-risk patients *(6)*, while raxibacumab and obiltoxaximab were approved in 2011 and 2016, respectively, for the treatment of anthrax *(207, 208)*. Antibodies may be appropriate therapeutics for a variety of other infectious diseases that cause serious disease in high-risk populations, including pertussis. An antibody therapeutic could be used to treat seriously ill infants in the developing world and prevent disease in high-risk areas, a strategy that is being pursued for pediatric HIV-1 *(209)* In this work, we have further explored the mechanism of synergy between the anti-PTx antibodies hu1B7 and hu11E6, and showed that a bispecific antibody captures this synergy in a single molecule.

We have previously demonstrated that an equimolar mixture of hu1B7 and hu11E6 exhibited synergistic PTx neutralization *in vitro*, requiring a lower antibody-to-toxin ratio to achieve the same effect as either hu1B7 or hu11E6 alone *(27)*. Here, we showed that while multiple antibodies can simultaneously bind the same toxin molecule (Fig. 8A), a single antibody is unlikely to crosslink two of those epitopes (Fig. 8B). Thus, if synergy depends upon simultaneous blockade of the hu1B7 and hu11E6 epitopes on PT, a bispecific antibody with native architecture would be expected to exhibit similar PTx-neutralizing abilities as the mixture. This was confirmed in several *in vitro* assays to assess PTx-binding and *in vitro* neutralization (Fig. 10, Fig. 11). Finally, *in vivo* PTx-neutralization data with a 7:1 molar excess of antibody not only demonstrated significant synergy between hu1B7 and hu11E6, but also confirmed that the bispecific format fully

recapitulated this effect (Fig. 13). These results confirm the hypothesis that synergy is due to more complete neutralization of the toxin when both the binding and catalytic activities are simultaneously blocked, which can be achieved by simultaneous binding of hu1B7 and hu11E6 or several bispecific antibodies.

A similar approach was recently reported for ricin toxin, another A-B toxin with an analogous intoxication pathway as PTx *(210)*. In that work, camelid variable heavy domains blocking the active and binding activities were only partially neutralizing on their own, and a mixture of the two top performers did not exhibit synergy *(211)*. In contrast, a flexible bispecific construct was developed that was able to crosslink the two epitopes, and in doing so significantly changed the dynamics of toxin binding and trafficking *(212)*. Thus even in the context of bacterial toxin neutralization, bispecific antibodies can be applied in several ways.

Avidity effects were difficult to deconvolute in this system, with the paratope:epitope stoichiometry, spatial presentation of the antigen, and relative amounts of toxin and antibody all impacting results differently in each assay. While structural modeling suggests that simultaneous engagement of two epitopes on the same toxin molecule by a single antibody is unlikely, it is possible that the presence of a second epitope nearby makes it easier for a bivalent construct to rebind the same toxin, essentially "wobbling" between the two epitopes. Avidity effects of multivalent and bispecific formats have been modeled *(213)*, and have been proposed as a way to drive higher-affinity and higher-specificity binding of targets with multiple epitopes. Alternatively, bridging of two toxin molecules by one monoclonal antibody can allow bivalent binding of a second antibody to a different epitope, which has been proposed as

a mechanism for synergy in the neutralization of anthrax toxin *(214)*. Regardless of the exact mechanism, bivalency enhanced the effective binding affinity (Fig. 11C) and *in vitro* neutralization (Fig. 12). In a therapeutic setting, Fabs would not typically be used due to their significantly shorter circulating half-life.

While the synergy between hu1B7 and hu11E6 is beneficial for potency and reducing the cost of goods, the inclusion of multiple specificities is also important for long-term safety and efficacy of a therapeutic. Suppression of escape variants is a particular concern for pertussis, as circulating *B. pertussis* strains appear to have changed in response to vaccine-induced immunity. Wide-spread use of acellular vaccines containing the adhesion pertactin appears to have provided a considerable fitness advantage for naturally occurring pertactin-deficient strains, with the result that 100% of clinical isolates in the United States now lack this protein *(215)*. Thus, there is basis for concern that widespread use of anti-PTx antibodies could lead to evolution or selection of escape variants. Fortunately, PTx appears to be more essential for pathogenesis than pertactin, as *B. pertussis* PTx knock-out strains are minimally infective and severely reduced in virulence *(143, 164)*. Moreover, PTx is a key component of all acellular vaccines, including a PTx-only vaccine in Denmark, yet only two PTx-deficient strains have been isolated in the past eight years worldwide. Both of these strains were recovered from unvaccinated individuals co-infected with other Bordetella strains *(216)*, suggesting that PT-deficient strains are unlikely to be successful pathogens. The majority of sequence variation occurs in the A subunit, which is immunodominant and has five distinct circulating alleles *(180)*. It is possible that antigenic drift could lead to PTx variants with reduced affinity for neutralizing antibodies, although changes in the A subunit are unlikely to affect hu11E6 binding and have previously been shown to have

minimal effect on hu1B7 binding *(157)*. However, an antibody therapeutic with multiple specificities further mitigates this concern.

The main drawbacks to antibody mixtures are the increased complexity and costs of manufacturing and regulatory approval processes. The binary mixture described here would likely be produced by separately manufacturing hu1B7 and hu11E6 and adding a final co-formulation step. Although this method is simple to implement, it is susceptible to batch failure from either individual antibody and requires development of two separate manufacturing chains *(69)*. In addition, antibody mixtures are subject to the same strict FDA approval processes as monoclonal preparations, and documentation for the safety of each individual component as well as the mixture is needed *(72)*. While bispecific antibodies have their own manufacturing challenges, detailed below, the regulatory pathway is expected to be simpler. We explored the use of a bispecific antibody as an alternative way to package the therapeutic potential of the antibody mixture.

Over 60 distinct bispecific architectures have been reported, ranging from constructs with near-native immunoglobulin structure to various scFv-fusions *(91)*. As our eventual goal is to use this antibody for passive immunization in high-risk infants, stability and a long-circulating half-life are essential characteristics, which suggested the use of a format including an Fc region for FcRn-mediated recycling. We chose to use the knobs-in-holes mutations *(184)* on a stabilized 4D5 framework, which is a validated approach with a simple protocol. The resulting huIgG1 antibody has a structure nearly identical to the parental hu1B7 and hu11E6 antibodies, facilitating direct comparisons with the antibody mixture. In several other applications of bispecific antibodies for infectious disease, it was found that the chosen bispecific format had a significant impact

on potency, with full neutralization only occurring when the molecule was engineered to be flexible enough to crosslink two epitopes *(182, 183)*. As hu1B7 and hu11E6 are able to neutralize PTx and exhibit synergy without crosslinking epitopes on a single PTx molecule, we did not pursue alternative formats.

Bispecific antibodies with native architectures are appealing for their high stability, long half-life, and low immunogenicity but are among the most difficult to manufacture. These designs require correct assembly of two unique heavy chains and two unique light chains into a single heterodimeric protein. In this case, the modular antibody domains that allow for diverse immune responses due to unbiased pairing of many heavy and light chain gene products is a detriment: there is minimal thermodynamic driving force to favor correct pairing, for instance between a hu1B7 heavy chain and a hu1B7 light chain versus a hu11E6 light chain. The simple knobs-in-holes design utilized here results in over 90% correct assembly of the knob-and-hole heavy chains *(184)*, but requires separate expression and purification of the half-antibodies to maintain proper pairing between the heavy and light chains. Several processing strategies using the knobs-in-holes designs have been developed *(186, 217)*, while engineering of orthogonal CH/CL Fab interfaces to drive proper heavy and light chain pairing *(218)* has paved the way for production of a bispecific antibody from a single cell line. Bispecific antibody manufacturing is currently a very active area of research, and it is likely that future improvements could be included in a second generation of the bispecific antibody described here.

The treatment of infectious diseases presents unique challenges, but antibody mixtures and bispecific formats have the potential to address currently unmet clinical

needs in this area. We have quantitatively demonstrated synergy *in vivo* between the two anti-pertussis toxin antibodies hu1B7 and hu11E6, and shown that this synergy is retained when these specificities are expressed as a knobs-and-holes bispecific antibody. As the antibody mixture was previously shown to be effective in both murine prophylactic and weanling baboon therapeutic models *(27)*, we expect a bispecific antibody to recapitulate the efficacy of the mixture in an infection setting. This bispecific antibody is particularly appealing, as the format simplifies the regulatory path while retaining the synergy and broader neutralization potential of the binary combination. We expect that bispecific and other multivalent antibody formats will see increased development for infectious disease applications.

ACKNOWLEDGEMENTS

We thank Andrea DiVenere for assistance with preparation of samples for mass spectrometry, Zachary P. Frye for assistance with PyMol and Greg Lyness for assistance with mouse studies. This work was supported by grants from Synthetic Biologics, the Welch Foundation (F-1767) and the National Institutes of Health (AI122753) to J.A.M., and a National Science Foundation Graduate Research Fellowship under grant no. DGE-1610403 to E. K. W.

Engineering a novel soluble TCR- Immunoglobulin hybrid molecule

ABSTRACT

T-cell receptors (TCRs) are structurally similar to antibodies and can be engineered in similar ways, however they are functionally distinct. While antibodies are well-suited for binding conformational epitopes found on extracellular pathogens or toxins, TCRs are highly specific for linear peptides displayed on the surface of cells in the context of major histocompatibility complexes (MHCs). Thus, soluble TCRs offer a complementary approach to antibody therapeutics, and are particularly relevant for viral diseases. We have proposed a new bispecific format called a T-cell Receptor-ImmunoGlobulin (TRIG) molecule, which is theoretically able to simultaneously bind a virally—infected cell via pMHC and a circulating T-cell via CD3. This "immune-redirecting" approach is becoming a more common strategy for targeting cancer, but is also in development for several infectious indications. The TRIG is also unique in that it can be expressed in mammalian cells, and contains an Fc region for long half-life and effector cell interaction. Herein we describe our efforts to engineer this new format. We have developed a CHO surface display method, and optimized it to display a TCR. We have generated focused libraries around CDR3α and CDR3β, and are currently screening them for higher affinity TCR variants. We have also expressed and purified the sTCR-Fc fusion, which is the parent molecule of the bispecific, and are currently optimizing expression variables. We believe the TRIG may be a useful format for the treatment and prevention of viral diseases, and in the future we hope to test the molecule in a human cytomegalovirus model.

INTRODUCTION

As we look towards finding cures for the next round of diseases- antibiotic-resistant infections, pandemic viruses, rare genetic disorders- we must also look for the next generation of therapeutic molecules. Biologic drugs, including recombinant antibodies, will likely continue to be key players due to favorable safety profiles and developmental timelines*(2)*. Further, there is now considerable interest in innovative new protein architectures which can open new pathways for treating disease.

In particular, bispecific antibodies have the powerful ability to harness both cellular and humoral immunity. Amgen's blinatumomab consists of an antibody single-chain variable fragment (scFv) which can bind CD19, a B cell surface antigen, linked to another scFv that binds CD3, part of the T-cell receptor (TCR) complex*(219)*. Simultaneous binding of CD3 on circulating cytotoxic T cells (CTLs) and CD19 on a tumor cell results in activation of the CTL and lysis of the lymphoma cell*(219)*. Thus, the bispecific molecule basically acts as an adaptor; it specifically decorates targeted host cells, but can then bind and activate any passing CTL. Blinatumomab was the first bispecific antibody approved in the US, and has since been shown to nearly double the overall survival rate in acute lymphoblastic leukemia patients over traditional chemotherapy*(220)*. Although initial development of bispecific antibodies has been for cancer indications, there is no reason this approach cannot be used for infectious, particularly viral, diseases. A nearly identical construct targeting the ectodomain of the influenza A matrix protein 2 (M2e), which is expressed on the surface of infected cells, has shown promise in a murine challenge study*(221)*. Several groups have reported on bispecific antibodies targeting CD3 and the HIV envelope protein, which can induce

significant cell lysis and reduction of HIV expression in *in vitro* and *ex vivo* models*(95, 222)*.

The ability to make such formats hinged on the maturation of the field of protein engineering and antibody production. The first bispecific antibodies were described in 1961, but these early bispecifics were difficult to produce and purify. In particular, as there is minimal driving force for correct assembly, co-expression of two different light chains and two different heavy chains results in a mixture of 10 possible proteins*(184)*. This problem was partly solved by the introduction of "knobs-into-holes" mutations in the CH3 region, which disrupt packing of mispaired products and thermodynamically favor correct pairing, resulting in up to 92% efficiency of desired heterodimeric pairing in the heavy chains*(184)*. However, heavy and light chain pairing remains an issue, and necessitates special production methods or non-native antibody formats. Over 60 such bispecific formats have been described, with several in clinical testing*(91)*. These approaches include using linked ScFvs*(223)* (as used in blinatumomab), adding variable region fusions*(224)*, and producing bispecifics *in vitro* from knob and hole or similar parent monoclonals*(186)*. Mutations in the heavy/light interface that allow production within a single cell have been identified, though are quite extensive and somewhat dependent on the variable region*(218, 225)*.

One unique bispecific format is called an immune-mobilizing monoclonal T-cell receptors against Cancer/Viruses (ImmTAC/ImmTAV), and has a high-affinity soluble TCR in place of the antigen-targeting ScFv*(226)*. While structurally related, TCRs are a different breed than antibodies; antibodies are adept at recognizing conformational epitopes on soluble proteins or cell surfaces, and TCRs recognize linear epitopes on

peptides derived from intracellular proteins. These peptides are displayed on the cell surface in complex with MHC molecules (peptide-MHC, pMHC), and cells displaying foreign or anomalous peptides will be recognized by CTLs and attacked. This ability to react to intracellular antigen fragments is a key way a healthy immune system eliminates endogenous virally infected and cancerous cells. As therapeutic antibodies binding viral glycoproteins are only functional in the extracellular space, using soluble TCR-like molecules to target infected cells themselves may be a complementary strategy for treating viral infections. For example, an ImmTAV specific for an immunodominant HIV peptide was able to kill resting and active HIV-positive cells *in vitro*, and may be an approach for eliminating reservoirs of latently infected cells*(96)*. Although this is an exciting new strategy there are several protein engineering challenges associated with this format. Firstly, wild-type TCRs typically have affinities in the micromolar range, and must be affinity matured to the picomolar range to have functional effects as soluble monomers*(227, 228)*. Secondly, soluble TCRs (sTCRs) are difficult to express, and are commonly expressed and refolded in E. coli*(229)*. Finally, the small size of this construct and lack of Fc region results in a half-life of hours rather than the weeks typical for IgG*(96)*. To put this into perspective, blinotumomab, which is antibody-based but similarly sized and formatted, must be continuously infused at high concentrations over several weeks to have therapeutic effects*(230)*.

In this chapter we describe our progress towards generating a novel TCR/Ig fusion molecule, called a TRIG (Fig. 14). This format is compelling as it can be expressed in mammalian cells without the need of a refolding step, and contains an antibody Fc region for long half-life *in vivo*. To do this, we first optimized a system to display RA14, a human TCR associated with human cytomegalovirus (CMV), on the

surface of CHO cells. We have designed and generated directed libraries of mutant RA14, and are in the process of using CHO cell display to discover high affinity variants. We have expressed and purified the wild-type RA14-Fc fusion and a human anti-CD3 antibody from CHO cells, and are in the process of cloning knob and hole mutations into the Fc regions to drive proper assembly. In the near future we hope to use an *in vitro* assembly method to generate bispecific molecules, and test the resulting TRIGs *in vitro* for activity against CMV-infected cells.

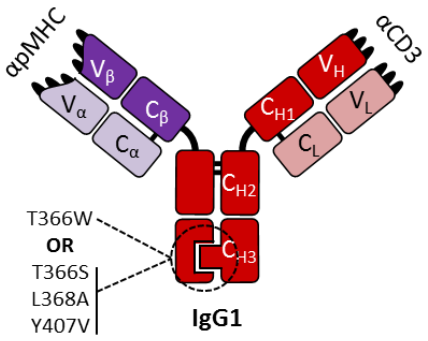

Figure 14. Diagram of the proposed hybrid T-cell receptor/Immunoglobulin molecule, or TRIG.

The molecule consists of a soluble TCR targeting a viral pMHC fused to an antibody Fc region. The antibody arm binds CD3. The C_H3 domains include knob and hole mutations*(231)* to ensure proper assembly. Purple, TCR domains. Red, antibody domains.

MATERIALS AND METHODS

Cloning of surface display, library screening, and soluble expression plasmids

The RA14 sequence was obtained from the protein data bank and synthesized as a gblock (IDT). The sequence was cloned into a pcDNA (general expression) or pPyEBV (Acyte Biotech) (library screening) backbone along with a murine Igk leader sequence, T2A peptide with furin cleavage site (RRKR) and GSG linker*(232)*, and PDGFR transmembrane region (Fig. 15A, Fig. 16A). Constructs were cloned in both α-2A-β-TM and β-2A-α-TM orientations. The constant region sequences were either the wild-type human germline sequence (UniProt), or included mutations to remove a free cysteine and move the terminal disulfide bond*(233)*. The soluble construct was generated by replacing the transmembrane region with a human IgG1 hinge, C_H2 and C_H3. Cloning was performed using Q5 hot-start polymerase (NEB) and either traditional cut and ligate methods or assembly methods (NEBuilder).

The sequence of 28F11, a human anti-CD3 antibody, was obtained from a patent*(234)*, synthesized, and cloned into expression vectors as above.

EpiCHO transfection

EpiCHO cells (CHO-T) (Acyte Biotech) were grown in CHO-S-SFM II media (Gibco) supplemented with 2x GlutaMax and penicillin/streptomycin. For transfection, cells were spun and resuspended at a concentration of $1.5x10^6$ cells/mL, with 2 mL plated per well in a 6-well plate. For each well, 250 µl of OptiMEM (ThermoFisher) was mixed with 10 µl of Lipofectamine 2000 (ThermoFisher), and added to another tube with 250 µl of OptiMEM and 4 µg of DNA. The solution was mixed and allowed to equilibrate for 30 minutes at room temperature, before adding the solution to the appropriate well. The next

day, cells were fed an additional 1 mL of media. Cells were scanned for transfection on day 2.

Tetramer preparation

Biotinylated HLA-A*0201 monomer loaded with the CMV-specific $pp65_{495-503}$ peptide (NLVPMVTAV) or an irrelevant HCV peptide (KLVALGINAV) were purchased from Biolegend and aliquoted. Streptavidin-APC, streptavidin-AF488 and streptavidin-AF647 were purchased from ThermoFisher and prepared at 200 μg/mL. To make the tetramer, one-tenth the required amount of streptavidin-fluor needed to make a 4:1 monomer:streptavidin molar ratio was added every 5 minutes on ice over 50 minutes. 30 μM biotin was then added to block any remaining unconjugated sites.

Flow cytometry

~$1x10^6$ transfected cells were centrifuged gently and resuspended in 50 μl of PBS plus 2% FBS (Sigma) with 9-30 μg/mL tetramer and a 1:50 dilution of antiVβ6-5-PE (Beckman Coulter). Cells were stained at room temperature for 1 hour, then rinsed and resuspended in 1 mL PBS plus FBS. Samples were run on a Fortessa (BD Biosciences). All analysis was done using FlowJo software with pre-gating on live cells.

Library design and cloning

Complementarity-determining regions (CDRs) 3α and 3β were targeted for saturation mutagenesis (Fig. 15A). The targeted region included all amino acids directly contacting the pMHC*(235)*, as well as an additional residue on either side to impart more backbone flexibility (Table 4.1). To limit library size and retain binding affinity, one (3α)

or two (3β) residues involved in hydrogen bonding were retained as the wild type sequence. To generate the insert, degenerate primers overlapping and extending past the CDR were used with upstream primers to synthesize the first fragment. This PCR was done 10 times to reduce bias using Q5 hot-start master mix (NEB). A second PCR, overlapping the first but outside of the mutagenized region, was performed to make the second fragment. The two fragments were run on an agarose gel and gel extracted, mixed in an equimolar ratio, put through 10 cycles of annealing and extension, and then amplified using primers at the distal ends. The insert and pPyEBV backbone were digested with the appropriate restriction enzymes (CDR3α, AgeI and NheI; CDR3β, BamHI and NheI, NEB), gel extracted and desalted. For each library ~1μg of vector was ligated with insert at a 3:1 (3α) or 6:1 (3β) ratio overnight using T4 ligase (NEB). The following day, ligations were desalted and transformed into ~1.5 mL of fresh NEB10β electrocompetent cells. After one hour of recovery, dilutions were plated and incubated, and colony counts used to estimate the library size. The library was grown to an OD_{600} of 2 in liquid culture, which was then used to make frozen stocks and inoculate a new flask for overnight growth. Library DNA was prepared the next morning using a Maxiprep kit (Qiagen).

Library transfection and sorting

1 or 2 T-150 flasks (24-48 mL total) of confluent EpiCHO cells were transfected as described above, with quantities scaled accordingly. To allow for only a single plasmid per cell, transfected DNA was diluted 1:4 with an irrelevant plasmid of similar size and no antibiotic resistance gene encoded. T-25 flasks of wild-type positive control as well as an irrelevant antibody display control were also transfected. On day 2, cells were scanned for surface display to verify transfection, and spun down and resuspended in half-strength

selective media (CHO-S-SFM II plus 2x GlutaMax plus 150 μg/mL Hygromycin). On day 4 or 5, cells were expanded as needed and transferred into full-strength selective media (300 μg/mL Hygromycin). Cells were split regularly in selective media until good viability was present in a confluent T-150 (~2 weeks).

For sorting, ~$1x10^7$ live cells were spun and resuspended in OptiMEM plus 1% BSA and stained as described above. Cells were sorted using a FACSAria, with the sort gate biased towards cells showing higher tetramer binding at the same display level. The gate was drawn to collect ~1% of the total population, thus resulting in a final sort count of ~$1x10^5$ cells. The sorted cells were grown up to a T-150 again (~1 week), and the process was repeated 1-2 more times.

Soluble protein expression and purification

For medium-scale expression of the TCR-Fc fusion and αCD3 antibody, two T-150 flasks of CHO-K1 cells were transfected using the same cell/media/reagent ratio as described above. Cells were grown in high-glucose DMEM (Sigma) with 10% low-IgG FBS (ThermoFisher) and no antibiotic. Media was collected and replaced over 1-2 weeks. Collected media was centrifuged to remove cells, neutralized with 1M Tris pH 8, and stored at 4C.

As an initial crude purification, soluble protein was precipitated out with 50% saturated ammonium sulfate. The precipitate was collected by centrifugation and resuspended in binding buffer (100 mM phosphate, 150 mM NaCl, pH 7.2). Protein in binding buffer was loaded onto a protein A column using an FPLC (ÅKTApure, GE healthcare), washed several times, and eluted with 100 mM glycine, pH 2.5. Elutate was

immediately neutralized with 1M Tris, pH 8, and buffer-exchanged into PBS pH 7.4 using a centrifugal filter.

3 μg of purified protein was prepared in reducing or non-reducing buffer and incubated for 5 minutes at 80C or 42C respectively. Samples were run on a 4-20% gradient gel (BioRad) at 200V for 30 minutes, and stained with GelCode Blue (ThermoFisher Scientific).

Enzyme-linked immune-sorbent assay (ELISA)

An Fc-capture ELISA was used to quantify protein in unpurified media. A high-binding plate (Costar) was coated with a 1:500 dilution of goat-anti-human-Fc (ThermoFisher) in PBS and incubated overnight at 4C, then blocked with a 5% milk/PBST solution. Neutralized media was diluted down the plate in duplicate and incubated at room temperature for 1 hour. After a 1 hour incubation with a 1:2500 dilution of goat-anti-human Fc- HRP (SouthernBiotech), the plate was developed with TMB and stopped with HCl. Absorbance was read at 450 nm. An irrelevant, high-expressing antibody with identical Fc region was used as a control.

To more stringently detect correctly assembled sTCR-Fc, binding of the soluble protein was assayed using an Fc/Vβ sandwich. The ELISA coat was identical to the Fc-capture, but the secondary was a 1:2500 dilution of the antiVβ-6-5-PE antibody used for flow cytometry. This mouse antibody was detected by a 1:2500 dilution of anti-mouse Fc-HRP (Sigma) and developed as above.

Jurkat cell staining

To test binding of the αCD3 antibody 28F11, ~$1x10^6$ Jurkat cells were collected, centrifuged, and resuspended in PBS plus 2% FBS with 1 μg/mL 28F11. Cells were stained on ice for 30 minutes, washed, then stained again with the same concentration of anti-human Fc-AF647 (Jackson Immunoresearch). Cells were washed again and then analysed on the Fortessa.

RESULTS

A CMV-specific TCR, RA14, can be displayed on the surface of CHO cells

As our long term goals were to make a soluble TCR from mammalian cells, we first wished to optimize an expression system for RA14. Initial testing using the wild-type sequence with leucine zippers for added stability*(236)* was not successful, so we instead moved to a surface display system for easier troubleshooting of parameters. The plasmid for this system (Fig. 16A) includes a murine Igκ leader sequence, which has been successful in our lab for antibody expression, and a PDGFR transmembrane which we have used for antibody display. The RA14 variable regions (Vα, Vβ) are paired with the human germline constant regions (Cα, Cβ), separated by a 2A sequence including a furin cleavage site (RRKR) and GSG linker. We used the 2A sequence from the Thosea asigna virus, which was shown to have the best cleavage efficiency in CHO cells expressing humanized antibodies*(232)*. Notably, readthrough of the 2A region obviates the need for a second secretion signal*(237)*. As only the second chain is fused to the transmembrane region, and the order may have some impact on expression, we cloned the construct with both the α (α/β-TM) and β (β/α–TM) chains in the first position. Finally, we assessed the wild-type constant regions (*wt*α/β) as well as modified constant regions (*ds*α/β), which have a moved interchain disulfide bond and eliminate a free cysteine, and have proved useful for phage and yeast display constructs*(238, 239)*.

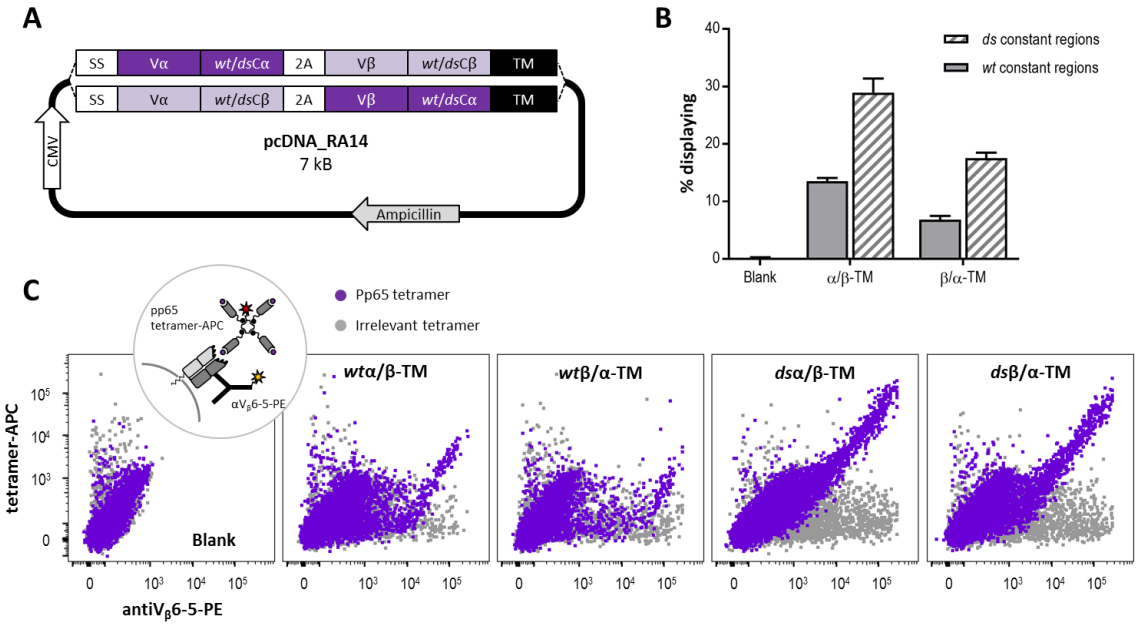

Figure 15. RA14 TCR is displayed on the surface of CHO cells.

A, Key elements of the surface display plasmid design. SS, secretion signal from murine Igκ. T2A includes a furin cleavage site (RRKR) and GSG linker. TM, transmembrane region from PDGFR. B, Display levels of the constructs, as measured by antiVβ6-5 antibody. EpiCHO cells were transfected with plasmid and stained 2 days later with pp65 tetramer-APC and antiVβ6-5-PE. Display is percent of live cells staining positive for PE. *wt*, wild-type constant regions. *ds*, disulfide-modified constant regions. C, Display and antigen binding of RA14 as measured by flow cytometry. Purple, pp65 tetramer staining. Grey, irrelevant tetramer staining.

The constructs were transiently transfected into EpiCHO cells, and scanned via flow cytometry two days later. As a measure of surface-bound TCR, cells were stained with antiVβ6-5-PE. We also made tetramers from biotinylated pMHC and streptavidin-APC, which increases the avidity and functional affinity of the reagent, and used these to check for pMHC binding. The cells had good viability, and the fraction of live cells displaying TCR was quantified by PE signal over background (Fig. 15B). The 2D plots

(Fig. 15C) show a population of cells that is binding tetramer proportionally to surface display, which is interpreted as properly-folded, surface-expressed TCR. Staining the same samples with an irrelevant tetramer did not show this same population. Although the tetramers seemed to have a small amount of non-specific binding, use of the antiVβ6-5 antibody helped confirm the population of interest. From this data it is clear that the disulfide-modified constant regions have a substantial positive effect on TCR display in both configurations. For either constant region, the α/β-TM configuration was better than the β/α-TM configuration, and even showed marginally better tetramer binding at the same display level. Transfection of a β-TM only construct confirmed that while the beta chain can be secreted alone and detected on the surface, it does not bind tetramer (data not shown). From these results, we chose to move forward with the dsα/β-TM construct.

A mammalian display system can be used to screen for affinity improvement

Although the wild-type affinity of RA14 is relatively high for a TCR, reported as 27.7μM*(235)* or 6.3 μM*(240)* depending on the experimental setup, a higher affinity will likely be required for therapeutic success*(227)*. Phage display and yeast display have both been used for affinity maturation of TCRs. Using a yeast display system, 100-fold*(239)* to 750-fold*(241)* affinity improvements were found by saturation mutagenesis of a single CDR. A phage display method with larger library sizes achieved a similar 720-fold improvement for a single CDR, but remarkably was able to reach a 10^6-fold affinity improvement by targeting multiple CDRs and repeating the process several times*(228)*. We have previously developed a CHO-cell surface display method for affinity maturation of antibodies (A. Nguyen, unpublished data). Although this method is limited to modest library sizes (10^6), a key benefit is that by screening in the final expression host, the soluble molecule is more likely to retain the characteristics selected for in the library. In

particular, as soluble TCR expression in mammalian cells is challenging, we decided that screening our TCR in this format was relevant and a good proof-of-concept for our CHO display system.

The layout of the original expression plasmid was maintained and cloned into the pPyEBV vector as shown (Fig. 16A). This large plasmid contains additional features, namely an OriP, EBNA-1 gene, and PyOri, which allow semi-stable transfection into modified CHO-T cells*(242)*. The PyOri and large T antigen (expressed in the EpiCHO cell line, CHO-T) allow plasmid amplification while OriP and EBNA-1 tether the plasmid to the chromosome during division. A hygromycin resistance gene allows for selection and maintenance of positive transfectants in mammalian culture.

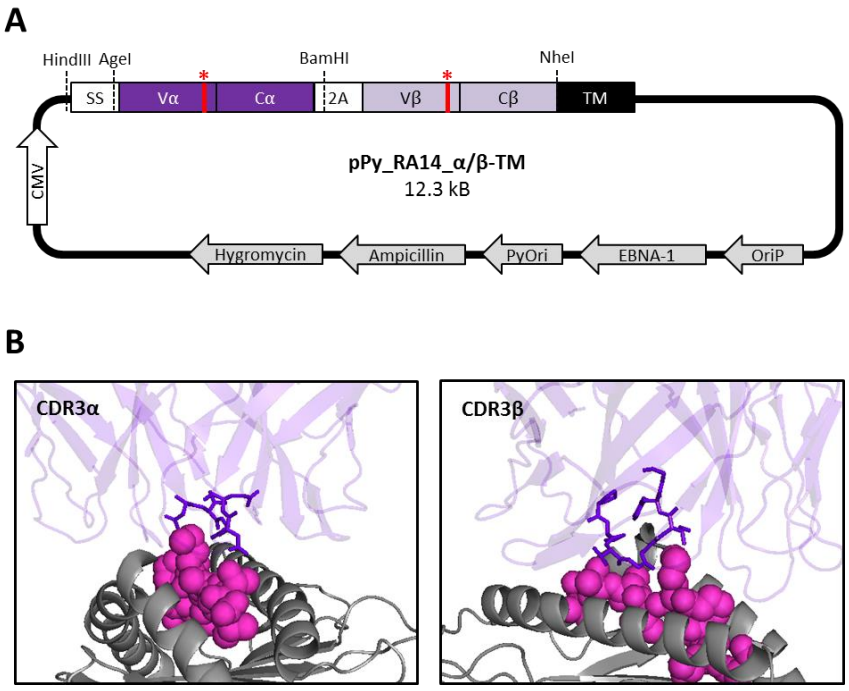

Figure 16. Design of CDR mutagenesis library.

A, Key elements of the surface display plasmid design for semi-stable transfection. SS, secretion signal from murine Igκ. T2A includes a furin cleavage site (RRKR) and GSG linker. TM, transmembrane region from PDGFR. Addition of an OriP and EBNA-1 gene allows episomal replication and chromosomal tethering. A hygromycin resistance gene allows selection in mammalian culture. Red starred regions indicate the approximate location of CDR3α and CDR3β. B, Structural rationale for CDR residues selected for mutagenesis. Grey, HLA-A*0201. Magenta spheres, NLV peptide. Purple, RA14 TCR. Based on PDB file 3GSN*(235)*.

Due to library size limitations with this system and the known role of TCR CDR3 loops in recognizing peptide antigens, we chose to make small, targeted libraries in the regions most important for binding. In particular, CDR3α and CDR3β make extensive contacts with both the peptide and HLA*(235)* (Fig. 16B), and are important for specificity. The final library designs consist of saturation or near-saturation mutagenesis of the contacting residues in one of these CDRs, plus one additional flanking residue on

either side to allow more flexibility in the backbone (Table 4.1). In each CDR there were 1 (3α) or 2 (3β) key residues that made hydrogen bonds with both peptide and HLA which were retained as wild type. Library inserts were generated using overlap PCR with degenerate primers, followed by an overlap extension step to make full-length inserts. The inserts and backbone were digested with the appropriate restriction enzymes, ligated overnight, and transformed into fresh electrocompetent cells. The final library size is estimated from the number of transformants after recovery (Table 1).

Table 4. Library design and size.

Library	**AA sequence**	**Codons**	**Library size**		
			AA, theo.	DNA, theo.	**DNA, actual**
CDR3α	NTG**N**Q	NNSNNSNNS**AAC**NNS	2E5	1E6	**4E5**
CDR3β	PV**T**GGI**Y**G	NBSVBC**ACC**VBCVBCVBC**TAC**NBS	1E6	4E6	**1E6**

Wild-type residues shown with retained residues in bold purple font. Library residues were randomized using primers with the degenerate nucleotides shown.

The libraries were transfected into EpiCHO cells, and transitioned into selective media during days 2-5. After two weeks. $1x10^7$ live cells were stained with the antiVβ6-5-PE antibody and pp65 tetramer-AF647. The cells were sorted based on higher tetramer staining for the same antiVβ6-5 staining, indicating improved affinity. Several rounds of sorting were performed, with an approximate growing time of 1 week per round (Fig. 17). The first round of sorting was able to pick out a population of clearly tetramer-binding cells, and R2 not only enriched that population but eliminated the majority of non-binding TCRs. By round 3, several distinct improved populations were observed.

Further analysis of clones pulled from the CDR3β library is ongoing, as is sorting of the CDR3α library.

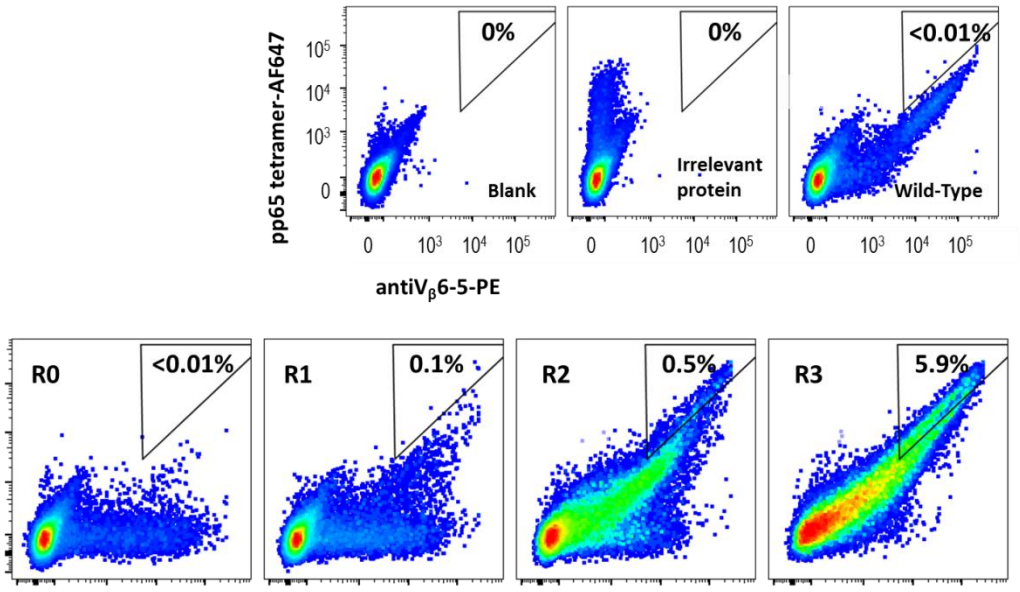

Figure 17. CDR3β library sorting.

Cells were stained with pp65 tetramer-AF647 and antiVβ6-5-PE. Live, single cells were sorted based on higher tetramer staining at the same antiVβ staining (display level). Sorting was performed three times. The percentage of cells falling within the boxed population is indicated in the upper right hand corner.

Bispecific TCR/Ig precursors can be expressed and purified from CHO cells

Our overall goal is to generate a novel bispecific TCR/Ig structure (Fig. 14), which replaces one arm of a full length antibody with a soluble TCR (T-cell Receptor Immunoglobulin Graft, or TRIG). We propose to make the TRIG by separate expression of a TCR-Fc and antibody (Fig. 18A), followed by a controlled reducing and re-oxidation step to make the bispecific molecule*(186)*. Knob and hole mutations in the Fc C_H3 domain (not shown)*(231)* will catalyze the formation of stable heterodimers. We have

considerable experience with this procedure, and have used it to make bispecific pertussis-toxin-binding antibodies with ~90% purity*(92)*.

We chose to work with a fully human CD3 binding antibody, 28F11, which is reported to have similar binding affinity and characteristics to OKT3, a commonly-used αCD3 reagent*(234)*. The variable regions were synthesized and cloned into separate κ and heavy chain expression plasmids, which were transfected into CHO-K1 cells. The media was collected over ~1 week, and purified by ammonium sulfate precipitation and protein A chromatography. SDS-PAGE of the purified protein (Fig. 18B) indicates high purity, with the expected ~50kD (heavy chain) and ~25kD (light chain) bands seen in the reduced sample, and a strong ~150kD band (full-length protein) seen in the non-reducing lane. The fainter, larger band in the non-reducing lane likely indicated a small amount of aggregates, which could be easily cleaned up using size exclusion chromatography. To confirm the binding specificity of our purified 28F11, we stained Jurkat cells, a human T-cell line with endogenous TCR expression, and analyzed them by flow cytometry (Fig. 18C). Staining of the Jurkat cells was ~91% efficient and resulted in a good differentiation from unstained cells, and looks very similar to staining with OKT3 (data not shown). Knob and hole mutations have been cloned into these constructs, and a small-scale transfection test indicated similar expression to the wild-type construct.

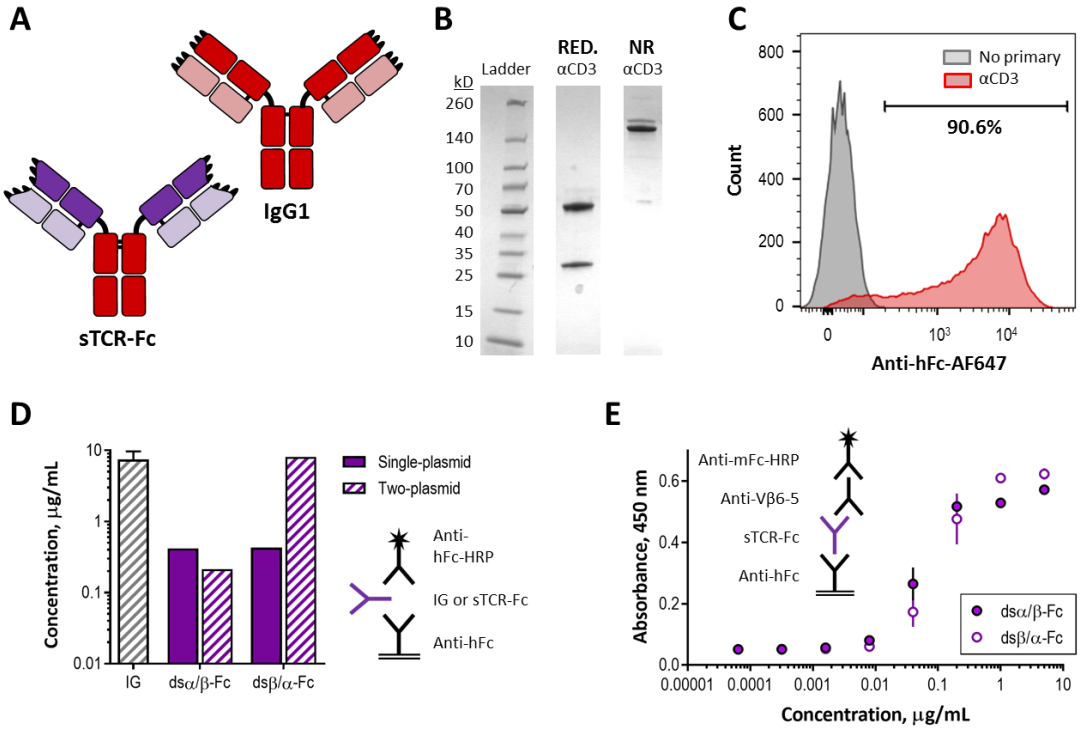

Figure 18. Design, expression, and characterization of αCD3 and sTCR-Fc.

A, Structure of TRIG parent molecules, an IgG1 antiCD3 antibody and sTCR-Fc. Red, antibody domains. Purple, TCR domains. B, SDS-PAGE of purified αCD3 antibody. 3µg of purified antibody was run under reducing and non-reducing conditions. C, Staining of Jurkat cells using the αCD3 antibody. Anti-hFc-AF647 was used to detect the αCD3 antibody, and samples were analyzed by flow cytometry. Grey, no primary antibody. Red, αCD3 primary antibody. D, Expression of sTCR-Fc constructs in EpiCHO cells. Expression level quantified using an Fc-capture ELISA. Grey, irrelevant high-expressing antibody control. Purple, sTCR-Ig constructs. Solid bars, single-plasmid design. Striped bars, split-plasmid design. E, Sandwich ELISA of purified sTCR-Ig. sTCR-Ig detected by anti-hFc and anti-Vβ6-5. Solid icons, dsα/β-Fc format. Hollow icons, dsβ/α-Fc format.

A soluble TCR-Fc expression construct was cloned by replacing the transmembrane region from the display plasmid with a human IgG1 Fc region. Due to the possibility of 2A readthrough, and to allow for further tuning of α and β chain expression

ratios, we also cloned the sequences into separate expression plasmids. Plasmids were transfected into EpiCHO cells, and the media was harvested 2 days later. An Fc capture ELISA of the media was used to detect expression levels as compared to a well-expressing irrelevant antibody (Fig. 18D). Although the sTCR expression level is much lower than the antibody expression, the yields achieved here are significantly higher than seen for similar TCR-Ig fusions*(243)*. Switching to a 2-plasmid system, which obviates the need for a 2A peptide, resulted in expression nearly as high as the antibody for the dsβ/α-Fc construct, but had minimal impact on the dsα/β-Fc construct. The cleavage efficiency of both the furin site and 2A peptide are impacted by the surrounding amino acids*(232)*, thus it is possible that good expression from the dsβ/α-Fc construct was limited by 2A cleavage efficiency. This suggests that 2A cleavage may not be complete in the surface displayed construct either, and further investigation of 2A peptides could be beneficial for library screening. Another possibility is that α chain expression is the limiting factor, and having the Fc fusion on the α chain helped increase expression, which is commonly observed*(244)*. A logical next experiment would be to try several ratios of α to β chain transfection and see if this impacts results. Finally, as the ELISA setup described here only detects Fc, further testing of the purified protein is needed to validate correct assembly.

A preliminary medium scale transfection (2x T-150s) of both the 2A-linked constructs, dsα/β-TM and dsβ/α-TM, was performed similarly with media collected over ~1 week. The media was purified using an ammonium sulfate precipitation followed by protein A chromatography. Full-length fusion protein was detected using an Fc/antiVβ6-5 sandwich ELISA (Fig. 18E), which is more stringent that the Fc-capture ELISA because it also detects the Vβ region. Both the dsα/β-Fc and dsβ/α-Fc constructs look similar on

the ELISA, suggesting that either order is amenable for soluble protein expression. We are currently doing further characterization of the soluble proteins, including affinity measurements and stability testing.

DISCUSSION

Herein we have proposed a novel T-cell receptor immunoglobulin fusion molecule, and demonstrated the progress we have made towards making this molecule. We have been able to express and purify the αCD3 antibody, and are currently optimizing high-yield expression of the sTCR-Fc. Although not required for generation of the TRIG, we have generated and are screening affinity libraries based on CDR3α and CDR3β, as it is likely that higher TCR affinity will be essential for therapeutic efficacy. We have extensive previous experience using knob and hole mutations to make bispecific antibodies *in vitro(92)*, and we are excited to try this method with the sTCR and antibody here. After validation of this new format, a long-term goal is to test its ability to redirect T-cells to kill CMV-infected cells.

We took a unique approach by first starting with a display system, which allowed for easy quantification and hence troubleshooting of expression. We were quickly able to identify key parameters, such as the disulfide-modified constant regions*(238)*, which resulted in robust surface expression of the RA14 TCR. For many other TCRs in other display systems it was necessary to first generate a random library and screen for increased expression to see anything*(245)*, so it is surprising that we were able to see such good display with RA14. Interestingly, the TCRs A6 and 1G4, which share the same Vβ germline with RA14, did not initially display on the surface of yeast at all, and expression mutations that worked for A6 did not work at all in 1G4*(246)*. RA14 does not have any of the stabilizing mutations found for A6, so it may just be that RA14 is a particularly stable TCR. A potential future application of this display system would be to screen for enhanced stability, which has been shown to correlate with expression level*(245)*. This would be particularly relevant for our system, since as our displaying

platform and expression platform use the same cell line, any improved clones found from the screening would likely demonstrate improved expression as soluble molecules. Although some engineering has been done using a T-cell display system*(247)*, to our knowledge this is the first report of recombinant TCR display on a production cell line.

Moving forward, the TCR affinity will likely be critical for efficacy of the TRIG *in vitro* and beyond. Experiments using various affinities of the ImmTAC format against a tumor antigen found that potency correlated with affinity, and TCRs with K_D values of 300-30pM were the most effective*(227)*. In an antiviral format, a very high affinity TCR (K_D of 3.6 pM) was less effective, and optimal efficacy occurred at a K_D of ~200 pM*(96)*. Another pertinent measure is the affinity ratio of the antigen and CD3 binding arms, as this will significantly influence the distribution and mechanism *in vivo*. In theory, affinity for the cellular antigen should be significantly higher to drive high concentrations of the therapeutic at the relevant site, rather than diluting the therapeutic throughout the entire circulating CTL population. While blinatumomab has a ~100-fold difference between its CD3 and CD19 binding arms*(219)*, ImmTAC formats are reported as having a ~1000-fold difference*(229)*. Interestingly, a flu-targeting bispecific with the same format as blinatumomab has the opposite affinity ratio, yet still showed some success in a murine challenge model*(221)*. As the affinity of our anti-CD3 antibody 28F11 is reported to be similar to that of OKT3 (300 nM)*(219, 234)*, our goal is to identify RA14 variants with at least low nM affinities for further testing.

We chose RA14 as our model TCR not only because of convenience, but also because we believe a CD3/RA14 TRIG has a potential therapeutic future. RA14 is a human TCR that recognizes the $pp65_{495\text{-}503}$ peptide (NLVPMVTAV) in the context of

HLA-A*0201, a relatively common HLA*(248)*. Pp65-directed TCRs make up 70-90% of the CTL response to CMV-infected cells*(249)*, suggesting that this antigen is relevant for viral targeting. Indeed, in many immunocompromised patients, the CMV TCR repertoire contains only a handful of conserved sequences, such as RA14, perhaps indicating that only a few CMV TCR clones are needed to control viremia*(248)*.

CMV infects 50-90% of adults worldwide, and while typically asymptomatic or latent in healthy individuals, CMV infection and reactivation is a major cause of morbidity and mortality of transplant recipients and congenitally-infected infants*(125, 250)*. Despite being listed as a top priority for decades, there is still no licensed CMV vaccine*(251)*, and a promising prophylactic antibody mixture from Genentech is no longer in active development*(126)*. Current treatments for high-risk individuals are limited to anti-viral drugs*(250)*, which can have poor safety profiles; and CMV hyperimmunoglobulin to prevent congenital infection, which has debatable efficacy*(252)*. Thus, recombinant proteins like antibodies or TRIGs could be a useful approach for preventing disease*(125)*. We propose that by using a bispecific molecule targeting a surface antigen, such as HLA-A*0201:$pp65_{495\text{-}503}$, and CD3, we can help circulating CTLs target newly infected or reactivating cells immediately rather than targeting virions that are already circulating. One very crude study has been done using chemically-conjugated antiCD3 and CMV hyperimmuneoglobulin, and was able to show that the bispecific conjugates enhanced cytotoxicity*(253)*. We hope that through conscious and creative engineering, the TRIG molecule will offer a new approach to preventing CMV.

ACKNOWLEDGEMENTS

We thank Ahlam Qerqez for soluble TCR-Fc expression, purification, and characterization. We thank Sam Karimaghaei and Cina Karimaghaei for anti-CD3 antibody and soluble CD3 expression, purification, and characterization. We thank Annalee Nguyen for assistance with cell sorting.

Appendix A

SUPPLEMENTARY MATERIALS FOR CHAPTER 2

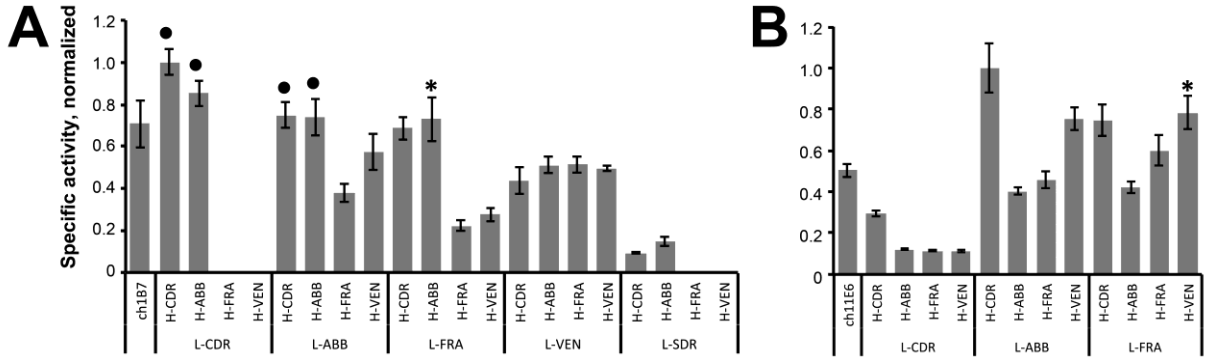

Figure 19. Specific activity of humanized antibody variants.

Humanized variants were designed in silico for each antibody heavy and light chain via five different methods: (a) 'veneering' (ven); (b) 'grafting of abbreviated complementarity determining regions (CDRs)' (abb); (c) 'specificity determining residue-transfer' (sdr); and (d) grafting of intact CDRs onto the hu4D5 framework or (e) a composite framework (fra). All pairwise combinations for a single antibody were transiently transfected into CHO cells. The crude supernatant was then screened for PTx binding activity and total antibody production level by ELISA, with the ratio of these values indicating the specific activity of a given heavy/ light chain combination. A, Screening of hu1B7 and B, hu11E6 variants. Combinations marked with • had high specific activity due to poor expression and were not considered for scale-up. Combinations marked with * were ultimately selected for large-scale production.

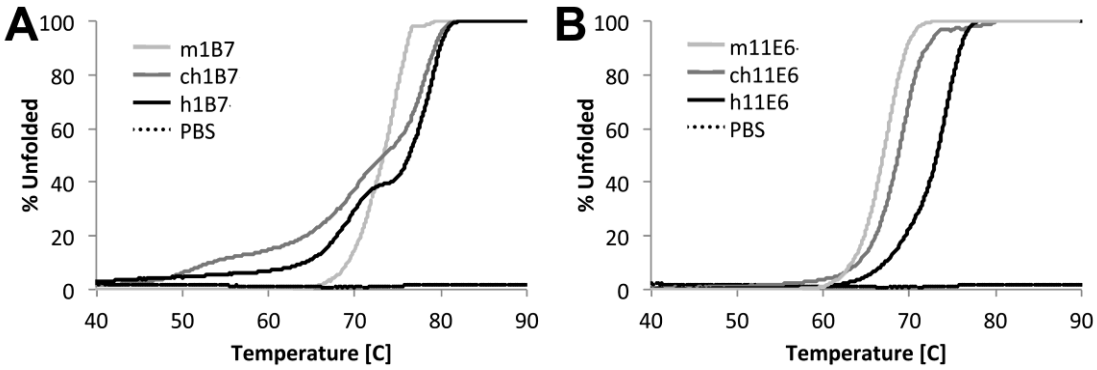

Figure 20. Antibody thermal stability.

Thermal denaturation melting curves for the A, 1B7 and B, 11E6 antibodies, comparing the murine, chimeric and humanized versions.

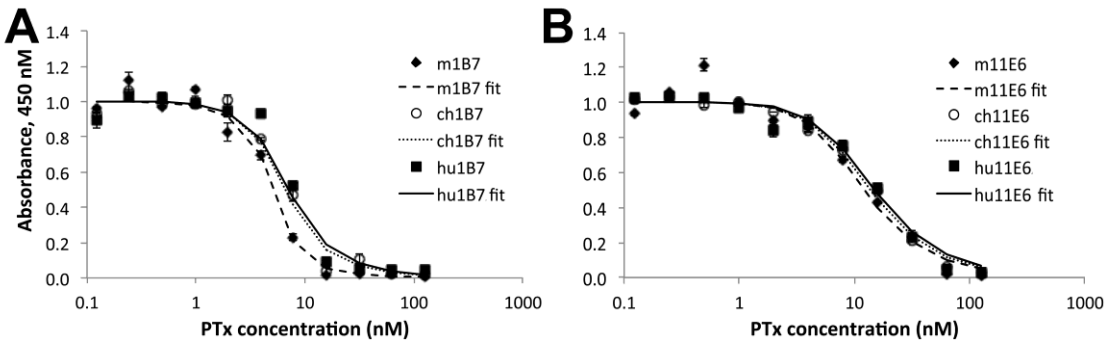

Figure 21. Competition ELISA to assess solution binding affinities of purified antibodies.

A, Comparison of m1B7, ch1B7 and hu1B7 antibodies. B, Comparison of m11E6, ch11E6 and hu11E6 antibodies. Calculated Kd values are reported in Table 1.

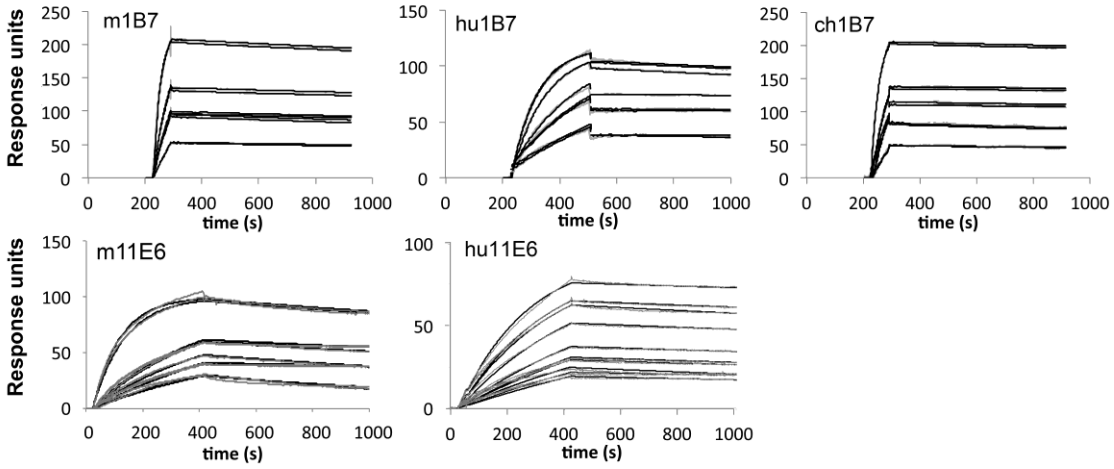

Figure 22. Binding kinetics of antibody-PTx interaction..

Black lines indicate experimental data; gray lines depict model fits. Association and dissociation rates and calculated Kd are reported in Table 1.

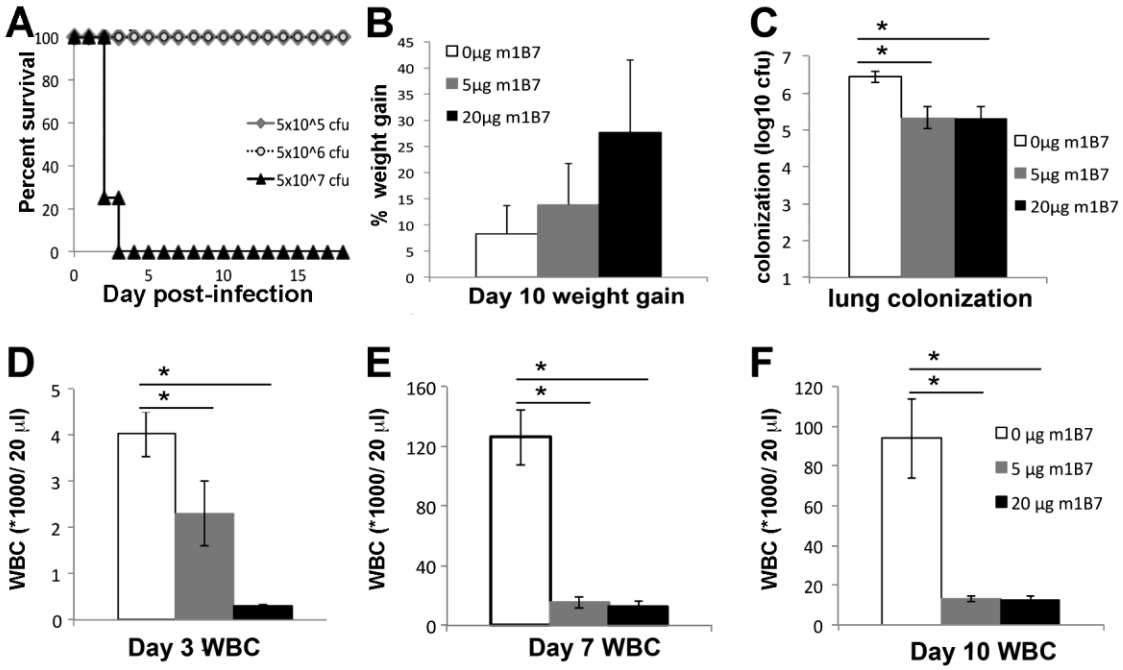

Figure 23. Pilot murine protection data with recent human clinical isolate D420 and murine 1B7.

A, B-F, Dosing study with murine 1B7 to determine antibody concentrations within the dose-response regime. At the study terminus on day 10, mice were monitored for weight gain (B) and bacterial lung colonization rates (C). The CD45+ lymphocyte population was monitored on days 3, 7 and 10. The reported WBC on day 7 are n=2; all others n=4. Statistical significance measured by Tukey's Test, with * indicating $p < 0.05$.

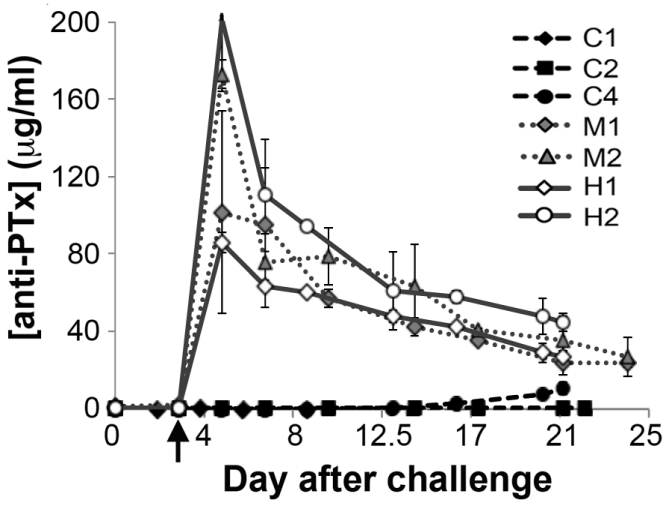

Figure 24. Concentrations of anti-PTx antibodies in baboons.

Baboons were infected on Day 0, and antibodies were administered to the treatment group on Day 3 (indicated by an arrow). Plot shows the serum levels of administered hu1B7+hu11E6 over time in treated animals and the induction of endogenous anti-PTx antibodies in control animals. An equimolar combination of hu1B7 and hu11E6 was used as a reference. Note, serum was not available for animal C3.

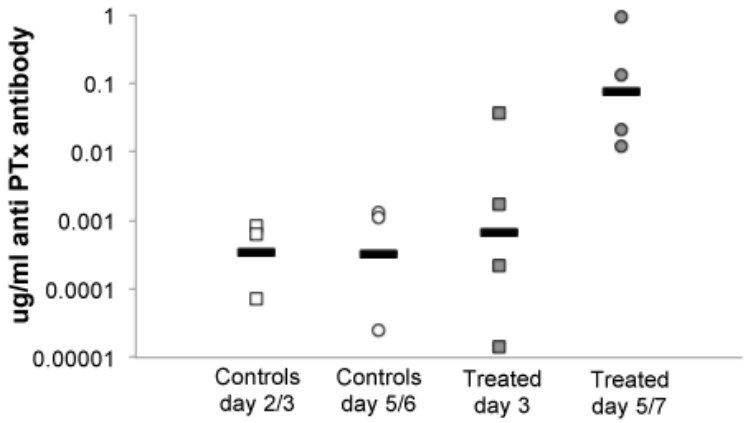

Figure 25. Detection of the hu1B7/hu11E6 combination in the nasopharyngeal wash of baboons.

Nasopharyngeal wash fluid for each baboon was tested for the presence of PTx-binding antibodies by PTx ELISA relative to a pure hu1B7/hu11E6 standard on day 2 or 3 (□ icons) and on day 5, 6, or 7 after infection (○ icons). Icons for control animals have no fill; icons for treated animals have gray fill. Geometric means for each population are shown as black bars.

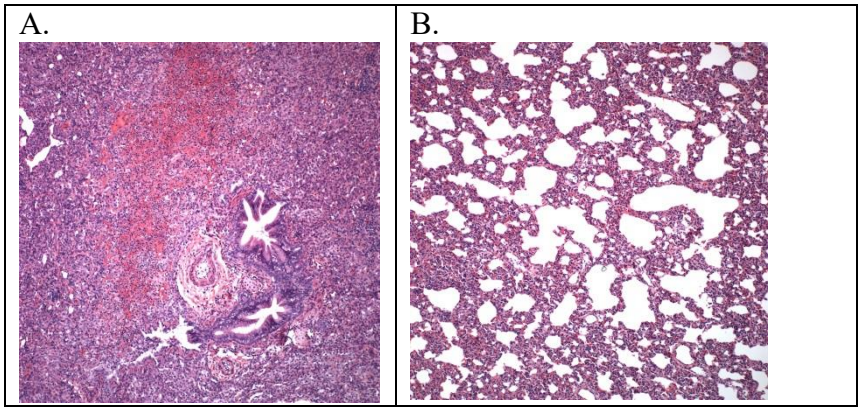

Figure 26. Histopathological analysis of lung tissue.

A, Heavily colonized, moribund animal C2 exhibited gross adhesions and areas of necrosis, probably associated with abscess formation in the lobes. Between 30% (right lobe) and 70% (left lobe) of terminal airways remained patent and were filled with inflammatory cells, primarily alveolar macrophages. The right lung of animal C2 is shown; *B. pertussis* was recovered from the trachea and right lung of this animal. B, Mildly colonized animals exhibited evidence of very mild interstitial pneumonia with no gross lesions, >90% of all terminal airways were partially to totally patent. The right lobe of animal M2 is shown.

Table 5. Humanized antibodies are more similar to the human repertoire than the original murine antibodies.

	Murine antibody Z score	Humanized antibody Z-score
1B7 light chain	-1.055	-0.033
1B7 heavy chain	-1.065	-0.093
11E6 light chain	-1.104	-0.215
11E6 heavy chain	-0.507	+0.086

Table 6. Baboon model challenge details

	Baboon Details			Day 2/3 levels			Day 16/17 levels	
	Day 0 Age (months)	Sex	Day 0 Weight (kg)	WBC (×1000/µl)	Colonization Level	Cough Count (/hr)	WBC (×1000/µl)	Colonization Level
C1	6.5	M	3.0	18	8.0×107	60.0	nd*	nd*
C2	5.9	M	2.1	34	3.0×107	24.0	42.9	4.5×107
C3	8.7	M	3.1	19	2.5×107	12.5	35.0	8.0×104
C4	7.1	F	2.6	28	1.8×107	2.5	24.0	5.0×103
M1	6.0	M	2.9	28	1.5×103	10.0	11.4	0
M2	6.0	M	2.4	23	1.7×104	13.0	7.0	0
H1	6.9	F	2.3	30	3.8×107	102.5	18.9	0
H2	8.3	M	2.3	14	1.3×108	64.0	9.8	0

*nd, not determined as animal was moribund/ removed from study on day 11.

References

1. World Health Organization, Causes of death, worldwide*Glob. Heal. Obs. data Repos.* (2012) (available at http://apps.who.int/gho/data/node.main.CODWORLD?lang=en).

2. D. M. Ecker, S. D. Jones, H. L. Levine, The therapeutic monoclonal antibody market, *MAbs* **7**, 9–14 (2015).

3. S. R. Aggarwal, What's fueling the biotech engine — 2012 to 2013, *Nat. Biotechnol.* **32**, 32–39 (2014).

4. M. Hay, D. W. Thomas, J. L. Craighead, C. Economides, J. Rosenthal, Clinical development success rates for investigational drugs., *Nat Biotechnol* **32**, 40–51 (2014).

5. J. M. Reichert, Therapeutic monoclonal antibodies approved or in review in the European Union or the United States*Antib. Soc.* (2017) (available at http://www.antibodysociety.org/news/approved-antibodies/).

6. The IMpact-RSV Study Group, Palivizumab, a Humanized Respiratory Syncytial Virus Monoclonal Antibody, Reduces Hospitalization From Respiratory Syncytial Virus Infection in High-risk Infants., *Pediatrics* **102**, 531–7 (1998).

7. T. Migone, G. M. Subramanian, J. Zhong, L. M. Healey, a. Corey, M. Devalaraja, L. Lo, S. Ullrich, J. Zimmerman, a. Chen, M. Lewis, G. Meister, K. Gillum, D. Sanford, J. Mott, S. D. Bolmer, Raxibacumab for the treatment of inhalational anthrax, *N. Engl. J. Med.* **361**, 135–144 (2009).

8. B. J. Yamamoto, A. M. Shadiack, S. Carpenter, D. Sanford, L. N. Henning, N. Gonzales, E. O'Connor, L. S. Casey, N. V. Serbina, Obiltoxaximab prevents disseminated Bacillus anthracis infection and improves survival during pre- and postexposure prophylaxis in animal models of inhalational anthrax, *Antimicrob. Agents Chemother.* **60**, 5796–5805 (2016).

9. P. Mitchell, M. Med, C. Wriedt, S. Graves, D. Phil, M. P. Staples, D. Ph, B. Murphy, B. Sc, Treatment with Monoclonal Antibodies against Clostridium difficile Toxins, *N. Engl. J. Med.* **362**, 197–205 (2010).

10. H. Wu, D. S. Pfarr, S. Johnson, Y. A. Brewah, R. M. Woods, N. K. Patel, W. I. White, J. F. Young, P. A. Kiener, Development of Motavizumab, an Ultra-potent Antibody for the Prevention of Respiratory Syncytial Virus Infection in the Upper and Lower Respiratory Tract, *J. Mol. Biol.* **368**, 652–665 (2007).

11. S. Mazumdar, Raxibacumab, *MAbs* **1**, 531–538 (2009).

12. J. a Maynard, C. B. M. Maassen, S. H. Leppla, K. Brasky, J. L. Patterson, B. L. Iverson, G. Georgiou, Protection against anthrax toxin by recombinant antibody fragments correlates with antigen affinity., *Nat. Biotechnol.* **20**, 597–601 (2002).

13. L. D. Hernandez, F. Racine, L. Xiao, E. DiNunzio, N. Hairston, P. R. Sheth, N. J. Murgolo, A. G. Therien, Broad coverage of genetically diverse strains of clostridium difficile by actoxumab and bezlotoxumab predicted by *in vitro* neutralization and epitope

modeling, *Antimicrob. Agents Chemother.* **59**, 1052–1060 (2015).

14. S. M. Lehar, T. Pillow, M. Xu, L. Staben, K. K. Kajihara, R. Vandlen, L. DePalatis, H. Raab, W. L. Hazenbos, J. Hiroshi Morisaki, J. Kim, S. Park, M. Darwish, B.-C. Lee, H. Hernandez, K. M. Loyet, P. Lupardus, R. Fong, D. Yan, C. Chalouni, E. Luis, Y. Khalfin, E. Plise, J. Cheong, J. P. Lyssikatos, M. Strandh, K. Koefoed, P. S. Andersen, J. A. Flygare, M. Wah Tan, E. J. Brown, S. Mariathasan, Novel antibody–antibiotic conjugate eliminates intracellular S. aureus, *Nature* **527**, 323–8 (2015).

15. D. A. Hill, C. Hoffmann, M. C. Abt, Y. Du, D. Kobuley, T. J. Kirn, F. D. Bushman, D. Artis, Metagenomic analyses reveal antibiotic-induced temporal and spatial changes in intestinal microbiota with associated alterations in immune cell homeostasis., *Mucosal Immunol.* **3**, 148–58 (2010).

16. R. A. Britton, V. B. Young, Role of the intestinal microbiota in resistance to colonization by Clostridium difficile, *Gastroenterology* **146**, 1547–1553 (2014).

17. Z. Yang, J. Ramsey, T. Hamza, Y. Zhang, S. Li, H. G. Yfantis, D. Lee, L. D. Hernandez, W. Seghezzi, J. M. Furneisen, N. M. Davis, A. G. Therien, H. Feng, Mechanisms of protection against Clostridium difficile infection by the monoclonal antitoxin antibodies actoxumab and bezlotoxumab, *Infect. Immun.* **83**, 822–831 (2015).

18. A. Hey, History and Practice: Antibodies in Infectious Diseases, *Microbiol. Spectr.* **3**, 1–15 (2015).

19. D. D. Richman, T. Wrin, S. J. Little, C. J. Petropoulos, Rapid evolution of the neutralizing antibody response to HIV type 1 infection., *Proc. Natl. Acad. Sci. U. S. A.* **100**, 4144–9 (2003).

20. E. Medina, D. H. Pieper, Tackling Threats and Future Problems of Multidrug-Resistant Bacteria, *Curr. Top. Microbiol. Immunol.* **398**, 3–33 (2016).

21. A.- Staphylococcus, H. I. Schwartz, T. Bellamy, M. Hernandez-illas, S. Jafri, Safety, Tolerability, and Pharmacokinetics of MEDI4893, an Investigational, Extended-Half-Life, Anti-Staphylococcus aureus Alpha-Toxin Human Monoclonal Antibody, in Healthy Adults, *Antimi* **61**, 1–9 (2017).

22. I. Desombere, S. Fafi-Kremer, F. Van Houtte, P. Pessaux, A. Farhoudi, L. Heydmann, L. Verhoye, S. Cole, J. A. Mckeating, G. Leroux-Roels, T. F. Baumert, A. H. Patel, P. Meuleman, Monoclonal anti-envelope antibody AP33 protects humanized mice against a patient-derived hepatitis C virus challenge, *Hepatology* **63**, 1120–1134 (2016).

23. M. Pelegrin, M. Naranjo-Gomez, M. Piechaczyk, Antiviral Monoclonal Antibodies: Can They Be More Than Simple Neutralizing Agents?, *Trends Microbiol.* **23**, 653–665 (2015).

24. S. Bournazos, F. Klein, J. Pietzsch, M. S. Seaman, M. C. Nussenzweig, J. V. Ravetch, Broadly Neutralizing Anti-HIV-1 Antibodies Require Fc Effector Functions for *In Vivo* Activity, *Cell* **158**, 1243–1253 (2014).

25. N. A.L., D. E., Development trends for human monoclonal antibody therapeutics,

Nat. Rev. Drug Discov. **9**, 767–774 (2010).

26. L. E. McCoy, D. R. Burton, Identification and specificity of broadly neutralizing antibodies against HIV, *Immunol. Rev.* **275**, 11–20 (2017).

27. A. W. Nguyen, E. K. Wagner, J. R. Laber, L. L. Goodfield, W. E. Smallridge, E. T. Harvill, J. F. Papin, R. F. Wolf, E. A. Padlan, A. Bristol, M. Kaleko, J. A. Maynard, A cocktail of humanized anti-pertussis toxin antibodies limits disease in murine and baboon models of whooping cough, *Sci. Transl. Med.* **7**, 1–9 (2015).

28. L. Hua, J. J. Hilliard, Y. Shi, C. Tkaczyk, L. I. Cheng, X. Yu, V. Datta, S. Ren, H. Feng, R. Zinsou, A. Keller, T. O'Day, Q. Du, L. Cheng, M. Damschroder, G. Robbie, J. Suzich, C. K. Stover, B. R. Sellman, Assessment of an anti-alpha-toxin monoclonal antibody for prevention and treatment of Staphylococcus aureus-induced pneumonia, *Antimicrob. Agents Chemother.* **58**, 1108–1117 (2014).

29. G. J. Babcock, T. J. Broering, H. J. Hernandez, R. B. Mandell, K. Donahue, N. Boatright, A. M. Stack, I. Lowy, R. Graziano, D. Molrine, D. M. Ambrosino, W. D. Thomas, Human monoclonal antibodies directed against toxins A and B prevent Clostridium difficile-induced mortality in hamsters, *Infect. Immun.* **74**, 6339–6347 (2006).

30. C. T. Baldari, F. Tonello, S. R. Paccani, C. Montecucco, Anthrax toxins : a paradigm of bacterial immune suppression, **27** (2006), doi:10.1016/j.it.2006.07.002.

31. P. Orth, L. Xiao, L. D. Hernandez, P. Reichert, P. R. Sheth, M. Beaumont, X. Yang, N. Murgolo, G. Ermakov, E. Dinunzio, F. Racine, J. Karczewski, S. Secore, R. N. Ingram, T. Mayhood, C. Strickland, A. G. Therien, Mechanism of action and epitopes of Clostridium difficile toxin B-neutralizing antibody bezlotoxumab revealed by X-ray crystallography, *J. Biol. Chem.* **289**, 18008–18021 (2014).

32. V. Oganesyan, L. Peng, M. M. Damschroder, L. Cheng, A. Sadowska, C. Tkaczyk, B. R. Sellman, H. Wu, W. F. Dall'Acqua, Mechanisms of Neutralization of a Human Anti-α-toxin Antibody, *J. Biol. Chem.* **289**, 29874–29880 (2014).

33. N. Abboud, S.-K. Chow, C. Saylor, A. Janda, J. V Ravetch, M. D. Scharff, A. Casadevall, A requirement for FcγR in antibody-mediated bacterial toxin neutralization., *J. Exp. Med.* **207**, 2395–2405 (2010).

34. N. Mohamed, M. Clagett, J. Li, S. Jones, S. Pincus, G. D'Alia, L. Nardone, M. Babin, G. Spitalny, L. Casey, A high-affinity monoclonal antibody to anthrax protective antigen passively protects rabbits before and after aerosolized Bacillus anthracis spore challenge, *Infect. Immun.* **73**, 795–802 (2005).

35. A. Nowakowski, C. Wang, D. B. Powers, P. Amersdorfer, T. J. Smith, V. A. Montgomery, R. Sheridan, R. Blake, L. A. Smith, J. D. Marks, Potent neutralization of botulinum neurotoxin by recombinant oligoclonal antibody, **99**, 11346–11350 (2002).

36. P. Warrener, R. Varkey, J. C. Bonnell, A. DiGiandomenico, M. Camara, K. Cook, L. Peng, J. Zha, P. Chowdury, B. Sellman, C. K. Stover, A novel anti-PcrV antibody

providing enhanced protection against pseudomonas aeruginosa in multiple animal infection models, *Antimicrob. Agents Chemother.* **58**, 4384–4391 (2014).

37. T. Secher, L. Fauconnier, A. Szade, O. Rutschi, S. C. Fas, B. Ryffel, M. P. Rudolf, Anti-Pseudomonas aeruginosa serotype O11 LPS immunoglobulin M monoclonal antibody panobacumab (KBPA101) confers protection in a murine model of acute lung infection, *J. Antimicrob. Chemother.* **66**, 1100–1109 (2011).

38. Y. A. Que, H. Lazar, M. Wolff, B. François, P. F. Laterre, E. Mercier, J. Garbino, J. L. Pagani, J. P. Revelly, E. Mus, A. Perez, M. Tamm, J. J. Rouby, Q. Lu, J. Chastre, P. Eggimann, Assessment of panobacumab as adjunctive immunotherapy for the treatment of nosocomial Pseudomonas aeruginosa pneumonia, *Eur. J. Clin. Microbiol. Infect. Dis.* **33**, 1861–1867 (2014).

39. J. J. Lim, R. Deng, M. A. Derby, R. Larouche, P. Horn, M. Anderson, M. Maia, S. Carrier, I. Pelletier, T. Burgess, P. Kulkarni, E. Newton, J. A. Tavel, Two Phase 1, Randomized, Double-Blind, Placebo-Controlled, Single-Ascending-Dose Studies To Investigate the Safety, Tolerability, and Pharmacokinetics of an Anti-Influenza A Virus Monoclonal Antibody, MHAA4549A, in Healthy Volunteers, *Antimicrob. Agents Chemother.* **60**, 5437–5444 (2016).

40. K. Ahmad, H. S. Malik, K. Bloom, K. J. Milks, a F. Straight, C. W. Carroll, B. Moree, C. J. Fuller, B. Gronemeyer, W. Lu, E. Eugster, J. E. Tomkiel, H. L. Chang, a Kagami, Y. Watanabe, M. C. Silva, K. M. Godek, L. E. Jansen, V. Kanelis, L. E. Kay, J. R. England, H. P. Yennawar, S. Tan, J. D. Garlick, D. Canzio, G. J. Narlikar, R. E. Kingston, G. H. Leno, S. Orthaus, S. Ohndorf, S. Diekmann, P. Hemmerich, H. Yang, N. Nozaki, T. Okazaki, K. Yoda, D. W. Cleveland, M. E. Lalonde, T. G. Kutateladze, a Kelly, C. Wu, H. Kurumizaka, N. Cancer, Structure of RSV Fusion Glycoprotein, *Science (80-.).* **340**, 1113–1117 (2013).

41. J. S. McLellan, Y. Yang, B. S. Graham, P. D. Kwong, Structure of respiratory syncytial virus fusion glycoprotein in the postfusion conformation reveals preservation of neutralizing epitopes., *J. Virol.* **85**, 7788–96 (2011).

42. L. van Mechelen, W. Luytjes, C. A. M. de Haan, O. Wicht, RSV neutralization by palivizumab, but not by monoclonal antibodies targeting other epitopes, is augmented by Fc gamma receptors, *Antiviral Res.* **132**, 1–5 (2016).

43. C. J. Bruno, J. M. Jacobson, Ibalizumab: An anti-CD4 monoclonal antibody for the treatment of HIV-1 infection, *J. Antimicrob. Chemother.* **65**, 1839–1841 (2010).

44. J. M. Jacobson, J. P. Lalezari, M. A. Thompson, C. J. Fichtenbaum, M. S. Saag, B. S. Zingman, P. D'Ambrosio, N. Stambler, Y. Rotshteyn, A. J. Marozsan, P. J. Maddon, S. A. Morris, W. C. Olson, Phase 2a study of the CCR5 monoclonal antibody PRO 140 administered intravenously to HIV-infected adults, *Antimicrob. Agents Chemother.* **54**, 4137–4142 (2010).

45. M. Rao, D. Valentini, E. Dodoo, A. Zumla, M. Maeurer, Anti-PD-1/PD-L1 therapy for infectious diseases: learning from the cancer paradigm, *Int. J. Infect. Dis.* **56**, 221–228

(2017).

46. A. Zumla, M. Rao, E. Dodoo, M. Maeurer, Potential of immunomodulatory agents as adjunct host-directed therapies for multidrug-resistant tuberculosis., *BMC Med.* **14**, 89 (2016).

47. Y. Delmas, B. Vendrely, B. Clouzeau, H. Bachir, H. N. Bui, A. Lacraz, S. H??lou, C. Bordes, A. Reffet, B. Llanas, S. Skopinski, P. Rolland, D. Gruson, C. Combe, Outbreak of Escherichia coli O104:H4 haemolytic uraemic syndrome in France: Outcome with eculizumab, *Nephrol. Dial. Transplant.* **29**, 565–572 (2014).

48. N. S. Laursen, I. A. Wilson, Broadly neutralizing antibodies against influenza viruses, *Antiviral Res.* **98**, 476–483 (2013).

49. G. Nakamura, N. Chai, S. Park, N. Chiang, Z. Lin, H. Chiu, R. Fong, D. Yan, J. Kim, J. Zhang, W. P. Lee, A. Estevez, M. Coons, M. Xu, P. Lupardus, M. Balazs, L. R. Swem, An *in vivo* human-plasmablast enrichment technique allows rapid identification of therapeutic influenza A antibodies, *Cell Host Microbe* **14**, 93–103 (2013).

50. N. L. Kallewaard, D. Corti, P. J. Collins, U. Neu, J. M. McAuliffe, E. Benjamin, L. Wachter-Rosati, F. J. Palmer-Hill, A. Q. Yuan, P. A. Walker, M. K. Vorlaender, S. Bianchi, B. Guarino, A. De Marco, F. Vanzetta, G. Agatic, M. Foglierini, D. Pinna, B. Fernandez-Rodriguez, A. Fruehwirth, C. Silacci, R. W. Ogrodowicz, S. R. Martin, F. Sallusto, J. A. A. Suzich, A. Lanzavecchia, Q. Zhu, S. J. Gamblin, J. J. Skehel, Structure and Function Analysis of an Antibody Recognizing All Influenza A Subtypes, *Cell* **166**, 596–608 (2016).

51. K. Tharakaraman, V. Subramanian, K. Viswanathan, S. Sloan, H.-L. Yen, D. L. Barnard, Y. H. C. Leung, K. J. Szretter, T. J. Koch, J. C. Delaney, G. J. Babcock, G. N. Wogan, R. Sasisekharan, Z. Shriver, A broadly neutralizing human monoclonal antibody is effective against H7N9., *Proc. Natl. Acad. Sci. U. S. A.* **112**, 10890–5 (2015).

52. S. Zolla-Pazner, T. Cardozo, Structure-function relationships of HIV-1 envelope sequence-variable regions refocus vaccine design., *Nat. Rev. Immunol.* **10**, 527–35 (2010).

53. R. a Buonpane, H. R. O. Churchill, B. Moza, E. J. Sundberg, M. L. Peterson, P. M. Schlievert, D. M. Kranz, Neutralization of staphylococcal enterotoxin B by soluble, high-affinity receptor antagonists., *Nat. Med.* **13**, 725–9 (2007).

54. H. Wu, D. S. Pfarr, Y. Tang, L. L. An, N. K. Patel, J. D. Watkins, W. D. Huse, P. A. Kiener, J. F. Young, Ultra-potent antibodies against respiratory syncytial virus: Effects of binding kinetics and binding valence on viral neutralization, *J. Mol. Biol.* **350**, 126–144 (2005).

55. A. Mejias, C. Garcia-Maurino, R. Rodriguez-Fernandez, M. E. Peeples, O. Ramilo, Development and clinical applications of novel antibodies for prevention and treatment of respiratory syncytial virus infection, *Vaccine* **35**, 496–502 (2016).

56. X.-Z. Wang, V. W. Coljee, J. A. Maynard, Back to the future: recombinant polyclonal

antibody therapeutics., *Curr. Opin. Chem. Eng.* **2**, 1–11 (2013).

57. E. Von Behring, S. Kitasato, Ueber das zustandekommen der diphtherie-immunität und der tetanus-immunität bei thieren, *Dtsch. Medizinische Wochenschrift* **49**, 1113–1114 (1890).

58. S. H. E. Kaufmann, crossm Remembering Emil von Behring : from Tetanus Treatment to Antibody Cooperation with Phagocytes, **8**, 1–6 (2017).

59. A. Casadevall, E. Dadachova, L. Pirofski, Passive antibody therapy for infectious diseases, *Nat. Rev. Microbiol.* **2**, 695–703 (2004).

60. M. a. Keller, E. R. Stiehm, Passive Immunity in Prevention and Treatment of Infectious Diseases, *Clin. Microbiol. Rev.* **13**, 602–614 (2000).

61. E. R. Stiehm, M. A. Keller, G. N. Vyas, Preparation and use of therapeutic antibodies primarily of human origin, *Biologicals* **36**, 363–374 (2008).

62. S. Johnson, C. Oliver, G. A. Prince, V. G. Hemming, S. David, S. Wang, M. Dormitzer, J. O. Grady, S. Koenig, K. James, R. Woods, G. Bansal, D. Couchenour, E. Tsao, W. C. Hall, J. F. Young, S. The, I. Diseases, N. Nov, S. Johnson, C. Oliver, G. A. Prince, V. G. Hemming, D. S. Pfarr, S. Wang, M. Dormitzer, J. O. Grady, S. Koenig, J. K. Tamura, R. Woods, G. Bansal, D. Couchenour, E. Tsao, W. C. Hall, J. F. Young, Development of a Humanized Monoclonal Antibody (MEDI-493) with Potent *in vitro* and *in vivo* Activity against Respiratory Syncytial Virus, *J. Infect. Dis.* **176**, 1215–1224 (1997).

63. H. C. Meissner, S. S. Long, A. A. of P. C. on I. D. and C. on F. and Newborn, Revised indications for the use of palivizumab and respiratory syncytial virus immune globulin intravenous for the prevention of respiratory syncytial virus infections., *Pediatrics* **112**, 1447–1452 (2003).

64. M. Bouvin-Pley, M. Morgand, L. Meyer, C. Goujard, A. Moreau, H. Mouquet, M. Nussenzweig, C. Pace, D. Ho, P. J. Bjorkman, D. Baty, P. Chames, M. Pancera, P. D. Kwong, P. Poignard, F. Barin, M. Braibant, Drift of the HIV-1 envelope glycoprotein gp120 toward increased neutralization resistance over the course of the epidemic: a comprehensive study using the most potent and broadly neutralizing monoclonal antibodies., *J. Virol.* **88**, 13910–7 (2014).

65. R. Kong, M. K. Louder, K. Wagh, R. T. Bailer, A. DeCamp, K. Greene, H. Gao, J. D. Taft, A. Gazumyan, C. Liu, M. C. Nussenzweig, B. Korber, D. C. Montefiori, J. R. Mascola, Improving neutralization potency and breadth by combining broadly reactive HIV-1 antibodies targeting major neutralization epitopes, *J. Virol.* **89**, 2659–71 (2015).

66. M. Shingai, Y. Nishimura, F. Klein, H. Mouquet, O. K. Donau, R. Plishka, A. Buckler-White, M. Seaman, M. Piatak, J. D. Lifson, D. Dimitrov, M. C. Nussenzweig, M. A. Martin, Antibody-mediated immunotherapy of macaques chronically infected with SHIV suppresses viraemia, *Nature* **503**, 277–80 (2013).

67. K. Dutta, A. K. Varshney, M. C. Franklin, M. Goger, X. Wang, B. C. Fries,

Mechanisms mediating enhanced neutralization efficacy of staphylococcal enterotoxin B by combinations of monoclonal antibodies, *J. Biol. Chem.* **290**, 6715–6730 (2015).

68. J. D. Murga, M. Franti, D. C. Pevear, P. J. Maddon, W. C. Olson, Potent antiviral synergy between monoclonal antibody and small-molecule CCR5 inhibitors of human immunodeficiency virus type 1, *Antimicrob. Agents Chemother.* **50**, 3289–3296 (2006).

69. S. K. Rasmussen, H. Naested, C. Muller, A. B. Tolstrup, T. P. Frandsen, Recombinant antibody mixtures: Production strategies and cost considerations, *Arch. Biochem. Biophys.* **526**, 139–145 (2012).

70. D. Corti, J. D. Kearns, Promises and pitfalls for recombinant oligoclonal antibodies-based therapeutics in cancer and infectious disease, *Curr. Opin. Immunol.* **40**, 51–61 (2016).

71. L. S. Nielsen, A. Baer, C. Müller, K. Gregersen, N. T. Mønster, S. K. Rasmussen, D. Weilguny, A. B. Tolstrup, Single-batch production of recombinant human polyclonal antibodies, *Mol. Biotechnol.* **45**, 257–266 (2010).

72. FDA Center for Drug Evaluation and Research, *Guidance for industry: codevelopment of two or more new investigational drugs for use in combination* (2013).

73. V. Irani, A. J. Guy, D. Andrew, J. G. Beeson, P. A. Ramsland, J. S. Richards, Molecular properties of human IgG subclasses and their implications for designing therapeutic monoclonal antibodies against infectious diseases, *Mol. Immunol.* **67**, 171–182 (2015).

74. E. M. Morrison, L. A. Yoo, L. A. Wims, S. L. Chan, E. M. Yoo, L. A. Wims, L. A. Chan, S. L. Morrison, Human IgG2 Can Form Covalent Dimers, *J. Immunol.* **170**, 3134–3138 (2003).

75. M. van der Neut Kolfschoten, Anti-Inflammatory Activity of Human IgG4 Antibodies by Dynamic Fab Arm Exchange, *Science (80-.).* **317**, 1554–1558 (2007).

76. R. J. Brezski, G. Georgiou, Immunoglobulin isotype knowledge and application to Fc engineering, *Curr. Opin. Immunol.* **40**, 62–69 (2016).

77. B. M. Gunn, G. Alter, Modulating Antibody Functionality in Infectious Disease and Vaccination, *Trends Mol. Med.* **22**, 969–982 (2016).

78. D. O. Beenhouwer, E. M. Yoo, C. W. Lai, M. A. Rocha, S. L. Morrison, Human immunoglobulin G2 (IgG2) and IgG4, but not IgG1 or IgG3, protect mice against Cryptococcus neoformans infection, *Infect. Immun.* **75**, 1424–1435 (2007).

79. D. J. DiLillo, G. S. Tan, P. Palese, J. V Ravetch, Broadly neutralizing hemagglutinin stalk-specific antibodies require FcγR interactions for protection against influenza virus *in vivo*., *Nat. Med.* **20**, 143–51 (2014).

80. T. T. Wang, J. Sewatanon, M. J. Memoli, J. Wrammert, S. Bournazos, S. K. Bhaumik, B. A. Pinsky, K. Chokephaibulkit, N. Onlamoon, K. Pattanapanyasat, J. K. Taubenberger, R. Ahmed, J. V. Ravetch, IgG antibodies to dengue enhanced for

FcγRIIIA binding determine disease severity, *Science (80-.).* **355**, 395–398 (2017).

81. M. J. Borrok, S. T. Jung, T. H. Kang, A. F. Monzingo, G. Georgiou, Revisiting the Role of Glycosylation in the Structure of Human IgG Fc, *ACS Chem Biol* **7**, 1596–1602 (2012).

82. R. Jefferis, Glycosylation as a strategy to improve antibody-based therapeutics., *Nat. Rev. Drug Discov.* **8**, 226–34 (2009).

83. T. Li, D. J. DiLillo, S. Bournazos, J. P. Giddens, J. V Ravetch, L. Wang, Modulating IgG effector function by Fc glycan engineering, *Proc. Natl. Acad. Sci.* **114**, 3485–3490 (2017).

84. E. S. Ward, S. C. Devanaboyina, R. J. Ober, Targeting FcRn for the modulation of antibody dynamics, *Mol. Immunol.* **67**, 131–141 (2015).

85. W. F. D. Acqua, R. M. Woods, E. S. Ward, S. R. Palaszynski, N. K. Patel, Y. A. Brewah, H. Wu, P. A. Kiener, S. Langermann, W. F. Dall' Acqua, R. M. Woods, E. S. Ward, S. R. Palaszynski, N. K. Patel, Y. A. Brewah, H. Wu, P. A. Kiener, S. Langermann, W. F. D. Acqua, R. M. Woods, E. S. Ward, S. R. Palaszynski, N. K. Patel, Y. A. Brewah, H. Wu, P. A. Kiener, S. Langermann, Increasing the Affinity of a Human IgG1 for the Neonatal Fc Receptor: Biological Consequences, *J. Immunol.* **169**, 5171–5180 (2002).

86. W. F. Dall'Acqua, P. A. Kiener, H. Wu, Properties of Human IgG1s engineered for enhanced binding to the neonatal Fc Receptor (FcRn), *J. Biol. Chem.* **281**, 23514–23524 (2006).

87. M. P. Griffin, A. A. Khan, M. T. Esser, K. Jensen, T. Takas, M. K. Kankam, T. Villafana, F. Dubovsky, Safety, tolerability, and pharmacokinetics of the respiratory syncytial virus-prefusion F-targeting monoclonal antibody with an extended half-life, MEDI8897, in healthy adults, *Antimicrob. Agents Chemother.* **61**, 1–9 (2017).

88. S. Foss, R. Watkinson, I. Sandlie, L. C. James, J. T. Andersen, TRIM21: A cytosolic Fc receptor with broad antibody isotype specificity, *Immunol. Rev.* **268**, 328–339 (2015).

89. M. Bottermann, H. E. Lode, R. E. Watkinson, S. Foss, I. Sandlie, J. T. Andersen, L. C. James, Antibody-antigen kinetics constrain intracellular humoral immunity, *Sci. Rep.* **6**, 37457 (2016).

90. K. Tsuchikama, Z. An, Antibody-drug conjugates: recent advances in conjugation and linker chemistries, *Protein Cell* , 1–14 (2016).

91. C. Spiess, Q. Zhai, P. J. Carter, Alternative molecular formats and therapeutic applications for bispecific antibodies, *Mol. Immunol.* **67**, 95–106 (2015).

92. E. K. Wagner, X. Wang, A. Bui, J. A. Maynard, D. L. Burns, Ed. Synergistic Neutralization of Pertussis Toxin by a Bispecific Antibody *In Vitro* and *In Vivo*, *Clin. Vaccine Immunol.* **23**, 851–862 (2016).

93. A. DiGiandomenico, A. E. Keller, C. Gao, G. J. Rainey, P. Warrener, M. M. Camara,

J. Bonnell, R. Fleming, B. Bezabeh, N. Dimasi, B. R. Sellman, J. Hilliard, C. M. Guenther, V. Datta, W. Zhao, C. Gao, X.-Q. Yu, J. A. Suzich, C. K. Stover, A multifunctional bispecific antibody protects against Pseudomonas aeruginosa, *Sci. Transl. Med.* **6**, 1–12 (2014).

94. R. Bargou, E. Leo, G. Zugmaier, M. Klinger, M. Goebeler, S. Knop, R. Noppeney, A. Viardot, G. Hess, M. Schuler, H. Einsele, C. Brandl, A. Wolf, P. Kirchinger, P. Klappers, M. Schmidt, G. Riethmüller, C. Reinhardt, P. A. Baeuerle, P. Kufer, Tumor regression in cancer patients by very low doses of a T cell – engaging antibody, *Science (80-.).* **321**, 974–977 (2008).

95. D. D. Sloan, C. Y. K. Lam, A. Irrinki, L. Liu, A. Tsai, C. S. Pace, J. Kaur, J. P. Murry, M. Balakrishnan, P. A. Moore, S. Johnson, J. L. Nordstrom, T. Cihlar, S. Koenig, Targeting HIV Reservoir in Infected CD4 T Cells by Dual-Affinity Re-targeting Molecules (DARTs) that Bind HIV Envelope and Recruit Cytotoxic T Cells, *PLoS Pathog.* **11**, 1–29 (2015).

96. H. Yang, S. Buisson, G. Bossi, Z. Wallace, G. Hancock, C. So, R. Ashfield, A. Vuidepot, T. Mahon, P. Molloy, J. Oates, S. J. Paston, M. Aleksic, N. J. Hassan, B. K. Jakobsen, L. Dorrell, Elimination of Latently HIV-infected Cells from Antiretroviral Therapy-suppressed Subjects by Engineered Immune-mobilizing T-cell Receptors, *Mol. Ther.* **24**, 1913–1925 (2016).

97. S. Sivapalasingam, D. Perez-caballero, M. Houghton, F. Yang, J. D. Davis, B. Gao, G. Geba, Phase 1 study evaluating safety , tolerability , pharmacokinetics and immunogenicity of REGN2222 in healthy adults : an investigational human monoclonal RSV-F antibody for RSV prevention, *IDWeek poster Sess.* (2015).

98. U. F. Power, C. Stortelers, K. Allosery, J. A. Melero, Generation and Characterization of ALX-0171 , a Potent Novel Therapeutic Nanobody for the Treatment of Respiratory Syncytial Virus Infection, *Antimicrob. Agents Chemother.* **60**, 6–13 (2016).

99. K. Dole, F. P. Segal, A. Feire, B. Magnusson, J. C. Rondon, J. Vemula, J. Yu, Y. Pang, P. Pertel, A First-in-Human Study To Assess the Safety and Pharmacokinetics of Monoclonal Antibodies against Human Cytomegalovirus in Healthy Volunteers, *Antimicrob. Agents Chemother.* **60**, 2881–2887 (2016).

100. S. H. Kim, Y. W. Shin, K. W. Hong, K. H. Chang, K. H. Ryoo, S. H. Paik, J. M. Kim, B. Brotman, W. Pfahler, A. M. Prince, Neutralization of hepatitis B virus (HBV) by human monoclonal antibody against HBV surface antigen (HBsAg) in chimpanzees, *Antiviral Res.* **79**, 188–191 (2008).

101. M. M. Soares, S. W. King, P. E. Thorpe, Targeting inside-out phosphatidylserine as a therapeutic strategy for viral diseases., *Nat. Med.* **14**, 1357–62 (2008).

102. S. U. Nayak, J. M. Griffiss, R. McKenzie, E. J. Fuchs, R. A. Jurao, A. T. An, A. Ahene, M. Tomic, C. W. Hendrix, J. M. Zenilman, Safety and pharmacokinetics of XOMA 3AB, A novel mixture of three monoclonal antibodies against botulinum toxin A, *Antimicrob. Agents Chemother.* **58**, 5047–5053 (2014).

103. T. Huynh, M. Stecher, J. Mckinnon, N. Jung, M. E. Rupp, C. H. System, Safety and Tolerability of 514G3, a True Human Anti-Protein A Monoclonal Antibody for the Treatment of S. aureus Bacteremia, *IDWeek poster Sess.* (2016), doi:10.1007/978-3-319-24741-0_8.

104. A. Pharmaceuticals, AR-301: Fully Human mAb Against Staphylococcus aureus (2017) (available at http://www.aridispharma.com/ar301.htm).

105. H. Rouha, A. Badarau, Z. C. Visram, M. B. Battles, B. Prinz, Z. Magyarics, G. Nagy, I. Mirkina, L. Stulik, M. Zerbs, M. Jägerhofer, B. Maierhofer, A. Teubenbacher, I. Dolezilkova, K. Gross, S. Banerjee, G. Zauner, S. Malafa, J. Zmajkovic, S. Maier, R. Mabry, E. Krauland, K. D. Wittrup, T. U. Gerngross, E. Nagy, Five birds, one stone: Neutralization of α-hemolysin and 4 bi-component leukocidins of Staphylococcus aureus with a single human monoclonal antibody, *MAbs* **7**, 243–254 (2015).

106. G. B. Pier, D. Boyer, M. Preston, F. T. Coleman, N. Llosa, S. Mueschenborn-Koglin, C. Theilacker, H. Goldenberg, J. Uchin, G. P. Priebe, M. Grout, M. Posner, L. Cavacini, Human monoclonal antibodies to Pseudomonas aeruginosa alginate that protect against infection by both mucoid and nonmucoid strains., *J. Immunol.* **173**, 5671–5678 (2004).

107. J. M. Jacobson, D. R. Kuritzkes, E. Godofsky, E. DeJesus, J. A. Larson, S. P. Weinheimer, S. T. Lewis, Safety, pharmacokinetics, and antiretroviral activity of multiple doses of ibalizumab (formerly TNX-355), an anti-CD4 monoclonal antibody, in human immunodeficiency virus type 1-infected adults, *Antimicrob. Agents Chemother.* **53**, 450–457 (2009).

108. C. Wang, W. Wong, H. Tsai, Y. Chen, M. Liao, S. Lynn, A Phase 2 Open-Label Trial of Antibody UB-421 Monotherapy as a Substitute for HAART, *Conf. Retrovir. Opportunistic Infect.* **Poster ses** (2017).

109. K. J. Bar, M. C. Sneller, L. J. Harrison, J. S. Justement, E. T. Overton, M. E. Petrone, D. B. Salantes, C. A. Seamon, B. Scheinfeld, R. W. Kwan, G. H. Learn, M. A. Proschan, E. F. Kreider, J. Blazkova, M. Bardsley, E. W. Refsland, M. Messer, K. E. Clarridge, N. B. Tustin, P. J. Madden, K. Oden, S. J. O'Dell, B. Jarocki, A. R. Shiakolas, R. L. Tressler, N. A. Doria-Rose, R. T. Bailer, J. E. Ledgerwood, E. V. Capparelli, R. M. Lynch, B. S. Graham, S. Moir, R. A. Koup, J. R. Mascola, J. A. Hoxie, A. S. Fauci, P. Tebas, T.-W. Chun, Effect of HIV Antibody VRC01 on Viral Rebound after Treatment Interruption, *N. Engl. J. Med.* **375**, 2037–2050 (2016).

110. S.-Y. Ko, A. Pegu, R. S. Rudicell, Z. Yang, M. G. Joyce, X. Chen, K. Wang, S. Bao, T. D. Kraemer, T. Rath, M. Zeng, S. D. Schmidt, J.-P. Todd, S. R. Penzak, K. O. Saunders, M. C. Nason, A. T. Haase, S. S. Rao, R. S. Blumberg, J. R. Mascola, G. J. Nabel, Enhanced neonatal Fc receptor function improves protection against primate SHIV infection., *Nature* **514**, 642–5 (2014).

111. J. F. Scheid, J. A. Horwitz, Y. Bar-On, E. F. Kreider, C.-L. Lu, J. C. C. Lorenzi, A. Feldmann, M. Braunschweig, L. Nogueira, T. Oliveira, I. Shimeliovich, R. Patel, L.

Burke, Y. Z. Cohen, S. Hadrigan, A. Settler, M. Witmer-Pack, A. P. West, Jr., B. Juelg, T. Keler, T. Hawthorne, B. Zingman, R. M. Gulick, N. Pfeifer, G. H. Learn, M. S. Seaman, P. J. Bjorkman, F. Klein, S. J. Schlesinger, B. D. Walker, B. H. Hahn, M. C. Nussenzweig, M. Caskey, HIV-1 antibody 3BNC117 suppresses viral rebound in humans during treatment interruption, *Nature* **535**, 556–560 (2016).

112. M. Caskey, T. Schoofs, H. Gruell, A. Settler, T. Karagounis, E. F. Kreider, B. Murrell, N. Pfeifer, L. Nogueira, T. Y. Oliveira, G. H. Learn, Y. Z. Cohen, C. Lehmann, D. Gillor, I. Shimeliovich, C. Unson-O'Brien, D. Weiland, A. Robles, T. Kümmerle, C. Wyen, R. Levin, M. Witmer-Pack, K. Eren, C. Ignacio, S. Kiss, A. P. West, H. Mouquet, B. S. Zingman, R. M. Gulick, T. Keler, P. J. Bjorkman, M. S. Seaman, B. H. Hahn, G. Fätkenheuer, S. J. Schlesinger, M. C. Nussenzweig, F. Klein, Antibody 10-1074 suppresses viremia in HIV-1-infected individuals, *Nat. Med.* **23**, 185–191 (2017).

113. J. Julien, S. Wang, A. Ramos, S. Fling, C. Wong, S. Phogat, T. Wrin, M. D. Simek, Broad neutralization coverage of HIV by multiple highly potent antibodies, *Nature* **477**, 466–470 (2012).

114. R. Diskin, J. F. Scheid, P. M. Marcovecchio, A. P. West, F. Klein, H. Gao, P. N. P. Gnanapragasam, A. Abadir, M. S. Seaman, M. C. Nussenzweig, P. J. Bjorkman, Increasing the potency and breadth of an HIV antibody by using structure-based rational design., *Science* **334**, 1289–93 (2011).

115. C. J. Costanzo, thesis, (2015).

116. D. C. Ekiert, R. H. E. Friesen, G. Bhabha, T. Kwaks, M. Jongeneelen, W. Yu, C. Ophorst, F. Cox, H. J. W. M. Korse, B. Brandenburg, R. Vogels, J. P. J. Brakenhoff, R. Kompier, M. H. Koldijk, L. A. H. M. Cornelissen, L. L. M. Poon, M. Peiris, W. Koudstaal, I. A. Wilson, J. Goudsmit, A Highly Conserved Neutralizing Epitope on Group 2 Influenza A Viruses, *Science (80-.).* **333**, 843–850 (2011).

117. D. C. Ekiert, G. Bhabha, M. Elsliger, R. H. E. Friesen, M. Jongeneelen, M. Throsby, J. Goudsmit, I. A. Wilson, Antibody recognition of a highly conserved influenza virus epitope, *Science (80-.).* **324**, 246–251 (2009).

118. A. M. Wollacott, M. F. Boni, K. J. Szretter, S. E. Sloan, M. Yousofshahi, K. Viswanathan, S. Bedard, C. A. Hay, P. F. Smith, Z. Shriver, J. M. Trevejo, Safety and Upper Respiratory Pharmacokinetics of the Hemagglutinin Stalk-Binding Antibody VIS410 Support Treatment and Prophylaxis Based on Population Modeling of Seasonal Influenza A Outbreaks, *EBioMedicine* **5**, 147–155 (2016).

119. E. Sparrow, M. Friede, M. Sheikh, S. Torvaldsen, A. T. Newall, Passive immunization for influenza through antibody therapies, a review of the pipeline, challenges and potential applications, *Vaccine* **34**, 5442–5448 (2016).

120. E. L. Ramos, J. L. Mitcham, T. D. Koller, A. Bonavia, D. W. Usner, G. Balaratnam, P. Fredlund, K. M. Swiderek, Efficacy and safety of treatment with an anti-M2e monoclonal antibody in experimental human influenza, *J. Infect. Dis.* **211**, 1038–1044 (2015).

121. PREVAIL II Writing Group, Multi-National PREVAIL II Study Team, A Randomized, Controlled Trial of ZMapp for Ebola Virus Infection., *N. Engl. J. Med.* **375**, 1448–1456 (2016).

122. M. Bitzan, R. Poole, M. Mehran, E. Sicard, C. Brockus, C. Thuning-Roberson, M. Rivière, Safety and pharmacokinetics of chimeric anti-shiga toxin 1 and anti-shiga toxin 2 monoclonal antibodies in healthy volunteers, *Antimicrob. Agents Chemother.* **53**, 3081–3087 (2009).

123. T. K. Hart, M. N. Blackburn, M. Brigham-Burke, K. Dede, N. Al-Mahdi, P. Zia-Amirhosseini, R. M. Cook, Preclinical efficacy and safety of pascolizumab (SB 240683): A humanized anti-interleukin-4 antibody with therapeutic potential in asthma, *Clin. Exp. Immunol.* **130**, 93–100 (2002).

124. D. Gardiner, J. Lalezari, E. Lawitz, M. DiMicco, R. Ghalib, K. R. Reddy, K. M. Chang, M. Sulkowski, S. O. Marro, J. Anderson, B. He, V. Kansra, F. McPhee, M. Wind-Rotolo, D. Grasela, M. Selby, A. J. Korman, I. Lowy, A Randomized, Double-Blind, Placebo-Controlled Assessment of BMS-936558, a Fully Human Monoclonal Antibody to Programmed Death-1 (PD-1), in Patients with Chronic Hepatitis C Virus Infection, *PLoS One* **8** (2013), doi:10.1371/journal.pone.0063818.

125. E. Acquaye-seedah, Z. P. Frye, J. A. Maynard, Immunotherapeutic Approaches To Prevent Cytomegalovirus-Mediated Disease, *Microbiol. Spectr.* **2**, 1–14 (2013).

126. J. H. Ishida, A. Patel, A. K. Mehta, P. Gatault, J. M. McBride, T. Burgess, M. A. Derby, D. R. Snydman, B. Emu, B. Feierbach, A. E. Fouts, M. Maia, R. Deng, C. M. Rosenberger, L. A. Gennaro, N. S. Striano, X. C. Liao, J. A. Tavel, Phase 2 Randomized, Double-Blind, Placebo-Controlled Trial of RG7667, a Combination Monoclonal Antibody, for Prevention of Cytomegalovirus Infection in High-Risk Kidney Transplant Recipients, *Antimicrob. Agents Chemother.* **61**, 1–11 (2016).

127. T. J. Gardner, K. R. Stein, J. A. Duty, T. M. Schwarz, V. M. Noriega, T. Kraus, T. M. Moran, D. Tortorella, Functional screening for anti-CMV biologics identifies a broadly neutralizing epitope of an essential envelope protein, *Nat. Commun.* **7**, 13627 (2016).

128. Y.-W. Shin, K.-H. Ryoo, K.-W. Hong, K.-H. Chang, J.-S. Choi, M. So, P.-K. Kim, J.-Y. Park, K.-T. Bong, S.-H. Kim, Human monoclonal antibody against Hepatitis B virus surface antigen (HBsAg)., *Antiviral Res.* **75**, 113–20 (2007).

129. S. Liu, Y. Zhang, M. Moayeri, J. Liu, D. Crown, R. J. Fattah, A. N. Wein, Z.-X. Yu, T. Finkel, S. H. Leppla, Key tissue targets responsible for anthrax-toxin-induced lethality., *Nature* **501**, 63–68 (2013).

130. B. Wang, C. H. Lee, E. L. Johnson, C. A. Kluwe, J. C. Cunningham, H. Tanno, R. M. Crooks, G. Georgiou, A. D. Ellington, Discovery of high affinity anti-ricin antibodies by B cell receptor sequencing and by yeast display of combinatorial VH:VL libraries from immunized animals, *MAbs* **8**, 1035–1044 (2016).

131. 1 Peter D. Kwong1 Tongqing Zhou,1 Ivelin Georgiev,1* Xueling Wu,1* Zhi-Yong

Yang,1* Kaifan Dai,1 Andrés Finzi,2 Young Do Kwon,1 Johannes F. Scheid,3 Wei Shi,1 Ling Xu,1 Yongping Yang,1 Jiang Zhu,1 Michel C. Nussenzweig,3 Joseph Sodroski,2,4 Lawrence Shapiro,1,5 Gary J. Nab, Structural Basis for Broad and Potent Neutralization ofHIV-1 byAntibody VRC01, *Science (80-.).* **120** (2010).

132. X. Qiu, G. Wong, J. Audet, A. Bello, L. Fernando, J. B. Alimonti, H. Fausther-Bovendo, H. Wei, J. Aviles, E. Hiatt, A. Johnson, J. Morton, K. Swope, O. Bohorov, N. Bohorova, C. Goodman, D. Kim, M. H. Pauly, J. Velasco, J. Pettitt, G. G. Olinger, K. Whaley, B. Xu, J. E. Strong, L. Zeitlin, G. P. Kobinger, Reversion of advanced Ebola virus disease in nonhuman primates with ZMapp, *Nature* **514**, 47–53 (2014).

133. J. de Kruif, A. B. H. Bakker, W. E. Marissen, R. A. Kramer, M. Throsby, C. E. Rupprecht, J. Goudsmit, A Human Monoclonal Antibody Cocktail as a Novel Component of Rabies Postexposure Prophylaxis, *Annu. Rev. Med.* **58**, 359–368 (2007).

134. S. S. Hasan, A. Miller, G. Sapparapu, E. Fernandez, T. Klose, F. Long, A. Fokine, J. C. Porta, W. Jiang, M. S. Diamond, J. E. Crowe Jr., R. J. Kuhn, M. G. Rossmann, A human antibody against Zika virus crosslinks the E protein to prevent infection, *Nat. Commun.* **8**, 14722 (2017).

135. K. E. Pascal, C. M. Coleman, A. O. Mujica, V. Kamat, A. Badithe, J. Fairhurst, C. Hunt, J. Strein, A. Berrebi, J. M. Sisk, K. L. Matthews, R. Babb, G. Chen, K.-M. V. Lai, T. T. Huang, W. Olson, G. D. Yancopoulos, N. Stahl, M. B. Frieman, C. A. Kyratsous, Pre- and postexposure efficacy of fully human antibodies against Spike protein in a novel humanized mouse model of MERS-CoV infection, *Proc. Natl. Acad. Sci.* **112**, 8738–8743 (2015).

136. C. E. Mire, J. B. Geisbert, V. Borisevich, K. A. Fenton, K. N. Agans, A. I. Flyak, D. J. Deer, H. Steinkellner, O. Bohorov, N. Bohorova, C. Goodman, A. Hiatt, D. H. Kim, M. H. Pauly, J. Velasco, K. J. Whaley, J. E. Crowe, L. Zeitlin, T. W. Geisbert, Therapeutic treatment of Marburg and Ravn virus infection in nonhuman primates with a human monoclonal antibody, *Sci. Transl. Med.* **9**, 1–9 (2017).

137. J. D. Cherry, J. Heitman, Ed. Pertussis: Challenges Today and for the Future, *PLoS Pathog.* **9**, e1003418 (2013).

138. R. E. Black, S. Cousens, H. L. Johnson, J. E. Lawn, I. Rudan, D. G. Bassani, P. Jha, H. Campbell, C. F. Walker, R. Cibulskis, T. Eisele, L. Liu, C. Mathers, Global, regional, and national causes of child mortality in 2008: a systematic analysis, *Lancet* **375**, 1969–1987 (2010).

139. C. D. Paddock, G. N. Sanden, J. D. Cherry, A. A. Gal, C. Langston, K. M. Tatti, K.-H. Wu, C. S. Goldsmith, P. W. Greer, J. L. Montague, M. T. Eliason, R. C. Holman, J. Guarner, W.-J. Shieh, S. R. Zaki, Pathology and Pathogenesis of Fatal Bordetella pertussis Infection in Infants, *Clin. Infect. Dis.* **47**, 328–338 (2008).

140. D. Nieves, J. S. Bradley, J. Gargas, W. H. Mason, D. Lehman, S. M. Lehman, E. L. Murray, K. Harriman, J. D. Cherry, Exchange Blood Transfusion In The Management Of Severe Pertussis In Young Infants, *Pediatr. Infect. Dis. J.* **32**, 698–699 (2013).

141. J. M. Warfel, L. I. Zimmerman, T. J. Merkel, Acellular pertussis vaccines protect against disease but fail to prevent infection and transmission in a nonhuman primate model, *Proc. Natl. Acad. Sci.* **111**, 787–792 (2014).

142. J. B. Robbins, R. Schneerson, J. M. Keith, M. A. Miller, J. Kubler-Kielb, B. Trollfors, Pertussis Vaccine: A critique, *Pediatr. Infect. Dis. J.* **28**, 237–241 (2009).

143. A. A. Weiss, E. L. Hewlett, G. A. Myers, S. Falkow, Pertussis Toxin and Extracytoplasmic Adenylate Cyclase as Virulence Factors of Bordetella pertussis, *J. Infect. Dis.* **150**, 219–222 (1984).

144. C. Andreasen, N. H. Carbonetti, Pertussis Toxin Inhibits Early Chemokine Production To Delay Neutrophil Recruitment in Response to Bordetella pertussis Respiratory Tract Infection in Mice, *Infect. Immun.* **76**, 5139–5148 (2008).

145. G. S. Kirimanjeswara, Pertussis toxin inhibits neutrophil recruitment to delay antibody-mediated clearance of Bordetella pertussis, *J. Clin. Invest.* **115**, 3594–3601 (2005).

146. G. Fedele, M. Bianco, A.-S. Debrie, C. Locht, C. M. Ausiello, Attenuated Bordetella pertussis Vaccine Candidate BPZE1 Promotes Human Dendritic Cell CCL21-Induced Migration and Drives a Th1/Th17 Response, *J. Immunol.* **186**, 5388–5396 (2011).

147. H.-H. MU, M. A. COOLEY, W. A. SEWELL, Studies on the lymphocytosis induced by pertussis toxin, *Immunol. Cell Biol.* **72**, 267–270 (1994).

148. B. Thierry-Carstensen, T. Dalby, M. A. Stevner, J. B. Robbins, R. Schneerson, B. Trollfors, Experience with monocomponent acellular pertussis combination vaccines for infants, children, adolescents and adults—A review of safety, immunogenicity, efficacy and effectiveness studies and 15 years of field experience, *Vaccine* **31**, 5178–5191 (2013).

149. J. Storsaeter, H. O. Hallander, L. Gustafsson, P. Olin, Low levels of antipertussis antibodies plus lack of history of pertussis correlate with susceptibility after household exposure to Bordetella pertussis, *Vaccine* **21**, 3542–3549 (2003).

150. M. Granstrom, K. Hanngren, A. M. Olinder-Nielson, P. Holmblad, A. Mark, Specific immunoglobulin for treatment of whooping cough, *Lancet* **338**, 1230–1233 (1991).

151. J. B. Bruss, R. Malley, S. Halperin, S. Dobson, M. Dhalla, J. McIver, G. R. Siber, Treatment of severe pertussis: a study of the safety and pharmacology of intravenous pertussis immunoglobulin, *Pediatr. Infect. Dis. J.* **18**, 505–511 (1999).

152. S. A. Halperin, W. Vaudry, F. D. Boucher, K. Mackintosh, T. B. Waggener, B. Smith, Is pertussis immune globulin efficacious for the treatment of hospitalized infants with pertussis?, *Pediatr. Infect. Dis. J.* **26**, 79–90 (2007).

153. H. Sato, Y. Sato, Protective activities in mice of monoclonal antibodies against pertussis toxin, *Infect. Immun.* **58**, 3369–3374 (1990).

154. Y. Sato, A. Ito, I. Ohishi, Effect of monoclonal antibody to pertussis toxin on toxin activity, *Infect. Immun.* **55**, 909–915 (1987).

155. J. M. Warfel, J. Beren, V. K. Kelly, G. Lee, T. J. Merkel, Nonhuman Primate Model of Pertussis, *Infect. Immun.* **80**, 1530–1536 (2012).

156. X. Wang, M. Gray, E. Hewlett, J. A. Maynard, The Bordetella adenylate cyclase repeat-in-toxin (RTX) domain is immunodominant and elicits neutralizing antibodies, *J. Biol. Chem.* **290**, 3576–3591 (2015).

157. J. N. Sutherland, J. a Maynard, Characterization of a Key Neutralizing Epitope on Pertussis Toxin Recognized by Monoclonal Antibody 1B7, *Biochemistry* **48**, 11982–11993 (2009).

158. M. Nishida, N. Uematsu, H. Kobayashi, Y. Matsunaga, S. Ishida, M. Takata, O. Niwa, E. A. Padlan, R. Newman, BM-ca is a newly defined type I/II anti-CD20 monoclonal antibody with unique biological properties, *Int. J. Oncol.* **38**, 335–344 (2011).

159. P. Martineau, in *Antibody Engineering*, (2010), vol. 1, pp. 657–665.

160. C. J. Boinett, S. R. Harris, G. C. Langridge, E. A. Trainor, T. J. Merkel, J. Parkhill, Complete Genome Sequence of Bordetella pertussis D420, *Genome Announc.* **3**, e00657-15 (2015).

161. M. A. Miller, T. A. Khan, K. J. Kaczorowski, B. K. Wilson, A. K. Dinin, A. U. Borwankar, M. A. Rodrigues, T. M. Truskett, K. P. Johnston, J. A. Maynard, Antibody nanoparticle dispersions formed with mixtures of crowding molecules retain activity and *In Vivo* bioavailability, *J. Pharm. Sci.* **101**, 3763–3778 (2012).

162. K. R. Abhinandan, A. C. R. Martin, Analyzing the "Degree of Humanness" of Antibody Sequences, *J. Mol. Biol.* **369**, 852–862 (2007).

163. K. H. G. Mills, M. Ryan, E. Ryan, B. P. Mahon, A Murine Model in Which Protection Correlates with PertussisVaccine Efficacy in Children Reveals Complementary Rolesfor Humoral and Cell-Mediated Immunity inProtection against Bordetella pertussis, *Infect. Immun.* **66**, 594–602 (1998).

164. N. H. Carbonetti, G. V Artamonova, R. M. Mays, Z. E. V Worthington, Pertussis Toxin Plays an Early Role in Respiratory Tract Colonization by Bordetella pertussis, *Infect. Immun.* **71**, 6358–6366 (2003).

165. S. Mattoo, J. D. Cherry, Molecular Pathogenesis, Epidemiology, and Clinical Manifestations of Respiratory Infections Due to Bordetella pertussis and Other Bordetella Subspecies, *Clin. Microbiol. Rev.* **18**, 326–382 (2005).

166. A. C. Moguinness, W. L. Bradford, J. G. Armstrong, The Production and Use of Hyperimmune Human Whooping Cough Serum, *J. Pediatr.* **16**, 21–29 (1940).

167. H. Macdonald, E. Macdonald, Experimental Pertussis, *J. Infect. Dis.* **53**, 328–330 (1933).

168. J. M. Warfel, J. Beren, T. J. Merkel, Airborne transmission of bordetella pertussis, *J. Infect. Dis.* **206**, 902–906 (2012).

169. E. M. Goebel, X. Zhang, E. T. Harvill, Bordetella pertussis infection or vaccination substantially protects mice against B. bronchiseptica infection, *PLoS One* **4** (2009), doi:10.1371/journal.pone.0006778.

170. S. Alonso, K. Pethe, N. Mielcarek, D. Raze, C. Locht, Role of ADP-Ribosyltransferase Activity of Pertussis Toxin in Toxin- Adhesin Redundancy with Filamentous Hemagglutinin during *Bordetella pertussis* Infection, *Infect. Immun.* **69**, 6038–6043 (2001).

171. W. E. Smallridge, O. Y. Rolin, N. T. Jacobs, E. T. Harvill, Different effects of whole-cell and acellular vaccines on Bordetella transmission, *J. Infect. Dis.* **209**, 1981–1988 (2014).

172. C. M. Healy, N. Ng, R. S. Taylor, M. A. Rench, L. S. Swaim, Tetanus and diphtheria toxoids and acellular pertussis vaccine uptake during pregnancy in a metropolitan tertiary care center, *Vaccine* **33**, 4983–4987 (2015).

173. M. Housey, F. Zhang, C. Miller, S. Lyon-Callo, J. McFadden, E. Garcia, R. Potter, Vaccination with Tetanus, Diphtheria, and Acellular Pertussis Vaccine of Pregnant Women Enrolled in Medicaid — Michigan, 2011–2013, *MMWR Morb. Mortal. Wkly. Rep.* **63**, 839–842 (2014).

174. B. Abu Raya, I. Srugo, A. Kessel, M. Peterman, D. Bader, R. Gonen, E. Bamberger, The effect of timing of maternal tetanus, diphtheria, and acellular pertussis (Tdap) immunization during pregnancy on newborn pertussis antibody levels - A prospective study, *Vaccine* **32**, 5787–5793 (2014).

175. J. M. Warfel, J. F. Papin, R. F. Wolf, L. I. Zimmerman, T. J. Merkel, Maternal and neonatal vaccination protects newborn baboons from pertussis infection, *J. Infect. Dis.* **210**, 604–610 (2014).

176. G. J. Robbie, R. Criste, W. F. Dall'Acqua, K. Jensen, N. K. Patel, G. A. Losonsky, M. P. Griffin, A novel investigational Fc-modified humanized monoclonal antibody, motavizumab-YTE, has an extended half-life in healthy adults, *Antimicrob. Agents Chemother.* **57**, 6147–6153 (2013).

177. Australian Government Department of Health, Notifiable diseases surveillance, 1917 to 1991 (2003) (available at https://www.health.gov.au/internet/main/publishing.nsf/Content/cda-pubs-annlrpt-oz_dis19_91.htm-copy3).

178. P. J. Spokes, H. E. Quinn, J. M. McAnulty, Review of the 2008–2009 pertussis epidemic in NSW: notifications and hospitalisations, *N. S. W. Public Health Bull.* **21**, 167–173 (2010).

179. S. L. Sheridan, K. Frith, T. L. Snelling, K. Grimwood, P. B. McIntyre, S. B. Lambert, Waning vaccine immunity in teenagers primed with whole cell and acellular

pertussis vaccine: recent epidemiology, *Expert Rev. Vaccines* **13**, 1081–1106 (2014).

180. F. R. Mooi, N. a T. Van Der Maas, H. E. De Melker, Pertussis resurgence: waning immunity and pathogen adaptation - two sides of the same coin, *Epidemiol. Infect.* **142**, 685–694 (2014).

181. K. Winter, J. Zipprich, K. Harriman, E. L. Murray, J. Gornbein, S. J. Hammer, N. Yeganeh, K. Adachi, J. D. Cherry, Risk factors associated with infant deaths from pertussis: a case-control study, *Clin. Infect. Dis.* **61**, 1099–1106 (2015).

182. A. Digiandomenico, A. E. Keller, C. Gao, G. J. Rainey, P. Warrener, M. M. Camara, J. Bonnell, R. Fleming, B. Bezabeh, N. Dimasi, B. R. Sellman, J. Hilliard, C. M. Guenther, V. Datta, W. Zhao, C. Gao, X. Yu, J. A. Suzich, C. K. Stover, A multifunctional bispecific antibody protects against Pseudomonas aeruginosa, *Sci. Transl. Med.* **6**, 1–12 (2014).

183. S. Bournazos, A. Gazumyan, M. S. Seaman, M. C. Nussenzweig, J. V Ravetch, Bispecific anti-HIV-1 antibodies with enhanced breadth and potency, *Cell* **165**, 1609–1620 (2016).

184. J. B. B. Ridgway, L. G. Presta, P. Carter, "Knobs-into-holes" engineering of antibody CH3 domains for heavy chain heterodimerization., *Protein Eng.* **9**, 617–621 (1996).

185. K. Smith, L. Garman, J. Wrammert, N.-Y. Zheng, J. D. Capra, R. Ahmed, P. C. Wilson, Rapid generation of fully human monoclonal antibodies specific to a vaccinating antigen, *Nat. Protoc.* **4**, 372–384 (2009).

186. A. F. Labrijn, J. I. Meesters, B. E. C. G. de Goeij, E. T. J. van den Bremer, J. Neijssen, M. D. van Kampen, K. Strumane, S. Verploegen, A. Kundu, M. J. Gramer, P. H. C. van Berkel, J. G. J. van de Winkel, J. Schuurman, P. W. H. I. Parren, Efficient generation of stable bispecific IgG1 by controlled Fab-arm exchange., *Proc. Natl. Acad. Sci. U. S. A.* **110**, 5145–50 (2013).

187. A. Sivasubramanian, A. Sircar, S. Chaudhury, J. Gray, Toward high-resolution homology modeling of antibody Fv regions and application of antibody-antigen docking, *Proteins* **74**, 497–514 (2009).

188. S. Lyskov, F. Chou, S. Conchuir, B. Der, K. Drew, D. Kuroda, J. Xu, B. Weitzner, P. Renfrew, P. Sripakdeevong, B. Borgo, J. Havranek, B. Kuhlman, T. Kortemme, R. Bonneau, J. Gray, R. Das, Serverification of molecular modeling applications: the Rosetta Online Server That Includes Everyone (ROSIE), *PLoS One* **8**, 1–11 (2013).

189. D. Duhovny, R. Nussinov, H. Wolfson, in *Algorithms in Bioinformatics*, (2002), pp. 185–200.

190. D. Schneidman-Duhovny, Y. Inbar, R. Nussinov, H. J. Wolfson, PatchDock and SymmDock: servers for rigid and symmetric docking, *Nucleic Acids Res.* **33**, 363–367 (2005).

191. P. E. Stein, A. Boodhoo, G. D. Armstrong, L. D. Heerze, S. A. Cockle, M. H. Klein,

R. J. Read, Structure of a pertussis toxin-sugar complex as a model for receptor binding., *Nat. Struct. Biol.* **1**, 591–596 (1994).

192. B. Friguet, A. F. Chaffotte, L. D. Ohaniance, M. E. Goldberg, Measurements of the true affinity constant in solution of antigen-antibody complexes by enzyme-linked immunosorbent assay, *J. Immunol. Methods* **77**, 305–319 (1985).

193. F. J. Stevens, Modification of an ELISA-based procedure for affinity determination: correction necessary for use with bivalent antibody, *Mol. Immunol.* **24**, 1055–1060 (1987).

194. P. Gillenius, E. Jaatmaa, P. Askelof, M. Granstrom, M. Tiru, The standardization of an assay for pertussis toxin and antitoxin in microplate culture of Chinese hamster ovary cells, *J. Biol. Stand.* **13**, 61–66 (1985).

195. H. Sato, Y. Sato, I. Ohishi, Comparison of pertussis toxin (PT)-neutralizing activities and mouse-protective activities of anti-PT mouse monoclonal antibodies, *Infect. Immun.* **59**, 3832–3835 (1991).

196. S. H. Millen, M. Watanabe, E. Komatsu, F. Yamaguchi, Y. Nagasawa, E. Suzuki, H. Monaco, A. A. Weiss, Single amino acid polymorphisms of pertussis toxin subunit S2 (PtxB) affect protein function, *PLoS One* **10**, 1–19 (2015).

197. E. O. Saphire, P. W. H. I. Parren, R. Pantophlet, M. B. Zwick, G. M. Morris, P. M. Rudd, R. A. Dwek, R. L. Stanfield, D. R. Burton, I. A. Wilson, Crystal structure of a neutralizing human IgG against HIV-1 : a template for vaccine design, *Science (80-.).* **293**, 1155–1159 (2001).

198. C. A. Kowalsky, M. S. Faber, A. Nath, H. E. Dann, V. W. Kelly, L. Liu, P. Shanker, E. K. Wagner, J. A. Maynard, C. Chan, T. a. Whitehead, Rapid fine conformational epitope mapping using comprehensive mutagenesis and deep sequencing, *J. Biol. Chem.* **290**, 26457–26470 (2015).

199. X. Zhang, L. Zhang, H. Tong, B. Peng, M. J. Rames, S. Zhang, G. Ren, 3D Structural Fluctuation of IgG1 Antibody Revealed by Individual Particle Electron Tomography, *Sci. Rep.* **5**, 1–13 (2015).

200. R. L. Stanfield, A. Zemla, I. a. Wilson, B. Rupp, Antibody elbow angles are influenced by their light chain class, *J. Mol. Biol.* **357**, 1566–1574 (2006).

201. A. J. Williams, G. Giese, J. Persson, Improved assembly of bispecific antibodies from knob and hole half-antibodies, *Biotechnol. Prog.* **31**, 1315–1322 (2015).

202. J. M. Elliott, M. Ultsch, J. Lee, R. Tong, K. Takeda, C. Spiess, C. Eigenbrot, J. M. Scheer, Antiparallel conformation of knob and hole aglycosylated half-antibody homodimers is mediated by a CH2-CH3 hydrophobic interaction, *J. Mol. Biol.* **426**, 1947–1957 (2014).

203. R. M. Ionescu, J. Vlasak, C. Price, M. Kirchmeier, Contribution of variable domains to the stability of humanized IgG1 monoclonal antibodies, *J. Pharm. Sci.* **97**, 1414–1426 (2007).

204. J. M. Reichert, Therapeutic monoclonal antibodies approved or in review in the European Union or United States*mAb Soc.* (2015) (available at http://www.antibodysociety.org/news/approved-antibodies/).

205. J. M. Reichert, Antibodies to watch in 2016, *MAbs* **8**, 197–204 (2016).

206. C. Morrison, Antibacterial antibodies gain traction, *Nat. Rev. Drug Discov.* **14**, 737–738 (2015).

207. C. Tsai, S. Morris, Approval of Raxibacumab for the Treatment of Inhalation Anthrax Under the US Food and Drug Administration "Animal Rule," *Front. Microbiol.* **6**, 1–5 (2015).

208. US Food and Drug Administration, FDA approves new treatment for inhalation anthrax*FDA news release* (2016) (available at http://www.fda.gov/NewsEvents/Newsroom/PressAnnouncements/ucm491470.htm).

209. Y. Voronin, L. M. Mofenson, C. K. Cunningham, M. G. Fowler, P. Kaleebu, E. J. McFarland, J. T. Safrit, B. S. Graham, W. Snow, HIV Monoclonal Antibodies: A New Opportunity to Further Reduce Mother-to-Child HIV Transmission, *PLoS Med.* **11**, 1–5 (2014).

210. B. Hazes, R. J. Read, Accumulating evidence suggests that several AB-toxins subvert the endoplasmic reticulum-associated protein degradation pathway to enter target cells, *Biochemistry* **36**, 11051–11054 (1997).

211. D. J. Vance, J. M. Tremblay, N. J. Mantis, C. B. Shoemaker, Stepwise engineering of heterodimeric single domain camelid VHH antibodies that passively protect mice from ricin toxin, *J. Biol. Chem.* **288**, 36538–36547 (2013).

212. C. Herrera, T. I. Klokk, R. Cole, K. Sandvig, N. J. Mantis, A bispecific antibody promotes aggregation of ricin toxin on cell surfaces and alters dynamics of toxin internalization and trafficking, *PLoS One* **11**, 1–18 (2016).

213. J. J. Rhoden, G. L. Dyas, V. J. Wroblewski, A modeling and experimental investigation of the effects of antigen Density, binding affinity, and antigen expression ratio on bispecific antibody binding to cell surface targets, *J. Biol. Chem.* **291**, 11337–11347 (2016).

214. M. M. Ngundi, B. D. Meade, S. F. Little, C. P. Quinn, C. R. Corbett, R. A. Brady, D. L. Burns, Analysis of defined combinations of monoclonal antibodies in anthrax toxin neutralization assays and their synergistic action, *Clin. Vaccine Immunol.* **19**, 731–739 (2012).

215. S. W. Martin, L. Pawloski, M. Williams, K. Weening, C. Debolt, X. Qin, L. Reynolds, C. Kenyon, G. Giambrone, K. Kudish, L. Miller, D. Selvage, A. Lee, T. H. Skoff, H. Kamiya, P. K. Cassiday, M. L. Tondella, T. a. Clark, Pertactin-negative bordetella pertussis strains: evidence for a possible selective advantage, *Clin. Infect. Dis.* **60**, 223–227 (2015).

216. M. Williams, K. Sen, M. Weigand, T. Skoff, V. Cunningham, T. Halse, M.

Tondella, CDC Pertussis Working Group, Bordetella pertussis strain lacking pertactin and pertussis toxin, *Emerg. Infect. Dis.* **22**, 319–322 (2016).

217. C. Spiess, M. Merchant, A. Huang, Z. Zheng, N.-Y. Yang, J. Peng, D. Ellerman, W. Shatz, D. Reilly, D. G. Yansura, J. M. Scheer, Bispecific antibodies with natural architecture produced by co-culture of bacteria expressing two distinct half-antibodies., *Nat. Biotechnol.* **31**, 753–758 (2013).

218. S. M. Lewis, X. Wu, A. Pustilnik, A. Sereno, F. Huang, H. L. Rick, G. Guntas, A. Leaver-Fay, E. M. Smith, C. Ho, C. Hansen-Estruch, A. K. Chamberlain, S. M. Truhlar, E. M. Conner, S. Atwell, B. Kuhlman, S. J. Demarest, Generation of bispecific IgG antibodies by structure-based design of an orthogonal Fab interface., *Nat. Biotechnol.* **32**, 191–198 (2014).

219. T. Dreier, G. Lorenczewski, C. Brandl, P. Hoffmann, U. Syring, F. Hanakam, P. Kufer, G. Riethmuller, R. Bargou, P. A. Baeuerle, Extremely potent, rapid and costimulation-independent cytotoxic T-cell response against lymphoma cells catalyzed by a single-chain bispecific antibody, *Int. J. Cancer* **100**, 690–697 (2002).

220. H. Kantarjian, A. Stein, N. Gökbuget, A. K. Fielding, A. C. Schuh, J.-M. Ribera, A. Wei, H. Dombret, R. Foà, R. Bassan, Ö. Arslan, M. A. Sanz, J. Bergeron, F. Demirkan, E. Lech-Maranda, A. Rambaldi, X. Thomas, H.-A. Horst, M. Brüggemann, W. Klapper, B. L. Wood, A. Fleishman, D. Nagorsen, C. Holland, Z. Zimmerman, M. S. Topp, Blinatumomab versus Chemotherapy for Advanced Acute Lymphoblastic Leukemia, *N. Engl. J. Med.* **376**, 836–847 (2017).

221. J. Pendzialek, K. Roose, A. Smet, B. Schepens, P. Kufer, T. Raum, P. A. Baeuerle, M. Muenz, X. Saelens, W. Fiers, Bispecific T cell engaging antibody constructs targeting a universally conserved part of the viral M2 ectodomain cure and prevent influenza A virus infection, *Antiviral Res.* **141**, 155–164 (2017).

222. C. Petrovas, S. Ferrando-Martinez, M. Y. Gerner, J. P. Casazza, A. Pegu, C. Deleage, A. Cooper, J. Hataye, S. Andrews, D. Ambrozak, P. M. Del Río Estrada, E. Boritz, R. Paris, E. Moysi, K. L. Boswell, E. Ruiz-Mateos, I. Vagios, M. Leal, Y. Ablanedo-Terrazas, A. Rivero, L. A. Gonzalez-Hernandez, A. B. McDermott, S. Moir, G. Reyes-Terán, F. Docobo, G. Pantaleo, D. C. Douek, M. R. Betts, J. D. Estes, R. N. Germain, J. R. Mascola, R. A. Koup, Follicular CD8 T cells accumulate in HIV infection and can kill infected cells *in vitro* via bispecific antibodies, *Sci. Transl. Med.* **9**, eaag2285 (2017).

223. M. Mack, G. Riethmüller, P. Kufer, A small bispecific antibody construct expressed as a functional single-chain molecule with high tumor cell cytotoxicity., *Proc. Natl. Acad. Sci. U. S. A.* **92**, 7021–5 (1995).

224. C. Wu, H. Ying, C. Grinnell, S. Bryant, R. Miller, A. Clabbers, S. Bose, D. McCarthy, R.-R. Zhu, L. Santora, R. Davis-Taber, Y. Kunes, E. Fung, A. Schwartz, P. Sakorafas, J. Gu, E. Tarcsa, A. Murtaza, T. Ghayur, Simultaneous targeting of multiple disease mediators by a dual-variable-domain immunoglobulin., *Nat. Biotechnol.* **25**,

1290–1297 (2007).

225. M. Dillon, Y. Yin, L. Mccarty, D. Ellerman, D. Slaga, T. T. Junttila, G. Han, W. Sandoval, M. A. Ovacik, K. Lin, Z. Hu, A. Shen, J. E. Corn, C. Spiess, P. J. Carter, Efficient production of bispecific IgG of different isotypes and species of origin in single mammalian cells, *MAbs* (2016).

226. J. Oates, B. K. Jakobsen, ImmTACs, *Oncoimmunology* **2**, e22891 (2013).

227. N. Liddy, G. Bossi, K. J. Adams, A. Lissina, T. M. Mahon, N. J. Hassan, J. Gavarret, F. C. Bianchi, N. J. Pumphrey, K. Ladell, E. Gostick, A. K. Sewell, N. M. Lissin, N. E. Harwood, P. E. Molloy, Y. Li, B. J. Cameron, M. Sami, E. E. Baston, P. T. Todorov, S. J. Paston, R. E. Dennis, J. V Harper, S. M. Dunn, R. Ashfield, A. Johnson, Y. McGrath, G. Plesa, C. H. June, M. Kalos, D. a Price, A. Vuidepot, D. D. Williams, D. H. Sutton, B. K. Jakobsen, Monoclonal TCR-redirected tumor cell killing., *Nat. Med.* **18**, 980–7 (2012).

228. Y. Li, R. Moysey, P. E. Molloy, A.-L. Vuidepot, T. Mahon, E. Baston, S. Dunn, N. Liddy, J. Jacob, B. K. Jakobsen, J. M. Boulter, Directed evolution of human T-cell receptors with picomolar affinities by phage display., *Nat. Biotechnol.* **23**, 349–54 (2005).

229. J. Oates, N. J. Hassan, B. K. Jakobsen, ImmTACs for targeted cancer therapy: Why, what, how, and which, *Mol. Immunol.* **67**, 67–74 (2015).

230. G. Friberg, D. Reese, Blinatumomab (Blincyto®); lessons learned from the bispecific t-cell engager (BiTE®) in acute lymphocytic leukemia (ALL), *Ann. Oncol.* (2017), doi:10.1093/annonc/mdx150.

231. S. Atwell, J. B. Ridgway, J. A. Wells, P. Carter, Stable heterodimers from remodeling the domain interface of a homodimer using a phage display library., *J. Mol. Biol.* **270**, 26–35 (1997).

232. J. Chng, T. Wang, R. Nian, A. Lau, K. M. Hoi, S. C. Ho, P. Gagnon, X. Bi, Y. Yang, Cleavage efficient 2A peptides for high level monoclonal antibody expression in CHO cells, *MAbs* **7**, 403–412 (2015).

233. J. M. Boulter, M. Glick, P. T. Todorov, E. Baston, M. Sami, P. Rizkallah, B. K. Jakobsen, Stable, soluble T-cell receptor molecules for crystallization and therapeutics, *Protein Eng. Des. Sel.* **16**, 707–711 (2003).

234. Anti-CD3 antibodies and methods of use thereof (2010).

235. S. Gras, X. Saulquin, J.-B. Reiser, E. Debeaupuis, K. Echasserieau, A. Kissenpfennig, F. Legoux, A. Chouquet, M. Le Gorrec, P. Machillot, B. Neveu, N. Thielens, B. Malissen, M. Bonneville, D. Housset, Structural bases for the affinity-driven selection of a public TCR against a dominant human cytomegalovirus epitope., *J. Immunol.* **183**, 430–7 (2009).

236. E. Walseng, S. Wälchli, L.-E. Fallang, W. Yang, A. Vefferstad, A. Areffard, J. Olweus, Soluble T-Cell Receptors Produced in Human Cells for Targeted Delivery, *PLoS*

One **10**, e0119559 (2015).

237. P. de Felipe, M. D. Ryan, Targeting of proteins derived from self-processing polyproteins containing multiple signal sequences, *Traffic* **5**, 616–626 (2004).

238. J. M. Boulter, M. Glick, P. T. Todorov, E. Baston, M. Sami, P. Rizkallah, B. K. Jakobsen, Stable, soluble T-cell receptor molecules for crystallization and therapeutics, *Protein Eng. Des. Sel.* **16**, 707–711 (2003).

239. P. D. Holler, P. O. Holman, E. V Shusta, S. O'Herrin, K. D. Wittrup, D. M. Kranz, *In vitro* evolution of a T cell receptor with high affinity for peptide/MHC., *Proc. Natl. Acad. Sci. U. S. A.* **97**, 5387–92 (2000).

240. D. M. Gakamsky, E. Lewitzki, E. Grell, X. Saulquin, B. Malissen, F. Montero-Julian, M. Bonneville, I. Pecht, Kinetic evidence for a ligand-binding-induced conformational transition in the T cell receptor., *Proc. Natl. Acad. Sci. U. S. A.* **104**, 16639–44 (2007).

241. L. K. Chlewicki, P. D. Holler, B. C. Monti, M. R. Clutter, D. M. Kranz, High-affinity, peptide-specific T cell receptors can be generated by mutations in CDR1, CDR2 or CDR3, *J. Mol. Biol.* **346**, 223–239 (2005).

242. R. Kunaparaju, M. Liao, N.-A. Sunstrom, Epi-CHO, an episomal expression system for recombinant protein production in CHO cells., *Biotechnol. Bioeng.* **91**, 670–7 (2005).

243. E. Lunde, G. Å. Løset, B. Bogen, I. Sandlie, Stabilizing mutations increase secretion of functional soluble TCR-Ig fusion proteins., *BMC Biotechnol.* **10**, 61 (2010).

244. J. Carter, J. Zhang, T. L. Dang, H. Hasegawa, J. D. Cheng, I. Gianan, J. W. O'Neill, M. Wolfson, S. Siu, S. Qu, D. Meininger, H. Kim, J. Delaney, C. Mehlin, Fusion partners can increase the expression of recombinant interleukins via transient transfection in 2936E cells, *Protein Sci.* **19**, 357–362 (2010).

245. M. Kieke, E. Shusta, E. Boder, L. Teyton, K. Wittrup, D. Kranz, Selection of functional T cell receptor mutants from a yeast surface- display library, *Proc Natl Acad Sci U S A* **96**, 5651–6. (1999).

246. D. H. Aggen, A. S. Chervin, F. K. Insaidoo, K. H. Piepenbrink, B. M. Baker, D. M. Kranz, Identification and engineering of human variable regions that allow expression of stable single-chain T cell receptors, *Protein Eng. Des. Sel.* **24**, 361–372 (2011).

247. A. S. Chervin, D. H. Aggen, J. M. Raseman, D. M. Kranz, Engineering higher affinity T cell receptors using a T cell display system, *J. Immunol. Methods* **339**, 175–184 (2008).

248. L. Trautmann, M. Rimbert, K. Echasserieau, X. Saulquin, B. Neveu, J. Dechanet, V. Cerundolo, M. Bonneville, Selection of T Cell Clones Expressing High-Affinity Public TCRs within Human Cytomegalovirus-Specific CD8 T Cell Responses, *J. Immunol.* **175**, 6123–6132 (2005).

249. M. R. Wills, A. J. Carmichael, K. Mynard, X. Jin, M. P. Weekes, B. Plachter, J. G.

Sissons, The human cytotoxic T-lymphocyte (CTL) response to cytomegalovirus is dominated by structural protein pp65: frequency, specificity, and T-cell receptor usage of pp65-specific CTL., *J. Virol.* **70**, 7569–79 (1996).

250. K. K. Biron, Antiviral drugs for cytomegalovirus diseases, *Antiviral Res.* **71**, 154–163 (2006).

251. P. R. Krause, S. R. Blalek, S. B. Boppana, P. D. Griffiths, C. A. Laughlin, P. Ljungman, E. S. Mocarski, R. F. Pass, J. S. Read, M. R. Schleiss, S. A. Plotkin, Priorities for CMV vaccine development, *Vaccine* **32**, 4–10 (2013).

252. M. G. Revello, T. Lazzarotto, B. Guerra, A. Spinillo, E. Ferrazzi, A. Kustermann, S. Guaschino, P. Vergani, T. Todros, T. Frusca, A. Arossa, M. Furione, V. Rognoni, N. Rizzo, L. Gabrielli, C. Klersy, G. Gerna, CHIP Study Group, A randomized trial of hyperimmune globulin to prevent congenital cytomegalovirus., *N. Engl. J. Med.* **370**, 1316–26 (2014).

253. L. G. Lum, M. Ramesh, A. Thakur, S. Mitra, A. Deol, J. P. Uberti, P. E. Pellett, Targeting Cytomegalovirus-Infected Cells Using T Cells Armed with Anti-CD3 × Anti-CMV Bispecific Antibody, *Biol. Blood Marrow Transplant.* **18**, 1012–1022 (2012).

Vita

Ellen Kathleen Wagner was born in Bakersfield, CA. but lived most of her formative years in Larkspur, CO. After graduating from Douglas County High School in 2007, Ellen pursued her bachelor's degree in chemical and biological engineering at the University of Colorado at Boulder. Her undergraduate highlights include spending a semester abroad at the University of Canterbury in Christchurch, New Zealand; writing an undergraduate thesis; and graduating Magna Cum Laude in 2007. Ellen worked as a process engineer for CH2M Hill for one year before starting graduate school at The University of Texas at Austin in the fall of 2012. During this time she was also able to spend 6 months as a visiting researcher at the University of Oslo in Oslo, Norway.

Ellen.Wagner@utexas.edu

This dissertation was typed by Ellen Kathleen Wagner.